

DNA 6168F

ADA130291

DNAF-1

An Analytical Fallout Prediction Model and Code

Atmospheric Science Associates
P.O. Box 307
363 Great Road
Bedford, Massachusetts 01730

31 October 1981

Final Report for Period 12 March 1980-31 October 1981

CONTRACT No. DNA 001-80-C-0197

APPROVED FOR PUBLIC RELEASE;
DISTRIBUTION UNLIMITED.

DTIC FILE COPY

THIS WORK WAS SPONSORED BY THE DEFENSE NUCLEAR AGENCY
UNDER RDT&E RMSS CODE B325080464 V99QAXNA01113 H2590D.

Prepared for
Director
DEFENSE NUCLEAR AGENCY
Washington, DC 20305

83 05 31 126

Destroy this report when it is no longer
needed. Do not return to sender.

PLEASE NOTIFY THE DEFENSE NUCLEAR AGENCY,
ATTN: STTI, WASHINGTON, D.C. 20305, IF
YOUR ADDRESS IS INCORRECT, IF YOU WISH TO
BE DELETED FROM THE DISTRIBUTION LIST, OR
IF THE ADDRESSEE IS NO LONGER EMPLOYED BY
YOUR ORGANIZATION.



UNCLASSIFIED

SECURITY CLASSIFICATION OF THIS PAGE (When Data Entered)

REPORT DOCUMENTATION PAGE		READ INSTRUCTIONS BEFORE COMPLETING FORM
1. REPORT NUMBER DNA 6168F	2. GOVT ACCESSION NO. DA6168F	3. RECIPIENT'S CATALOG NUMBER
4. TITLE (and Subtitle) DNAF-1 An Analytical Fallout Prediction Model and Code		5. TYPE OF REPORT & PERIOD COVERED Final Report for Period 12 Mar 80 - 31 Oct 81
7. AUTHOR(s) Hillyer G. Norment		6. PERFORMING ORG. REPORT NUMBER
9. PERFORMING ORGANIZATION NAME AND ADDRESS Atmospheric Science Associates P. O. Box 307, 360 Great Road Bedford, Massachusetts 01730		8. CONTRACT OR GRANT NUMBER(s) DNA 001-80-C-0197
11. CONTROLLING OFFICE NAME AND ADDRESS Director Defense Nuclear Agency Washington, D.C. 20305		10. PROGRAM ELEMENT PROJECT, TASK AREA & WORK UNIT NUMBERS Subtask V99QAXNA011-13
14. MONITORING AGENCY NAME & ADDRESS (if different from Controlling Office)		12. REPORT DATE 31 October 1981
		13. NUMBER OF PAGES 130
		15. SECURITY CLASS (of this report) UNCLASSIFIED
		15a. DECLASSIFICATION/DOWNGRADING SCHEDULE
16. DISTRIBUTION STATEMENT (of this Report) Approved for public release; distribution unlimited.		
17. DISTRIBUTION STATEMENT (of the abstract entered in Block 20, if different from Report)		
18. SUPPLEMENTARY NOTES This work was sponsored by the Defense Nuclear Agency under RDT&E Code B325080464 V99QAXNA01113 H2590D.		
19. KEY WORDS (Continue on reverse side if necessary and identify by block number) Nuclear Fallout Nuclear Weapons Effects Damage Assessment Fallout Modeling Fallout Prediction Analytical Model		
20. ABSTRACT (Continue on reverse side if necessary and identify by block number) DNAF-1 has been developed to rapidly predict fallout γ -ray activity from surface burst nuclear explosions. It is suitable for use in large-scale damage assessment studies. Explosion energy yield range is 10^{-3} to 10^5 KT. Minimum input data requirements of the code are: total and fission yields, speed and direction angle of a single effective wind vector, and a wind shear parameter. Wind data in terms of a vertical profile of wind vectors may be supplied by		

DD FORM 1473

EDITION OF 1 NOV 65 IS OBSOLETE

UNCLASSIFIED

SECURITY CLASSIFICATION OF THIS PAGE (When Data Entered)

UNCLASSIFIED

SECURITY CLASSIFICATION OF THIS PAGE(When Data Entered)

20. ABSTRACT (continued)

the user, in which case the code will process the data such as to compute the effective wind vector and shear parameter.

The code will automatically compute and print a fallout map in terms of H + 1 hour exposure rate ordinates for a spatially undistorted array of points on the ground. Alternatively, the user may specify his own map boundaries and grid increments. He also may specify any number of ground points at which the code will compute H + 1 hour exposure rate and maximum effective biological dose. Both model and code are fully documented, and user instructions for the code are presented.

Results of a validation study are presented. Predicted fallout patterns are compared with observed patterns for five test shots that cover a wide range of energy yields. Predictions by the DELFIC and WSEG-10 models also are included. Visual comparisons of contour maps and various statistical comparison methods are used. DNAF-1 predictions are found to be substantially better than those of WSEG-10 and almost as good as DELFIC predictions.

UNCLASSIFIED

SECURITY CLASSIFICATION OF THIS PAGE(When Data Entered)

PREFACE

The author gratefully acknowledges the support and cooperation of Dr. David L. Auton of the Defense Nuclear Agency, and Mr. Ralph B. Mason of the Command and Control Technical Center (CCTC) who made exhaustive runs of the code on the CCTC computer, analyzed the results, uncovered numerous problems, and thus substantially assisted in the development of the model.

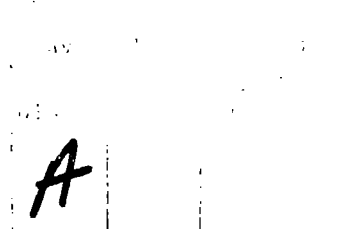


TABLE OF CONTENTS

<u>Section</u>		<u>Page</u>
	PREFACE - - - - -	1
1.	INTRODUCTION AND BACKGROUND - - - - -	7
2.	DATA BASE - - - - -	9
	2.1 ACTIVITY DEPOSITION RATE - - - - -	9
	2.2 FALLOUT ONSET TIME - - - - -	9
	2.3 FIREBALL AND STABILIZED CLOUD DATA - - - - -	19
	2.4 NOMINAL PARTICLE - - - - -	20
	2.5 OBSERVED FALLOUT DATA - - - - -	22
3.	MATHEMATICAL DESCRIPTION - - - - -	23
	3.1 ACTIVITY DEPOSITION RATE FUNCTION - - - - -	23
	3.2 DEPOSITION AS A FUNCTION OF DISTANCE FROM GROUND ZERO - - - - -	25
	3.3 FARFIELD CORRECTION - - - - -	30
	3.4 UPWIND CORRECTION - - - - -	34
	3.5 FALLOUT TIME OF ARRIVAL - - - - -	35
	3.6 HORIZONTAL SPREAD OF THE NUCLEAR CLOUD - - - - -	35
	3.7 TURBULENT DISPERSION OF FALLOUT - - - - -	40
	3.8 WIND SHEAR DISPERSION AND CROSSWIND SPREAD OF THE FALLOUT PATTERN - - - - -	41
	3.9 GAMMA RAY EXPOSURE RATE AND MAXIMUM EFFECTIVE BIOLOGICAL DOSE - - - - -	44
4.	USE OF WIND DATA - - - - -	47
	4.1 GENERAL CONSIDERATIONS - - - - -	47
	4.2 EFFECTIVE FALLOUT WIND - - - - -	47
	4.3 SHEAR PARAMETER - - - - -	50
5.	VALIDATION - - - - -	52
	5.1 DISCUSSION OF RESULTS - - - - -	52
	5.2 DISCUSSION OF THE TEST SHOT DATA AND PREDICTIONS	55

TABLE OF CONTENTS (Continued)

<u>Section</u>	<u>Page</u>
5.3 OBSERVED AND PREDICTED FALLOUT PATTERNS - - - - -	57
6. COMPUTER CODE - - - - -	81
6.1 GENERAL DISCUSSION - - - - -	81
6.2 FALLOUT MAPS - - - - -	83
6.3 INPUT OF WIND PROFILE DATA - - - - -	85
6.4 STORAGE AND COMPUTATION TIME REQUIREMENTS - - - - -	90
6.5 DESCRIPTION OF CARD INPUTS FOR THE DNAF-1 CODE - - - - -	91
6.6 EXAMPLE PROBLEM AND PRINTOUT DESCRIPTION - - - - -	93
REFERENCES - - - - -	97
APPENDIX A GLOSSARY OF SYMBOLS AND FORTRAN MNEMONICS - - - - -	99
APPENDIX B GROUND ROUGHNESS AND INSTRUMENT RESPONSE CORRECTION FACTORS - - - - -	103
APPENDIX C FALLOUT PATTERN COMPARISON BY THE FIGURE-OF-MERIT METHOD	105
APPENDIX D FORTRAN CODE FOR THE DNAF-1 FALLOUT MODEL - - - - -	107

LIST OF ILLUSTRATIONS

<u>Figure</u>		<u>Page</u>
1	Computer plots of activity fraction deposition rate vs. time as computed by DELFIC. - - - - -	10
2	Activity fraction deposition rate function, $g(t)$, (eq. (6)), without farfield correction, vs. time for $W = 1$ KT. A sampling of DELFIC results are included for comparison. - - - - -	24
3	Distribution of activity of depositing fallout in the hotline axis direction. - - - - -	27
4	Comparison of Gaussian function with the function used in DNAF-1 to approximate the spatial distribution of cloud activity along the hotline axis. - - -	28
5	Activity deposition rate, $g(t)_f$, including farfield correction, vs. time. A sampling of DELFIC results are included for comparison. - - - - -	32
6	Basis of the time-of-arrival calculation. - - - - -	36
7	Fallout time of arrival vs. distance from ground zero for several yields as computed by DNAF-1 and WSEG-10.	37
8	Crosswind-integrated activity fraction, $D(X)_f$ and $D(X)_u$, vs. distance from ground zero along the hotline. - - - - -	42
9	Wind data card input for the example data listed in Table 7. - - - - -	89
10	Test problem card input. - - - - -	94

LIST OF TABLES

<u>Table</u>		<u>Page</u>
1	SETTLING SPEEDS FOR THE NOMINAL PARTICLE, δ_{nom} = 229 μm - - - - -	21
2	TEST SHOT DATA - - - - -	52
3	COMPARISON OF OBSERVED AND PREDICTED FALLOUT PATTERN STATISTICS - - - - -	54
4	OVERALL MEAN ABSOLUTE PERCENT ERRORS - - - - -	55
5	EFFECTIVE FALLOUT WINDS AND SHEAR PARAMETERS COM- PUTED FROM H HOUR WIND PROFILES FOR USE BY DNAF-1 -	57
6	DESCRIPTION OF DNAF-1 CODE SUBROUTINES AND FUNCTIONS	82
7	EXAMPLE WIND DATA LISTING - - - - -	88

1. INTRODUCTION AND BACKGROUND

To quickly and efficiently estimate fallout radioactivity from large numbers of nuclear surface explosions, for example, for military damage assessment studies, a simple, very fast fallout prediction code is needed. While codes based on numerical models^{1,2,3} provide flexibility of usage and relatively high prediction accuracy, they are cumbersome, use too much computer storage, require more input data than desired, and use too much computer time per prediction. A model which uses analytical equations rather than a numerical approach is appropriate for this purpose.

The model that has best satisfied these requirements in the past, the WSEG-10 model, has been used for more than twenty years for damage assessment studies^{4,5}. WSEG-10 has recently been analyzed⁶ and its prediction capabilities compared with those of several other models⁷. It was found that, while in several respects WSEG-10 is satisfactory in terms of its mathematical structure, its data base is obsolete, and this deficiency alone was seen to substantially compromise its prediction capability.

To upgrade prediction capability the easiest course would be to upgrade the WSEG-10 data base, but retain its mathematical structure. However owing to several deficiencies of the model itself, this course has turned out to be undesirable. The most important of these deficiencies are as follows. WSEG-10 mathematics are based on a curve fit of an exponential function to radioactivity deposition rate data that were calculated by an early fallout model. The particular model used was developed to predict fallout from surface bursts of large yield (i.e., megaton range) nuclear weapons. For these large yield cases the exponential function fits the deposition rate data reasonably well at intermediate and late times. Unfortunately, this is not the case for low yield explosions. Also, in no case does the exponential function go to zero at detonation time as a physically realistic function should do. Thus, to fit the low yield deposition rate data as well as the high yield data, and to force the fitted function to go to zero at zero time, a new mathematical base is needed.



Another serious problem with WSEG-10 is that it assumes that a Gaussian function describes the vertical distribution of activity in the nuclear cloud. For shots with yields less than about 50 KT, this is a very poor assumption since much of the activity which will fall out locally is in the cloud stem, whereas the WSEG-10 Gaussian peaks near the cloud cap center height. In effect this procedure ignores the stem, even for low yield cases, and this also seriously compromises prediction capability.

To substantially improve prediction capability, and to extend the range of applicability to lower yields, an entirely new model is required. The DNAF-1 model has been developed to fill this need.

DNAF-1 also is based on a curve fit to calculated activity deposition rate data, though a new set of data is used, and a more appropriate function is used to fit the data. An entirely new approach is used to account for vertical structure of the stabilized cloud, which does account for fallout from the cloud stem. Indeed, revised data and updated modeling concepts are used throughout the development of the new model. Also, the yield range has been extended downward from 1 KT, the lower limit for WSEG-10, to 10^{-3} KT. The upper yield limit is 10^5 KT.

The model computes gamma radiation from dry ground-deposited particulate fallout from the nuclear cloud cap and stem. This radiation issues from weapon debris fission products and from induced activity in the fallout. Contributions from throwout and induced activity in the crater or elsewhere are not included. Alpha and beta radiation are not treated.

In the next section, section 2, we discuss the more critical aspects of the data base used for the new model. In section 3 we detail the mathematical structure of the model, and in section 4 we discuss how wind data are used. Section 5 contains results of a validation study: predicted fallout patterns are compared with observed patterns for five test shots, and predictions by the WSEG-10 and DELFIC models are included as well as those by the DNAF-1 model. Finally, the computer code is described in section 6.

Throughout the presentation, we make comparisons between DNAF-1 and WSEG-10 modeling approaches and results wherever such is appropriate.

2. DATA BASE

2.1 ACTIVITY DEPOSITION RATE

As mentioned above, the DNAF-1 model is based on a mathematical function that is fitted to activity deposition rate data. These data represent rate of deposition of total fallout activity as a function of time and yield. Of course, it would be best to use observed data, but there are none, so instead we have used results generated by a special version of the DELFIC code^{1,2}.

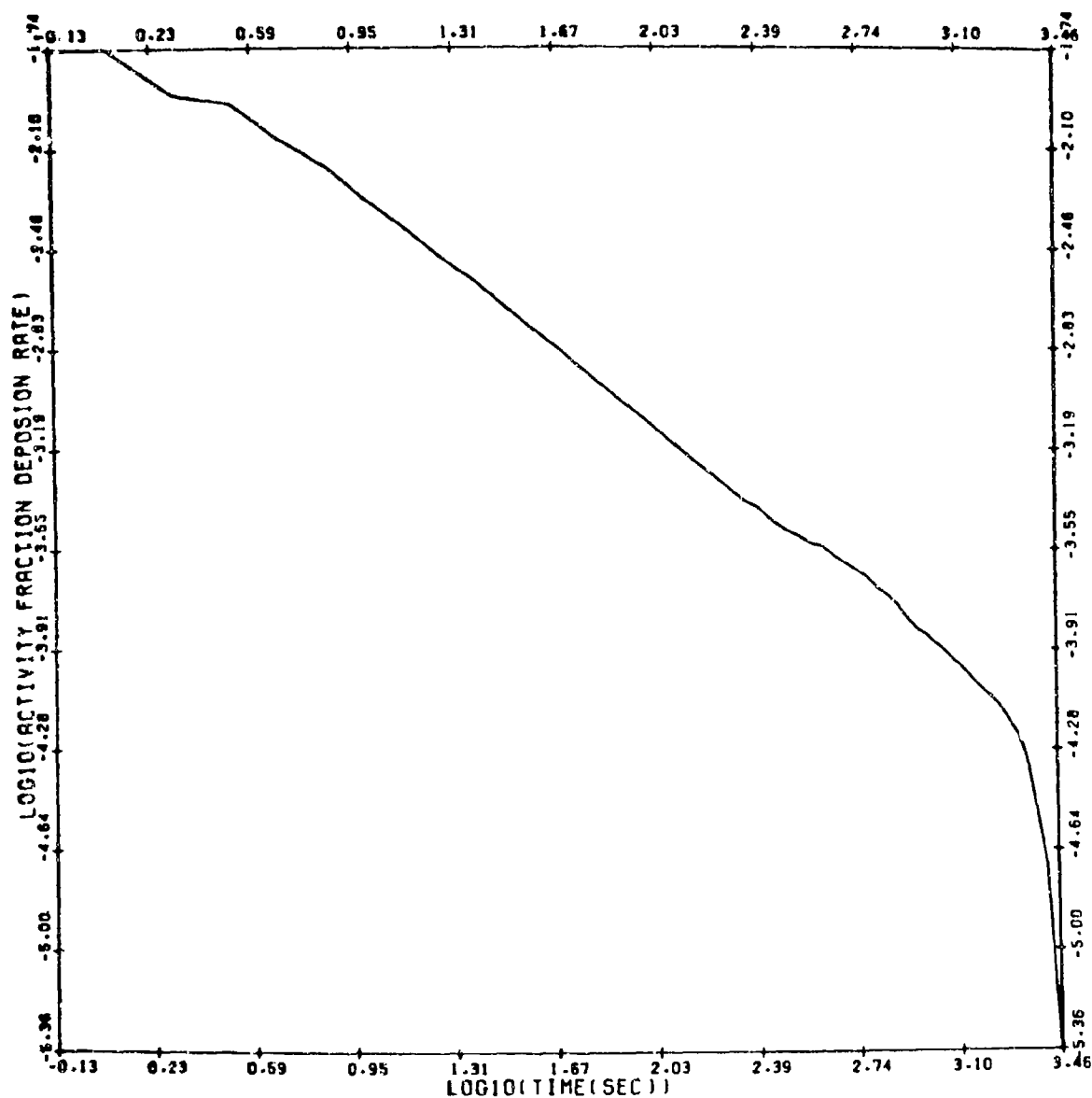
Nuclear cloud rise was calculated through the 1976 U.S. Standard Atmosphere⁸ for every decade of yield from 10^{-3} KT to 10^5 KT. Explosion was taken to be at sea level. Fission yield was taken to equal energy yield. Twenty thousand fallout parcels (100 particle size classes and 200 cloud subdivisions) were followed for each calculation. Cumulative activity tabulated as a function of time was differentiated to give deposition rate by the method of cubic splines⁹. Results are given in Figure 1. The uneven appearance of the curves at early times was caused by poor deposition statistics for the sparse, though highly radioactive, early fallout. Some numerical experimentation showed that increased resolution of the calculations produced curves of essentially the same shape; therefore, to save computer time the curves shown were accepted as an adequate compromise.

The fitting of a mathematical function to these data is described in section 3.1.

2.2 FALLOUT ONSET TIME

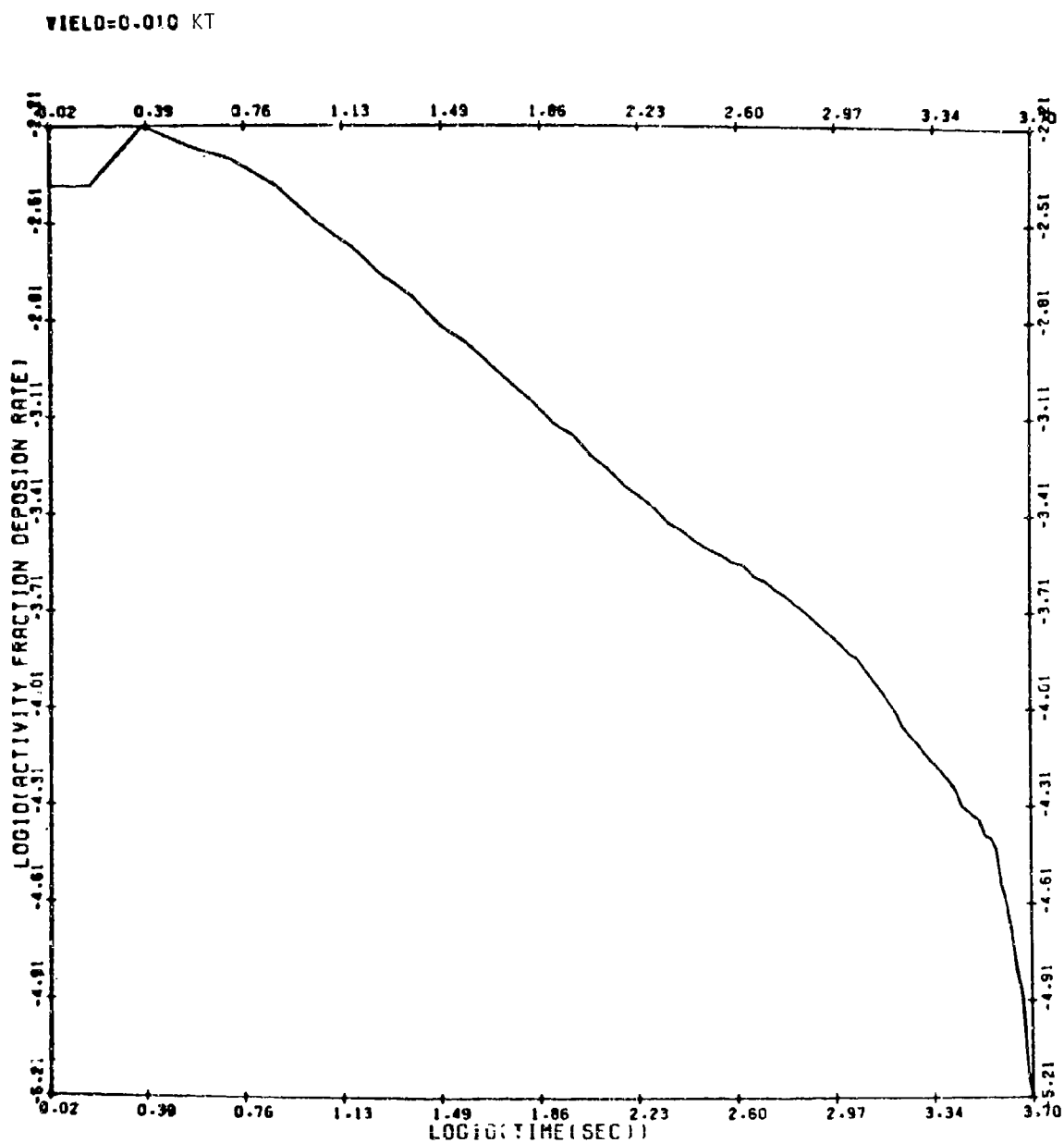
Fallout onset time, t_0 , is the time of first impact of fallout on the ground. It is needed to calculate fallout time of arrival as a function of distance from ground zero, which in turn, is required for calculation of several critical parameters. Onset times for each decade of yield were tabulated from the DELFIC deposition rate data, and $\ln(t_0)$ was fitted by least squares to a polynomial in $\ln(W)$. The result is

YIELD=0.001 KT



a.

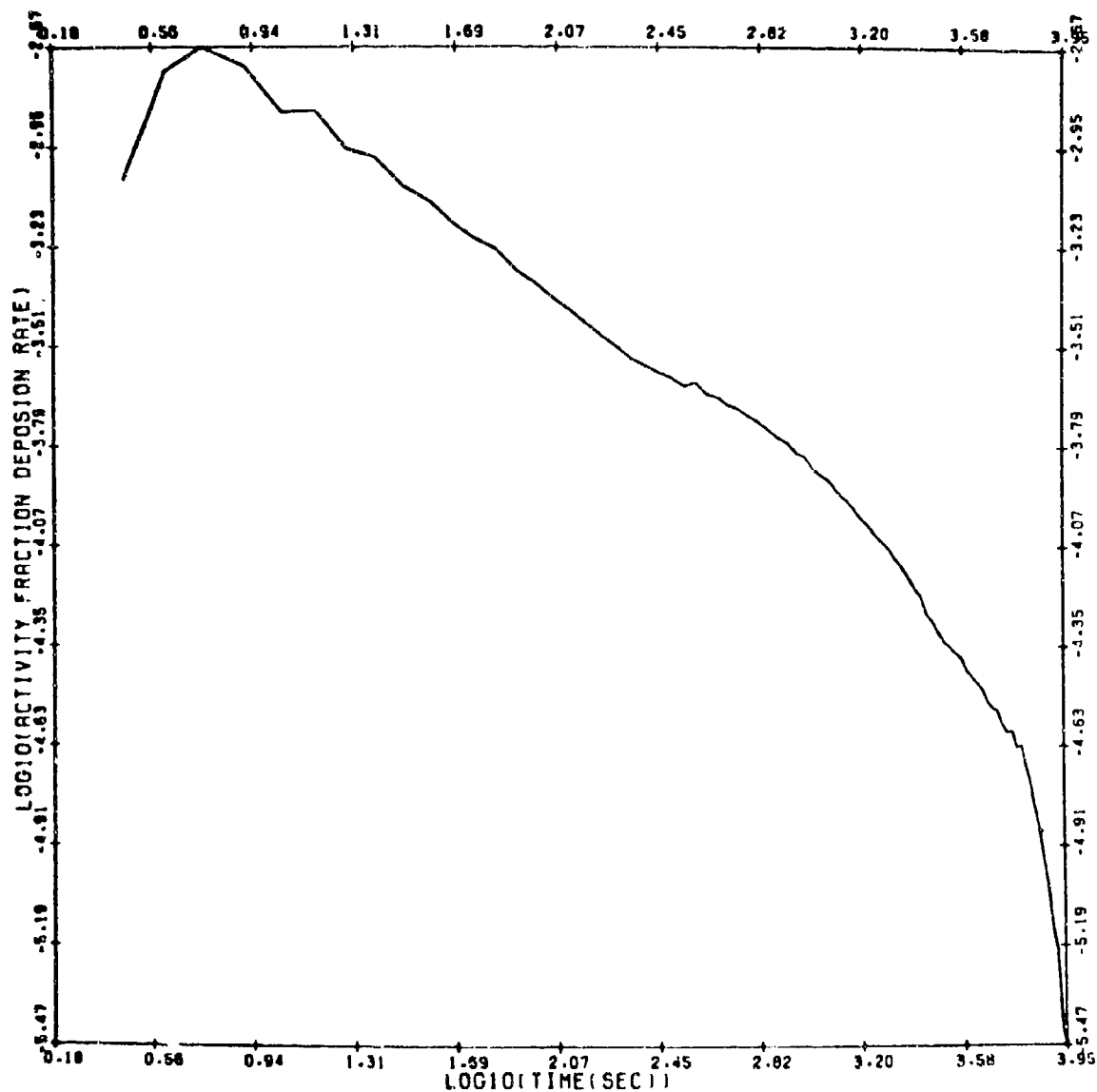
Figure 1. Computer plots of activity fraction deposition rate vs. time as computed by DELFIC.



b.

Figure 1. Computer plots of activity fraction deposition rate vs. time as computed by DELFIC.
(continued)

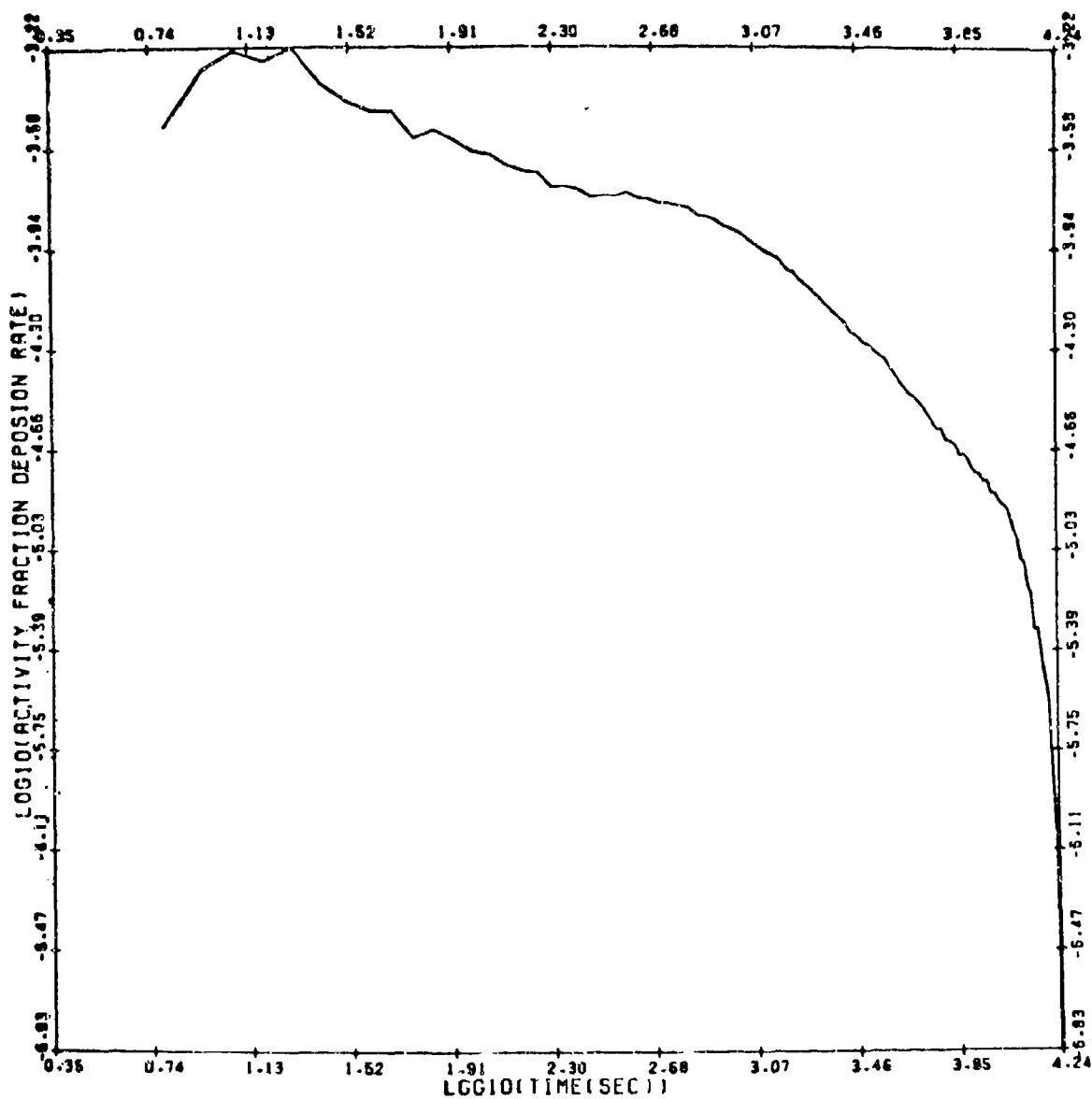
YIELD=0.100 KT



C.

Figure 1. Computer plots of activity fraction deposition rate vs. time as computed by DELFIC (continued)

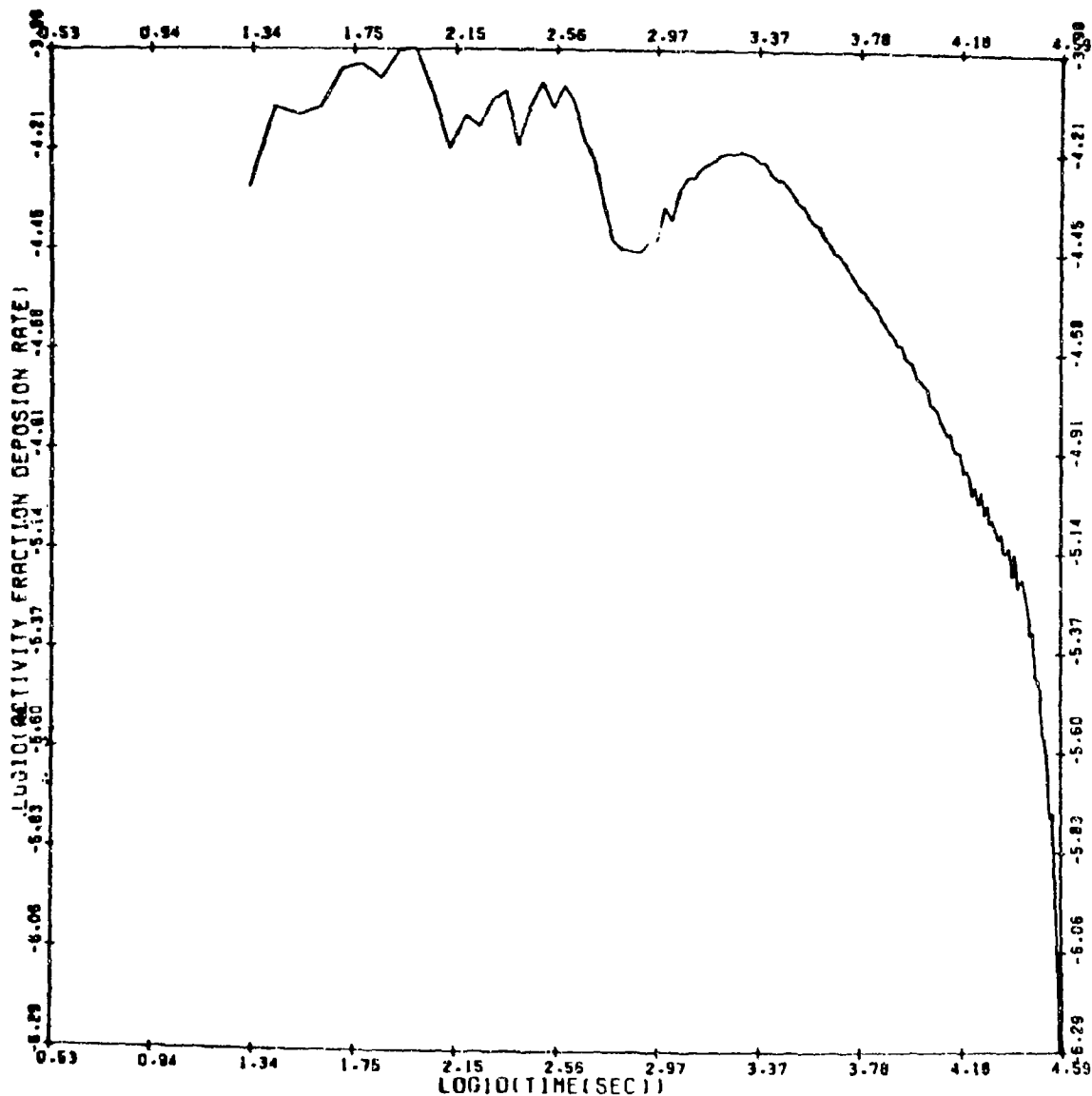
YIELD=1.000 KT



d.

Figure 1. Computer plots of activity fraction deposition rate vs. time as computed by DEIFIC.
(continued)

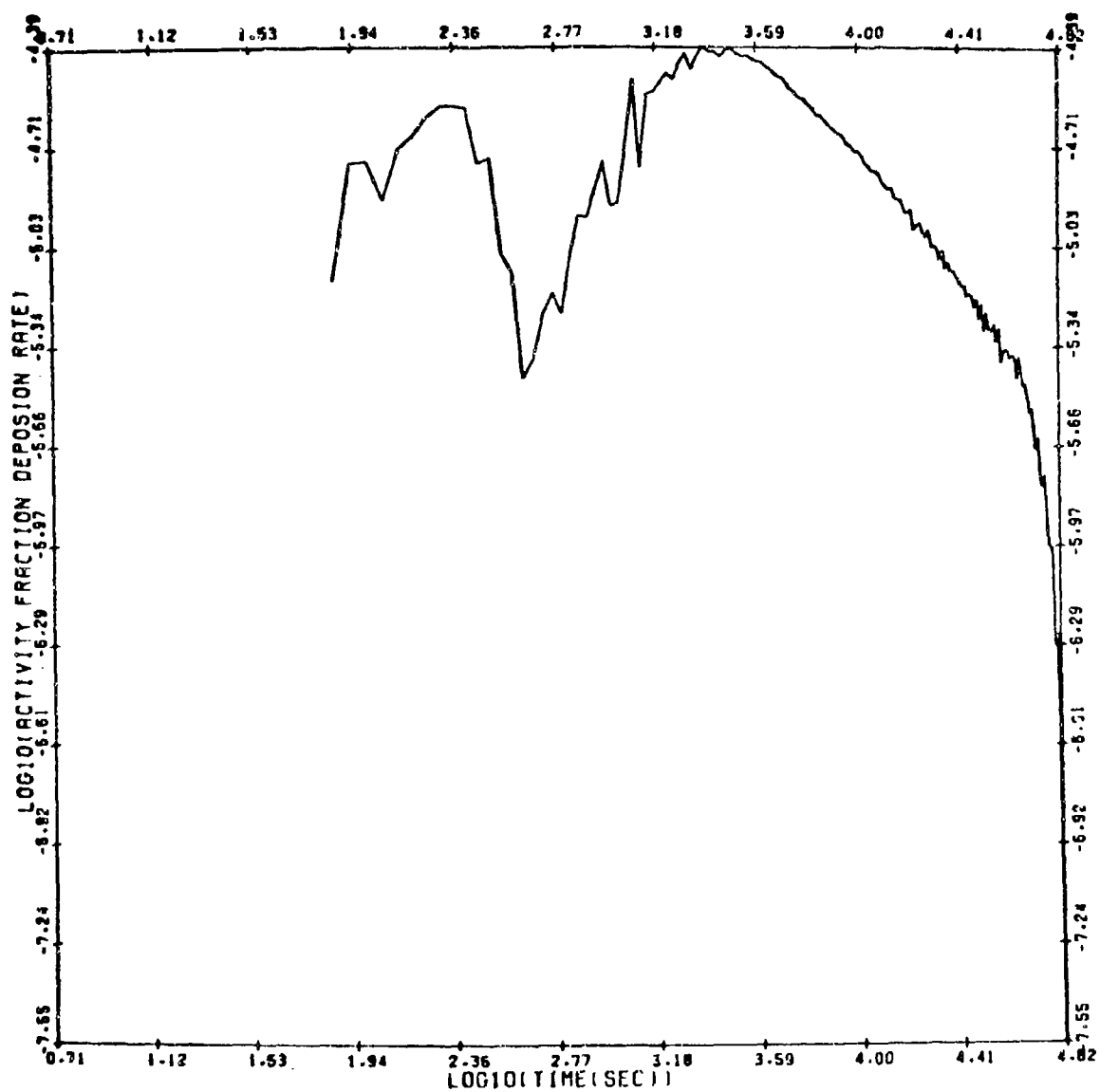
YIELD=10.000 KT



e.

Figure 1. Computer plots of activity fraction deposition rate vs. time as computed by DELFIC.
(continued)

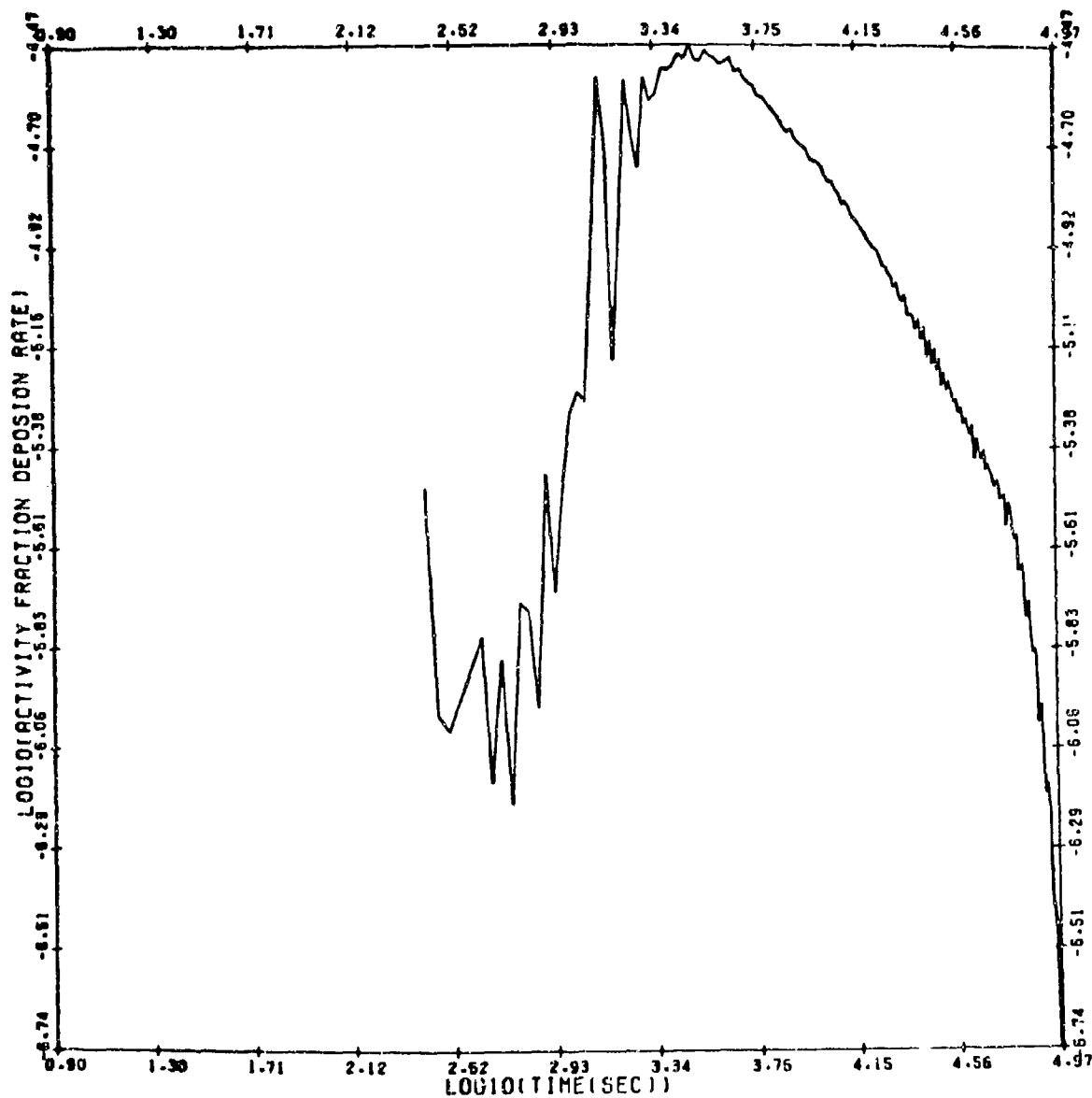
YIELD=100.000 KT



f.

Figure 1. Computer plots of activity fraction deposition rate vs. time as computed by DELFIC.
(continued)

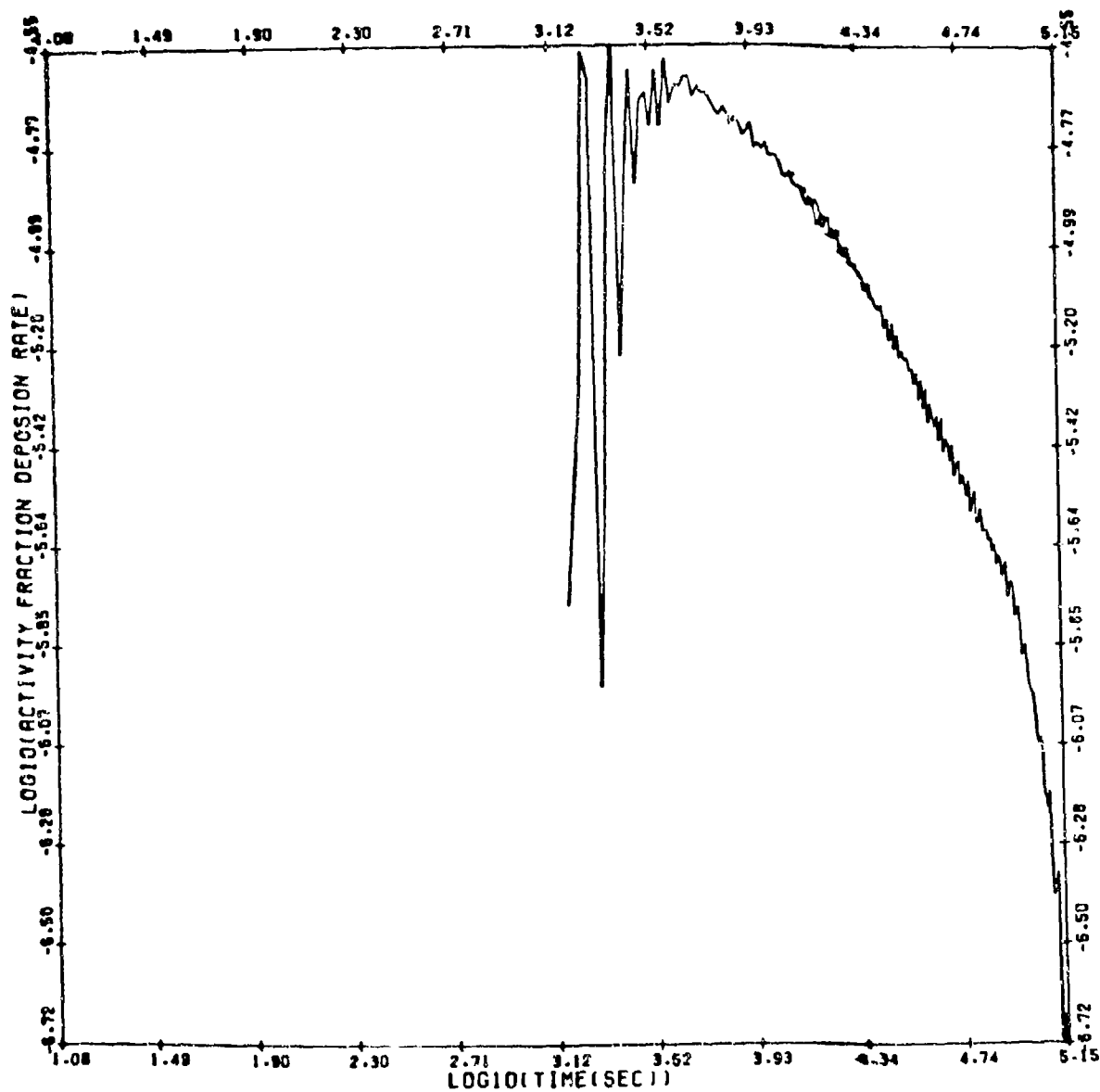
YIELD=1000.070 KT



9.

Figure 1. Computer plots of activity fraction deposition rate vs. time as computed by DLIFIC.
(continued)

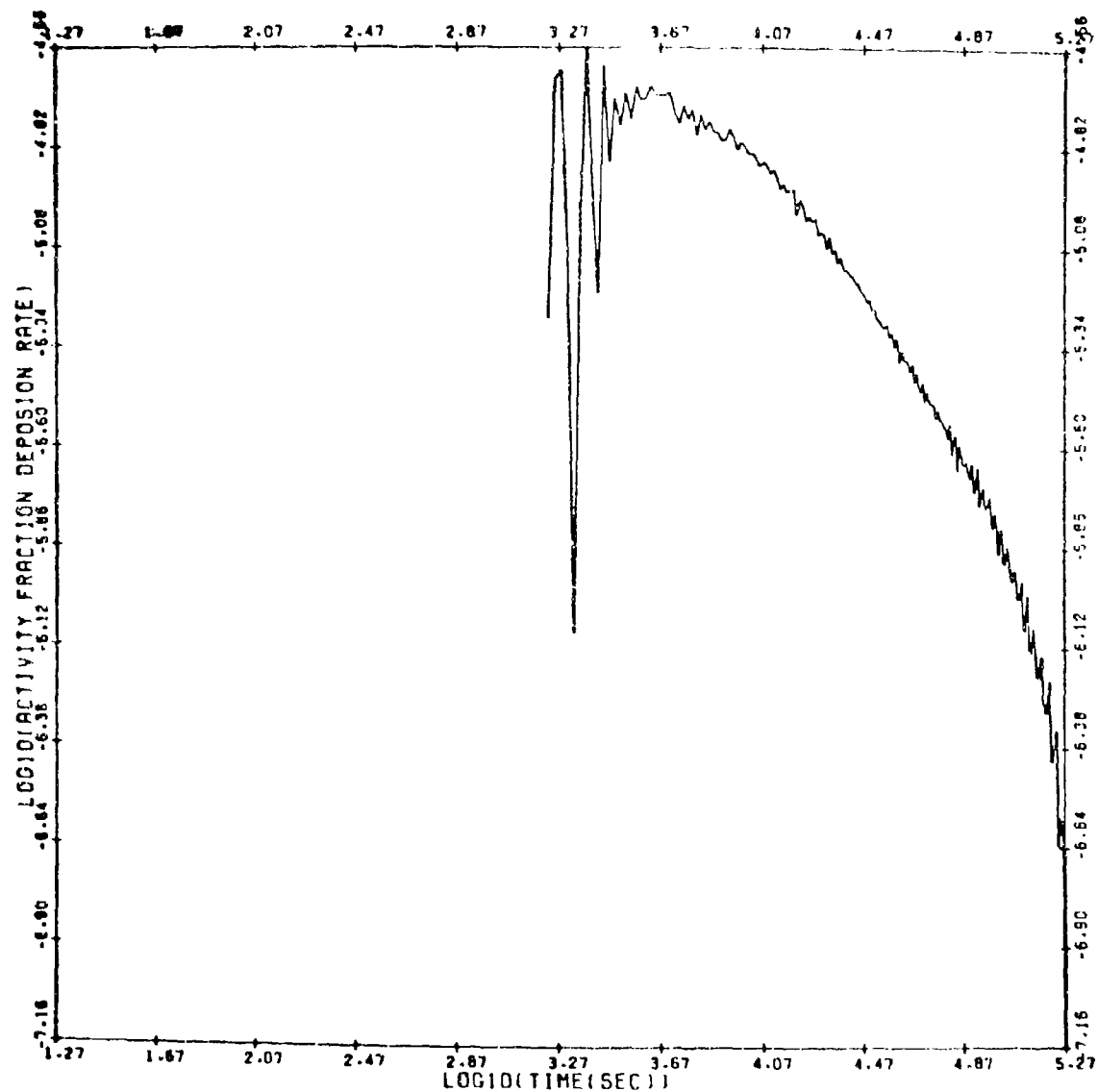
YIELD=10000.000 KT



h.

Figure 1. Computer plots of activity fraction deposition rate vs. time as computed by DELFIC.
(continued)

YIELD=100000.000



i.

Figure 1. Computer plot of activity fraction deposition rate vs. time as computed by DELFIC.
(continued)

$$t_c = \exp \left[1.527667 + 0.4089466 \ln W + 0.02064322 (\ln W)^2 \right] ; \quad W \cdot 10^{-3} \text{ KT} \quad (1)$$

$$t_c = 1147.54 ; \quad W \cdot 10^{-3}$$

where t_c is in units of seconds.

2.3 FIREBALL AND STABILIZED CLOUD DATA

The model also requires fireball (i.e., early cloud) radius, as well as radius and top and base heights of the stabilized cloud. The latter are taken to be above mean sea level.

The early cloud radius, R_f (m), is computed from a function used to initialize the SIMIC cloud rise¹,

$$R_f = 108W^{0.23}; \quad W \text{ in KT.} \quad (2)$$

Stabilized cloud cap base height, z_B , and top height, z_T , are computed from functions fitted to observed data by Wilsey and Crisco¹⁰,

$$z_B = aW^b \quad (3)$$

$$z_T = cW^d \quad (4)$$

where W is energy yield in kilotons, the heights are in meters, and

$$\begin{aligned} a &= 2228, b = 0.3463; & W &\leq 4.07 \text{ KT} \\ a &= 2661, b = 0.2198; & W &> 4.07 \\ c &= 3597, d = 0.2553; & W &\leq 2.29 \\ c &= 3170, d = 0.4077; & 2.29 &< W \leq 19 \\ c &= 6474, d = 0.1650; & W &> 19 \end{aligned}$$

Stabilized cloud radius, R_s , is computed from a least squares polynomial curve fit to DELFIC results,

$$R_s = \exp \left[6.7553 + 0.32055 \ln W + 0.01137478 (\ln W)^2 \right] \quad (5)$$

where R_s is in meters and W is yield in kilotons.

2.4 NOMINAL PARTICLE

The model requires that a single, "effective fallout wind" vector, \vec{v} , be calculated from a given vertical profile of wind data. This effective fallout wind vector is an average of the given data, where in the averaging each vector is weighted according to the time required for a "nominal particle" to settle through the wind space stratum represented by that vector.

The nominal particle diameter was calculated from DELFIC results to be the activity-weighted average diameter over all particle sizes. The standard DELFIC lognormal particle size distribution was used,

$$\delta_{50} = 0.407 \text{ } \mu\text{m}$$

$$s = 4.0$$

where δ_{50} is the median diameter and s the geometric standard deviation of the distribution of particle number with respect to particle diameter. (See Appendix A of reference 1.)

Calculations were performed for the full range of yields, at every decade of W starting with 10^{-3} KT, using a special version of DELFIC. The low yield results were averaged separately from the high yield results, to give

$$\delta_{\text{nom}} = 217.05 \text{ } \mu\text{m}; \quad W \leq 100 \text{ KT}$$

$$\delta_{\text{nom}} = 240.95 \text{ } \mu\text{m}; \quad W > 100$$

The average of these diameters is 229 μm , which is the value used in the model.

Using $\delta_{\text{nom}} = 229 \mu\text{m}$, a table (Table 1) of particle settling speeds as a function of altitude in the 1976 U.S. Standard Atmosphere⁸, was computed via the equations given in section 2.2.3 of the DELFIC documentation¹. This table is used by subroutine EFWIND to calculate effective fallout wind.

TABLE 1
SETTLING SPEEDS FOR THE NOMINAL PARTICLE, $\delta_{\text{nom}} = 229 \mu\text{m}$

<u>Altitude</u> <u>(km above MSL)</u>	<u>Settling</u> <u>Speed</u> <u>(m s⁻¹)</u>	<u>Altitude</u> <u>(km above MSL)</u>	<u>Settling</u> <u>Speed</u> <u>(m s⁻¹)</u>
0	1.6538	20	3.5222
1	1.7124	21	3.6322
2	1.7744	22	3.8122
3	1.8401	23	3.9243
4	1.9097	24	3.9994
5	1.9836	25	4.0806
6	2.0621	26	4.1746
7	2.1458	28	4.3565
8	2.2350	30	4.5328
9	2.3303	32	4.7083
10	2.4324	34	4.8517
11	2.5419	36	5.0023
12	2.6446	38	5.1767
13	2.7489	40	5.3910
14	2.8551	42	5.6632
15	2.9630	44	6.0155
16	3.0723	46	6.4727
17	3.1831	48	7.0778
18	3.2951	50	7.8819
19	3.0482		

2.5 OBSERVED FALLOUT DATA

After development of the model, its capability must be evaluated by comparison against observed data. For this purpose, we have used the best whole-pattern fallout data available. Comparison results are not greatly different from those obtained by use of presumably much more capable models^{1,2,3,4}. Details are given below in section 5.

3. MATHEMATICAL DESCRIPTION

3.1 ACTIVITY DEPOSITION RATE FUNCTION

Ideal specifications for the activity deposition rate function, $q(t)$, are as follows:

1. It should be a simple single function, requiring as few yield dependent parameters as practicable, which fits the deposition rate data (Fig. 1) over the entire nine decades of yield range.
2. The product of $q(t)$ with a downwind dispersion factor, $F(X,t)$, should be analytically integrable over time to yield activity as a function of downwind distance. (See the next section.)
3. Both downwind and crosswind dispersion functions, $F(X,t)$ and $G(r)$, should have Gaussian forms as required by theory and confirmed by experiment for diffusion by homogeneous turbulence¹¹, in the absence of firm data to support alternative functions. Thus, specification 2 is extended to require that $q(t)$ be such as to allow analytical integration of the product $q(t)F(X,t)$ where $F(X,t)$ is specifically a Gaussian function.
4. $q(t)$ should go to zero at the limits of zero and infinite time.
5. Normalization should be exact such that activity is conserved.

These specifications are so restrictive as to require some compromise. Even so, only requirements 3 and 5 are not met by the function selected.

The function which comes closest to satisfying the specifications was found to be

$$q(t) = \frac{4 \sin[\pi(3-\alpha)/2]}{\pi\Gamma(3-\alpha)} \left(\frac{t}{T}\right)^{\alpha} \left[1 + \left(\frac{t}{T}\right)^2\right]^{-2} ; \quad \alpha < 4. \quad (6)$$

Here $q(t)$ is rate of deposition of activity fraction (s^{-1}), t is time (s), and α (dimensionless) and T (s) are yield dependent constants.

Figure 2 shows a representative plot of eq. (6), for $W = 1$ KT, and compares this with a sampling of the DEFFIC results. Except for a tendency to overpredict the maximum deposition rate (also see Fig. 5) for some cases, the function is capable of reproducing the DEFFIC results reasonably well.

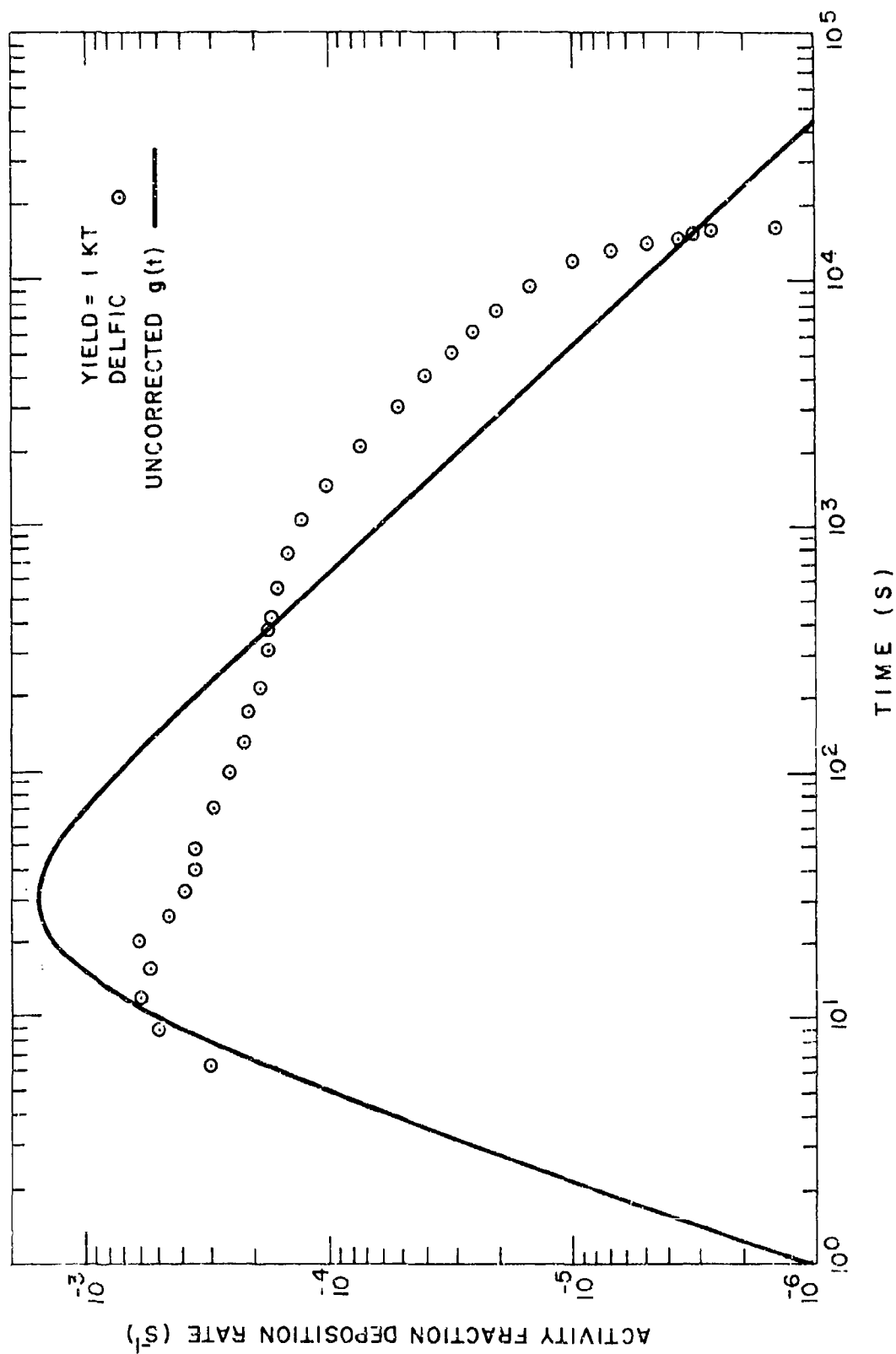


Figure 2. Activity fraction deposition rate function, $g(t)$, (eq. (6)), without farfield correction, vs. time for $W = 1 \text{ } \mu\text{T}$. A sampling of DELFIC results are included for comparison.

for early and intermediate times. At late time the eq. (6) function becomes linear (on the log-log plot) whereas the deposition rate data drop off rapidly. This discrepancy requires application of a "far field" correction factor which is discussed in section 3.3.

The maximum of the $g(t)$ function occurs at time t_{\max} which is given by

$$t_{\max} = T \sqrt{\frac{4-\alpha}{\alpha}} \quad (7)$$

The significance of this relation is that only two of these three parameters need to be specified as functions of yield. Approximate best fit values of α and t_{\max} were determined somewhat subjectively by trial and error for each decade of yield. These were fitted to simple functions of yield as follows:

$$\begin{aligned} \alpha &= 1.06 & ; & 10^{-3} \leq W \leq 10^{-1} \text{ KT} \\ \alpha &= 1.0875 + .0119431 \ln W; & 10^{-1} < W < 10^3 & \\ \alpha &= 1.17 & ; & 10^3 \leq W \end{aligned} \quad (8)$$

and

$$\begin{aligned} t_{\max} &= 30W^{0.41556} & ; & 10^{-3} \leq W \leq 1 \text{ KT} \\ t_{\max} &= 30W^{0.65407} & ; & 1 < W \leq 10^3 \\ t_{\max} &= 893.616W^{0.16273} & ; & 10^3 < W \leq 10^4 \\ t_{\max} &= 2497.18W^{0.05115} & ; & 10^4 < W \leq 10^5 \end{aligned} \quad (9)$$

where t_{\max} is in units of seconds.

3.2 DEPOSITION AS A FUNCTION OF DISTANCE FROM GROUND ZERO

The action of effective fallout wind v is to transport the stabilized cloud downwind such that at time t it is centered over downwind distance point $X = vt$. We assume that fallout deposited from the cloud at this time

has a continuous distribution along the X (i.e. hotline) axis with the distribution centered and peaked at $X = vt$. The situation is illustrated in Figure 3. To determine the total, crosswind integrated fallout deposited at any distance X from ground zero, the contributions of all fallout deposits must be summed over all time, and in this case, this is accomplished by analytical integration from $t = 0$ to $t = \infty$ of the product of $q(t)$ with the downwind distribution function.

As explained in the previous section, a most desirable selection for the downwind distribution function for depositing fallout would be a Gaussian function. It turned out, however, that we could not find a satisfactory function for $q(t)$ that is analytically integrable in combination with a Gaussian distribution in $X-vt$. Thus, we were forced to use the distribution function

$$F(X,t) = \left\{ \pi \sigma^2 \left[1 + \left(\frac{X-vt}{\sigma} \right)^2 \right] \right\}^{-1}, \quad (10)$$

where σ is analogous to the Gaussian standard deviation. Figure 4 shows a comparison of the eq. (10) function with the Gaussian function.

Thus, total, crosswind integrated activity fraction, $D(X)$, deposited at distance X along the windward, or hotline, axis is

$$D(X) = \int_0^{\infty} q(t) F(X,t) dt$$

or

$$D(X) = \frac{4 \sin \left[\frac{\pi}{2} (3-\alpha) \right]}{\pi^2 \Gamma(\alpha) (3-\alpha)} \int_0^{\infty} \frac{(1/t)^{\alpha} dt}{\left[1 + \left(\frac{1}{t} \right)^2 \right]^2 \left[1 + \left(\frac{X-vt}{\sigma} \right)^2 \right]} \quad (11)$$

A result is obtained in closed form provided we take $\alpha=1$ inside the integral. This result is

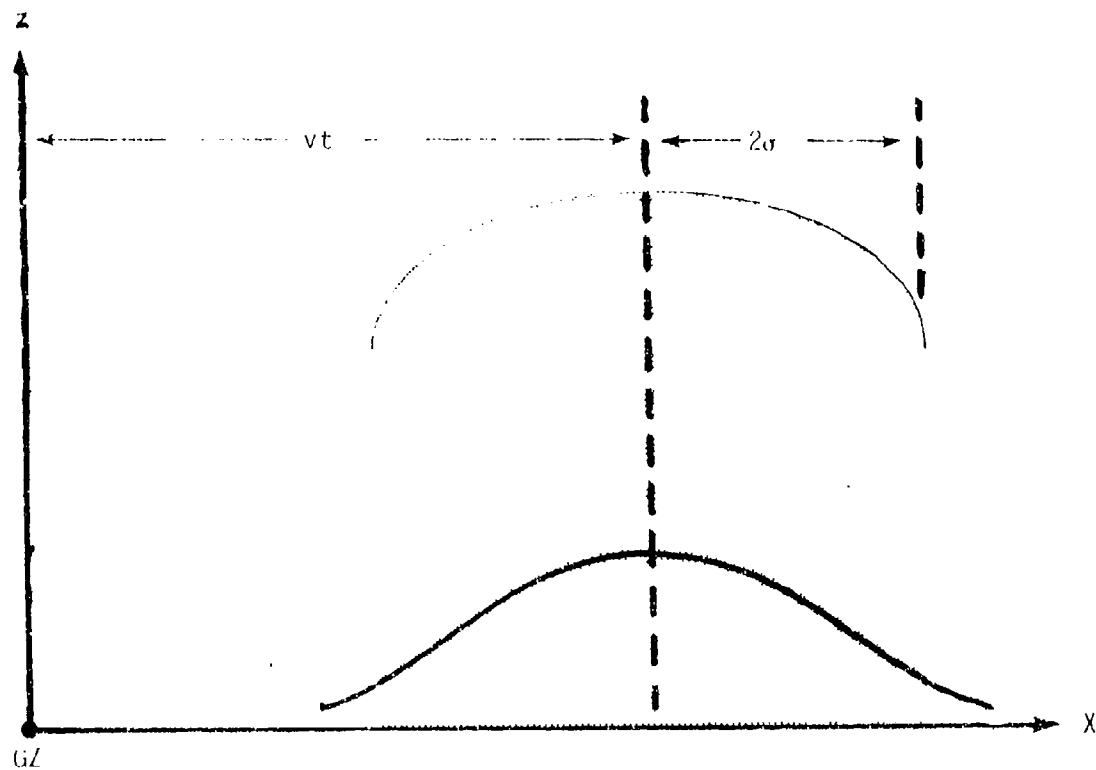


Figure 3. Distribution of activity of depositing fallout in the hotline axis direction.

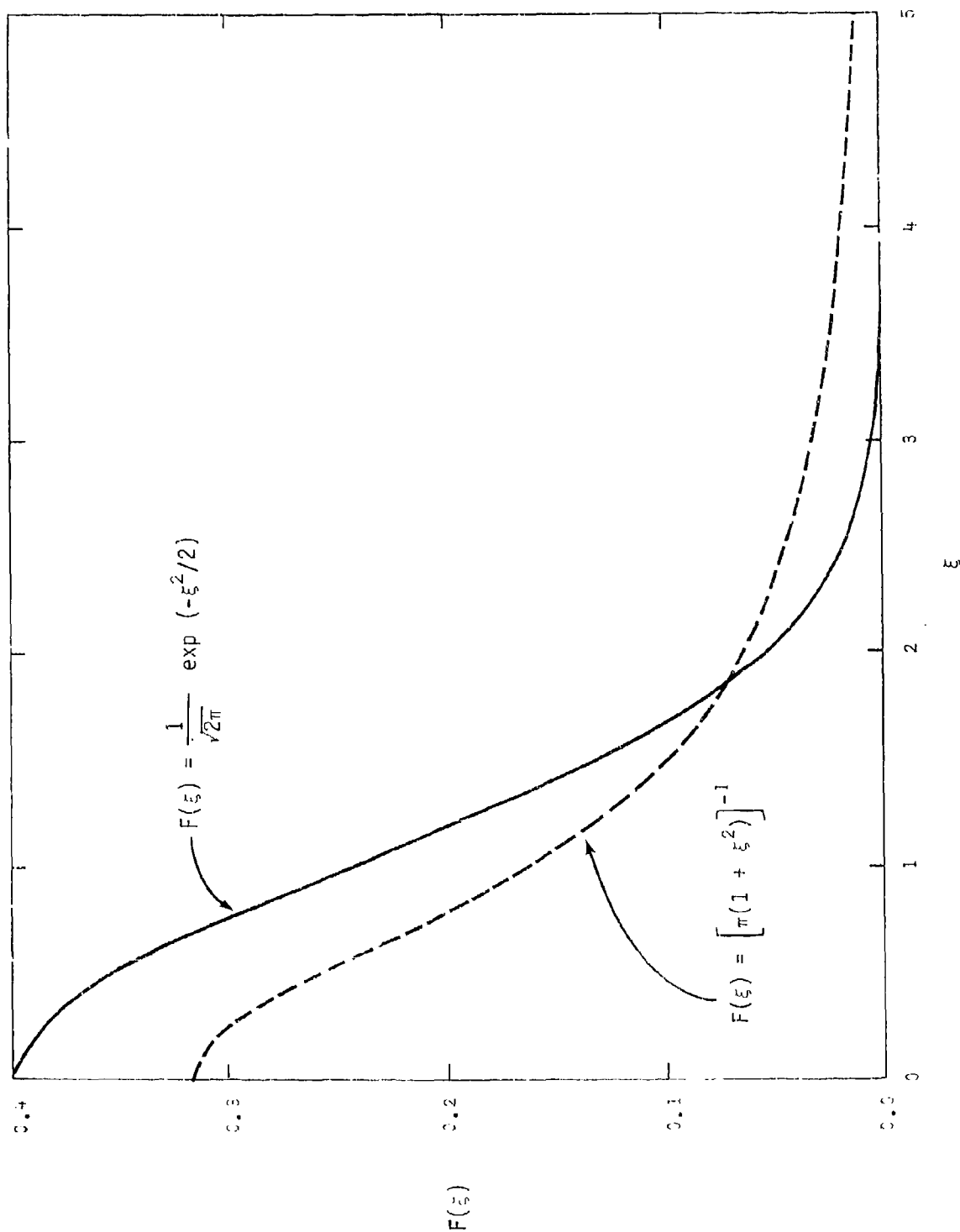


Figure 4. Comparison of Gaussian function with the function used in DNAF-1 to approximate the spatial distribution of cloud activity along the hotline axis.

$$\begin{aligned}
D(X) \sim \frac{2\sigma \sin [\pi(3-\alpha)/2]}{\pi^2 X_4^8 (3-\alpha)} \left\{ -\pi X X_1 \left[(3X_2^2 + X_1^2) X_3^2 + 4X^2 X_1^2 \right] \right. \\
- (X_3^4 + 4X^2 X_1^2) X_3^2 + (X_2^2 X_3^4 - 4X^2 X_1^4) \ln \left(\frac{X_2^2}{X_1^2} \right) \\
\left. + \frac{X}{\sigma} \left[(X_2^2 + 3X_1^2) X_2^2 X_3^2 + 4X^2 X_1^4 \right] \left[\pi + 2 \tan^{-1} \left(\frac{X}{\sigma} \right) \right] \right\} \quad (12a)
\end{aligned}$$

where

$$\begin{aligned}
X_1 &= vT \\
X_2^2 &= X^2 + \sigma^2 \\
X_3^2 &= X_2^2 - X_1^2 \\
X_4^8 &= (X_3^4 + 8X^2 X_1^2) X_3^4 + 16X^4 X_1^4,
\end{aligned}$$

and $D(X)$ has units m^{-1} .

This is the basic equation for the DNAF-1 model. In the computer code (function DNAF1), an alternative form of eq. (12a) is also used, which is required because of limitations of some computers

$$\begin{aligned}
D(X) \sim \frac{2\sigma \sin [\pi(3-\alpha)/2]}{\pi^2 X_5^4 (3-\alpha)} \left\{ -\pi X X_1 \left[(3X_2^2 + X_1^2)/X_3^2 + 4X^2 X_1^2/X_3^4 \right] \right. \\
- X_3^2 \left(1 + 4X^2 X_1^2/X_3^4 \right) + (X_2^2 - 4X^2 X_1^4/X_3^4) \ln \left(\frac{X_2^2}{X_1^2} \right) \\
\left. + \frac{X}{\sigma} \left[X_2^2 (X_2^2 + 3X_1^2)/X_3^2 + 4X^2 X_1^4/X_3^4 \right] \left[\pi + 2 \tan^{-1} \left(\frac{X}{\sigma} \right) \right] \right\} ; |X_3^2| \geq 1. \quad (12b)
\end{aligned}$$

where

$$X_5^4 = X_3^4 + 8X^2 X_1^2 + 16X^4 X_1^4/X_3^4$$

Thus eq. (12a) is used for small values of $|X_3|$ and eq. (12b) for large values.

Negative values of X (i.e., upwind distances) are accommodated as well as positive values in eqs. (12a) and (12b).

For a point cloud, defined by $\sigma = 0$, eq. (12) reduces to

$$D(X)_{\sigma=0} = \frac{4 \sin[\pi(3-\alpha)/2]}{\pi(3-\alpha)} \frac{X^3}{(X^2 + X_1^2)^2} ; X \geq 0 \quad (13)$$

which, on substitution of $X = vt$, becomes

$$vD(vt)_{\sigma=0} = \frac{4 \sin[\pi(3-\alpha)/2]}{\pi(3-\alpha)} \frac{t^3}{(t^2 + T^2)^2} \quad (14)$$

The right hand side of eq. (14) is equivalent to eq. (6) with $(T/t)^\alpha$ replaced by T/t .^{*} Thus, provided that α is not much different from unity, eqs. (13) or (14) may be used instead of eq. (6) to represent activity deposition rate as a function of either distance from ground zero or time for a point cloud. These equations are used below for the development of the farfield correction.

3.3 FARFIELD CORRECTION

As already noted, the eq. (6) function for deposition rate fits the DELFIC results adequately at early and intermediate times, but at late times (which correspond to farfield deposition) the DELFIC results drop off much more rapidly. Moreover, this discrepancy becomes more acute as yield increases. Indeed, as inspection of eq. (14) shows, $g(t) \propto 1/t$; $t \rightarrow \infty$, whereas the DELFIC results for large time are proportional to $\exp[-(t/\tau)^n]$, $n=1$ or 2 and τ constant.

A correction to the functions for $g(t)$ and $D(X)$ which have general applicability, but are effective only for late times and correspondingly large X are as follows. As shown at the end of the last section,

^{*}Recall that α was taken to be unity inside the integral in eq. (11).

$D(X)_{\sigma=0}$, (i.e., downwind deposition for a point cloud) is equivalent to $g(t)/v$. It also turns out that $D(vt)_{\sigma \neq 0} = g(t)/v$ for large t . Thus, we can derive a correction factor for the $g(t)$ function for large t , which will also apply to the $D(X)$ function for large X , where X and t are related by $X = vt$.

The correction factor is derived by means of an exponential interpolation, $1 - \exp[-X/(avt_c)]$, between the functions $\ln\{D(X)\}$ and $\ln\left\{\frac{k}{v} \exp\left[-\left(\frac{X}{vt_c}\right)^2\right]\right\}$, where a is constant and t_c , k and v are functions of yield. The farfield corrected $D(X)$, $D(X)_f$ (m^{-1}), is

$$D(X)_f = D(X) \exp \left\{ - \left[\ln(vD(X)/k) + \left(\frac{X}{vt_c}\right)^2 \right] \left[1 - \exp \left\{ -X/(avt_c) \right\} \right] \right\} ;$$

$$X \geq 0 \quad (15)$$

where $D(X)$ is computed by eq. (12a) or (12b), and

$$\begin{aligned} a &= 1.443 \\ k &= 9.867 \times 10^{-4} W^{-0.26045} \quad (s^{-1}) \\ T &= 8160 W^{0.2463} \quad (s) \\ t_c &= 14667 W^{0.26208} \quad (s); \quad W \leq 98.787 \text{ KT} \\ t_c &= \exp \left[10.124706 + 0.1861768 \ln W \right. \\ &\quad \left. - 0.008660444 (\ln W)^2 \right] \quad (s); \quad W > 98.787 \text{ KT} \end{aligned} \quad (16)$$

Figure 5 shows the function $g(t)_f$ (actually $vD(vt)_f$, $\sigma=0$, see eq. 14)) for every other decade of yield along with a sampling of the DELFIC results and the corresponding quantity for the WSEG-10 model.

The WSEG-10 model uses the deposition rate function

$$g(t)_{\text{WSEG-10}} = \frac{1}{T' \Gamma(1+1/n)} \exp \left[- (t/T')^n \right] \quad (17)$$

where Γ is the gamma function, T' is a yield dependent constant and n has a value between 1 and 2. In calculating the results shown in Figure 5, we have used $n = 1.5$. Notice in Figure 5 that the WSEG-10 function

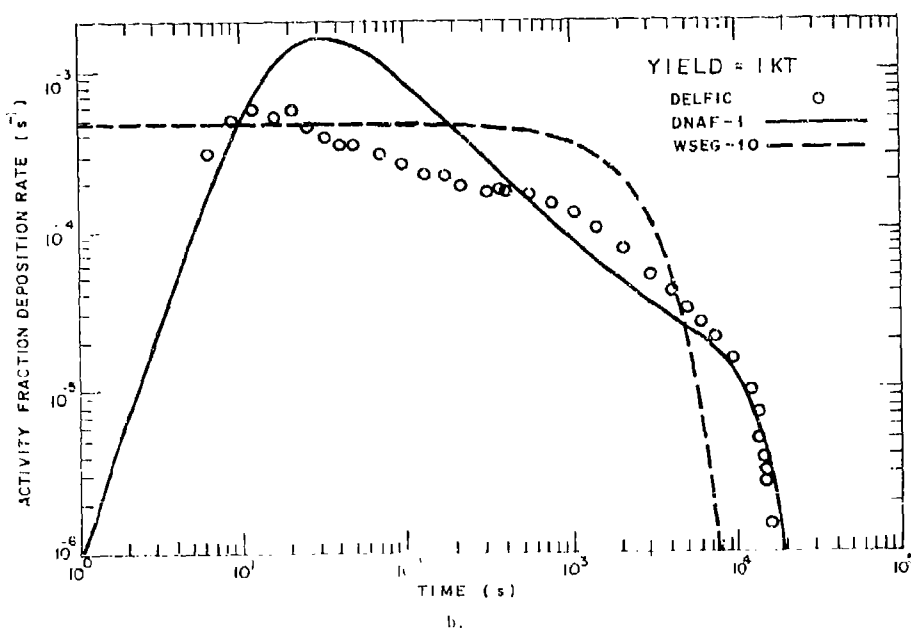
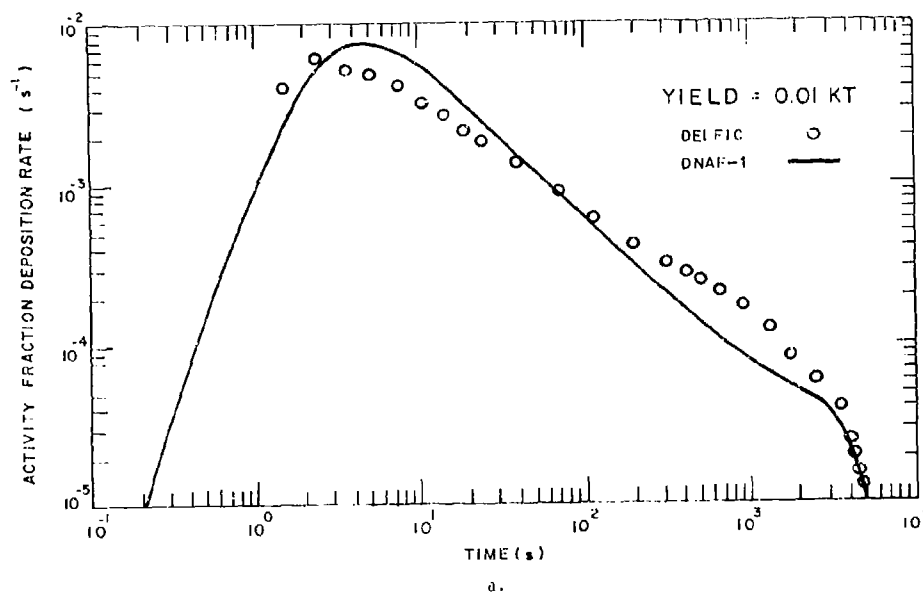


Figure 5. Activity deposition rate, $q(t)_f$, including farfield correction, vs. time. A sampling of DEL FIC results are included for comparison.

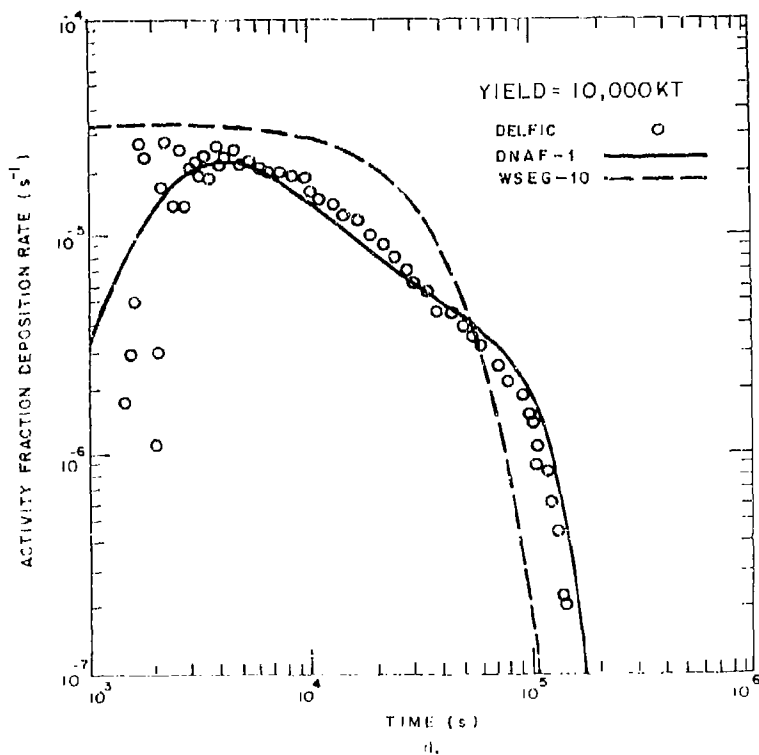
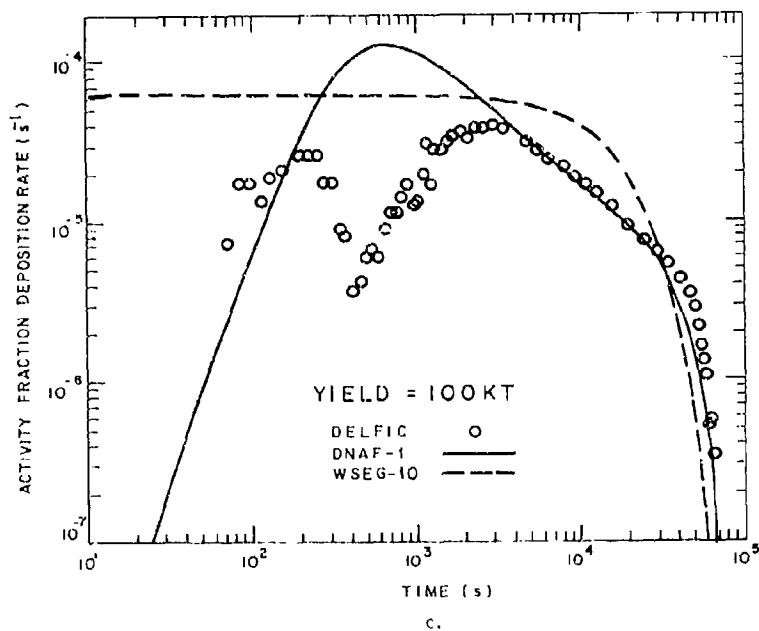


Figure 5. Activity deposition rate, $q(t)$, including farfield correction, vs. time. A sampling of DELFIC results are included for comparison. (continued)

matches the DELFIC deposition rate data only in the farfield region, and that instead of going to zero at $t = 0$, it actually peaks there. Also note that the WSEG-10 curve fit probably is adequate for very high yields, but is very poor for low yields.

3.4 UPWIND CORRECTION

In comparing calculated fallout patterns with observed patterns for low yield test shots, it was found that the calculated activities decreased too slowly with upwind distance from ground zero. Analysis of the discrepancies indicated a correction factor that is independent of both yield and wind speed for yields less than 10KT.*

For high yield shots there is little credible upwind fallout data to serve as a guide. However, a correction was developed that is reasonably consistent with data available for shots Koon, Zuni and Bravo, and that provides a continuous transition to the low yield correction at $W = 10$ KT.

As with the farfield correction, an exponential interpolation in $\log(D) - \log(X)$ space is used to compute the upwind-corrected activity deposited, $D(X)_u$, which is given by

$$D(X)_u = D(X) \exp \left\{ bX \left[1.0 - \exp(X/c) \right] \right\} ; \quad X < 0 \quad (18)$$

where $D(X)$ is calculated by eqs. (12a) or (12b), and

$$\begin{aligned} b &= 0.0176 \\ c &= 570 & W \leq 10 \text{ KT} \\ b &= 0.08045W^{-0.66} \\ c &= -8179.82 + 3800 \ln W & W > 10 \text{ KT} \end{aligned} \quad (19)$$

*Though one would guess that this correction should be a function of wind speed, there is not enough variation of v among the cases available to allow for a quantitative evaluation of the dependence.

3.5 FALLOUT TIME OF ARRIVAL

An estimate of fallout time of arrival as a function of distance from ground zero is required for computation of maximum effective biological dose and turbulent and wind shear dispersion of the nuclear cloud during atmospheric transport. By time of arrival we mean the time of deposition of the first fallout at distance X from ground zero along the hotline.

Time of arrival, t_a , is estimated by means of the following simple model. The first fallout to touch ground anywhere does so at onset time t_0 (eq. (1)) in the form of a horizontally distributed parcel centered at $X = vt_0$. We take the radius of this parcel to be that of the early cloud, R_i (eq. (2)). Thus, for any point with coordinate $X \leq vt_0 + R_i$, we take $t_a = t_0$. For $X > vt_0 + R_i$, we take $t_a = t_0 + (X - vt_0 - R_i)/v$. The geometry is shown in Figure 6a.

Figure 6b shows that the plot of t_a vs X consists of two straight lines that intersect at point $(t_0, vt_0 + R_i)$. We desire a smooth transition between the two curves rather than the discontinuous transition shown. This is achieved by replacing the straight lines with a hyperbola that is asymptotic to both lines and has its center at the intersection point of the lines. Thus t_a (s) is calculated from the equation

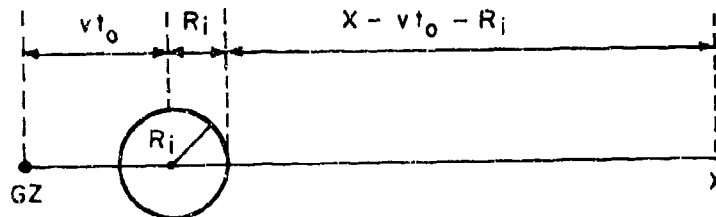
$$t_a = t_0 + \frac{1}{2} \left[\frac{X}{v} - t_0 - \frac{R_i}{v} + \sqrt{\left(\frac{X}{v} - t_0 - \frac{R_i}{v} \right)^2 + \left(t_0 + \frac{R_i}{v} \right)^2 / 100} \right];$$

$$v \geq 0.01 \text{ m s}^{-1} \quad (20)$$

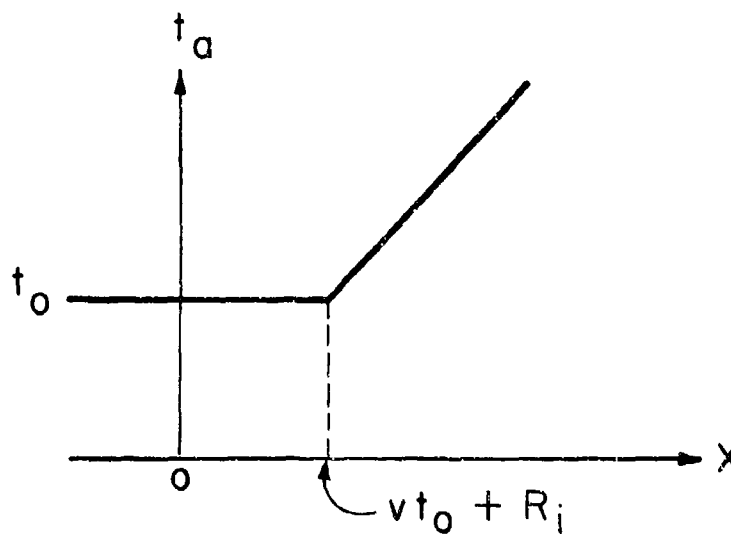
Figure 7 shows plots of t_a vs X for an effective fallout wind speed of 10 m s^{-1} at several different yields. WSEG-10 results also are shown. Since according to WSEG-10 the minimum t_a is 30 minutes, we see that for low yield shots WSEG-10 grossly overestimates t_a , and hence correspondingly underestimates maximum effective biological dose (eq. (32)).

3.6 HORIZONTAL SPREAD OF THE NUCLEAR CLOUD

In this section we consider horizontal spread of the nuclear cloud before we account for dispersing effects of atmospheric turbulence and wind



a. Geometry of the time-of-arrival model.



b. Representative plot of t_a vs X .

Figure 6. Basis of the time-of-arrival calculation.

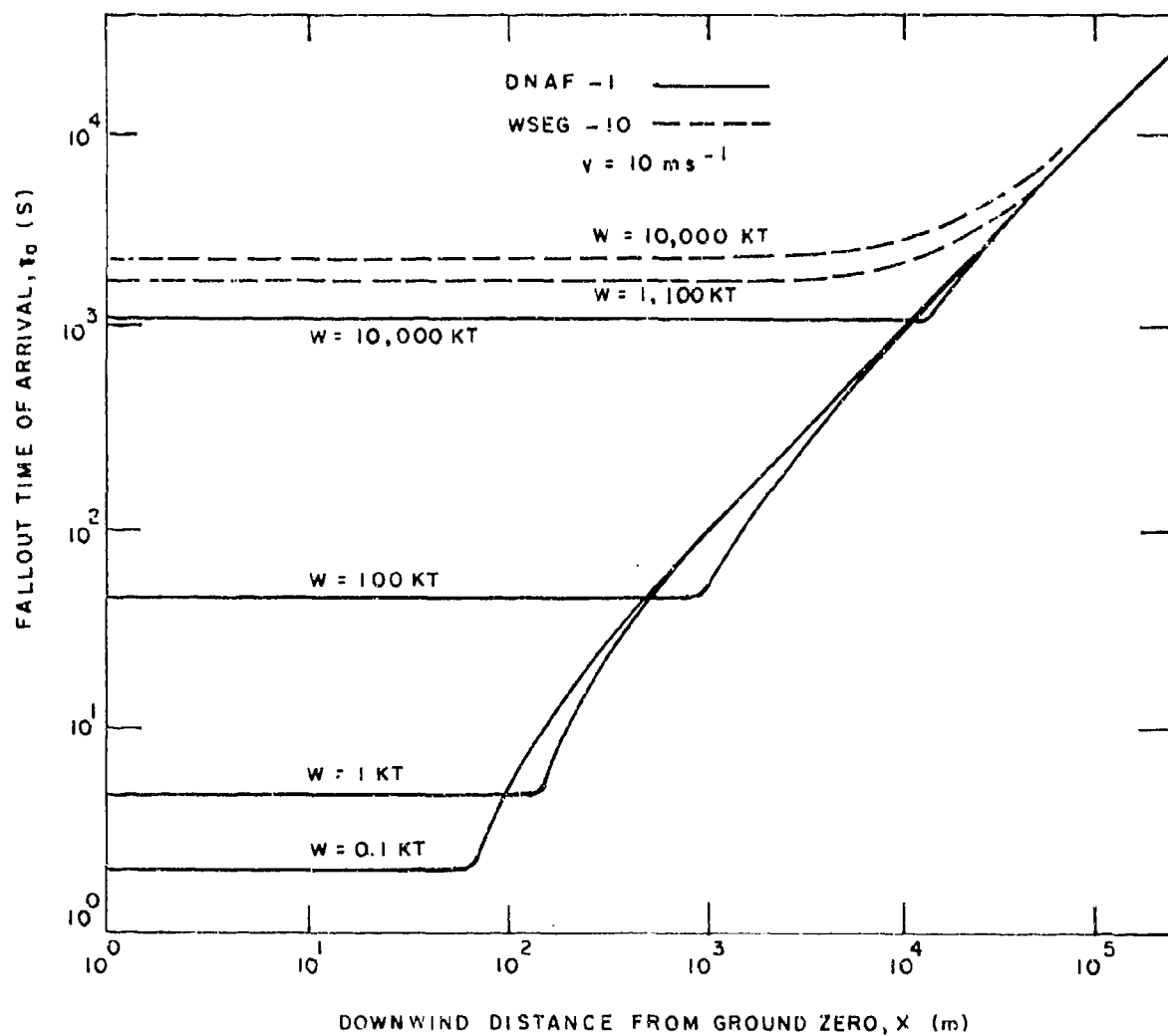


Figure 7. Fallout time of arrival vs. distance from ground zero for several yields as computed by DNAF-1 and WSEG-10.

shear. Vertical cloud structure is included implicitly. We have shown elsewhere^{6,7} that close-in fallout patterns from surface bursts of yields less than roughly 50 KT are dominated by fallout from the cloud stem. Thus, for a low yield shot we cannot make the conventional assumption that close-in fallout comes from the cloud cap, nor that it begins its atmospheric transport with a horizontal spread derived from the stabilized cloud radius. Accordingly, in the following analysis we differentiate between stem and cap fallout.

Three critical times are involved here:

t_o fallout onset time (eq. (1))

t_a fallout arrival time (eq. (20))

t_B time of ground impact of a nominal particle which begins its descent at the stabilized cloud base, z_B .

Time t_B (s) is approximated by use of a simple relation between settling speed of water drops and altitude¹², which for this purpose is found to apply well enough to fallout particles. The settling speed of a particle at altitude z , $f(z)$, is

$$f(z) = f(o)e^{\zeta z} \quad (21)$$

where $\zeta = 2.90 \times 10^{-5} \text{ m}^{-1}$ and from Table 1, $f(o) = 1.6538 \text{ (m s}^{-1}\text{)}$ for our nominal particle. Thus,

$$t_B = - \int_{z_B}^0 dz/f(z) = \left(1 - e^{-\zeta z_B}\right) / \left(\zeta f(o)\right) \quad (22)$$

where z_B is given by eq. (3).

Horizontal dimension of the cloud prior to atmospheric transport is specified in terms of the standard deviation of its spread, σ_c (m). Define a yield dependent parameter, σ_w , as

$$\sigma_w = R_i \quad ; W \leq 10 \text{ KT} \quad (23a)$$

$$\begin{aligned} \sigma_w &= R_i + (2.5R_i - R_i)(\log_{10}W - 1)/2 \\ &= R_i(1 + 3\log_{10}W)/4; 10 < W < 1000 \text{ KT} \end{aligned} \quad (23b)$$

$$\sigma_w = 2.5 R_i \quad ; W \geq 1000 \text{ KT}, \quad (23c)$$

where R_i is given by eq. (2). Then upwind and in the region of ground zero we have

$$\sigma_c = \sigma_w \quad ; X \leq vt_o. \quad (24)$$

For fallout from the stem we have

$$\sigma_c = \sigma_w + \left(\frac{t_a - t_o}{t_B - t_o} \right) \left(\frac{R_s}{2} - \sigma_w \right) ; X > vt_o \text{ and } t_a < t_B \quad (25)$$

and for fallout from the cap we have

$$\sigma_c = R_s/2; \quad t_a \geq t_B \quad (26)$$

where R_s is given by eq. (5).

Equations (24) and (23a) express the fact that onset of fallout from low yield shots is early enough that the upwind and ground zero area fallout has essentially the spread of the late fireball. Equations (24) and (23c) account for the fact that the debris from high yield shots is carried aloft rapidly, which causes the earliest fallout to traverse a substantial vertical path and thus experience substantial horizontal dispersion. Equation (23b) is simply a linear interpolation in $\log_{10}(W)$ between eqs. (23a) and (23c).

Equation (26) sets the standard deviation of horizontal spread of fallout in the stabilized cloud cap at one half of the stabilized cloud radius, and eq. (25) provides for stem fallout via a linear interpolation in altitude (in terms of arrival time) between the base and top of the stem.

3.7 TURBULENT DISPERSION OF FALLOUT

During transport from its initial location in the stabilized cloud to the ground, fallout is acted upon by the ambient atmospheric turbulence such as to produce additional dispersion. To calculate this effect, we use the scale dependent equations of Walton¹³ which require specification of turbulence level in terms of a quantity called turbulent energy density dissipation rate, ϵ . Of course, ϵ will depend on local conditions in the atmosphere, but Wilkins¹⁴ has found that ϵ can be approximated, with surprisingly consistent accuracy, by a simple reciprocal function of altitude. Thus, the variance of the horizontal spread of fallout at ground level, σ^2 (m²), not including crosswind dispersion owing to wind shear, is given by

$$\sigma^2 = \left(\sigma_c^{2/3} + \frac{2}{3} \langle \epsilon \rangle^{1/3} t_a \right)^3 \quad ; \quad \sigma^2 \leq 10^9 \text{ m}^2 \quad (27a)^*$$

$$\sigma^2 = 10^6 \left(3\sigma_c^{2/3} + 2 \langle \epsilon \rangle^{1/3} t_a - 2000 \right) \quad ; \quad \sigma^2 > 10^9 \text{ m}^2 \quad (27b)^*$$

where t_a is given by eq. (20) and σ_c is calculated as described in the preceding section.

Wilkins' relation for ϵ is $\epsilon \approx 0.03/z$, and we have taken for our average value, $\langle \epsilon \rangle = 0.03/z_B$. Using a power function in W relation for z_B which is approximately valid over the entire yield range¹⁵, we obtain

$$\frac{2}{3} \langle \epsilon \rangle^{1/3} = 0.016522 W^{-0.10233} \quad ; \quad W \text{ in KT.}$$

The value of t_a at which $\sigma^2 = 10^9 \text{ m}^2$ is given by

$$(t_a)_\ell = \left(10^3 - \sigma_c^{2/3} \right) / \left(\frac{2}{3} \langle \epsilon \rangle^{1/3} \right) .$$

*See ref. 1, sec. 3.3 for a more complete presentation of these equations.

Thus if $t_a \leq (t_a)_L$, use eq. (27a); otherwise use eq. (27b).

The value of σ calculated by one of eqs. (27) is used in one of eqs. (12) to calculate crosswind integrated fraction of activity deposited at hotline distance X from ground zero.

At this point in the presentation we have discussed how to determine all of the quantities needed to calculate $D(X)$ via one of eqs. (12a) or (12b). Figure 8 shows plots of $D(X)$, including upwind and farfield corrections, at every other decade of yield for an effective fallout wind of 10 m s^{-1} . WSEG-10 results also are shown for comparison.

The most obvious difference between the DNAF-1 and WSEG-10 predictions is the much sharper peak downwind of ground zero (GZ) predicted by DNAF-1. For the higher yields this peak falls off more rapidly toward GZ, according to DNAF-1, such that the DNAF-1 GZ activity is substantially less than predicted by WSEG-10. The farfield activity curves have nearly the same shape, as expected, though they are significantly displaced, except for 10^4 KT for which case they are essentially coincident. Upwind, the curves have similar shapes, though again the displacements are significant. Shapes and displacements at near and intermediate downwind distances are significantly different.

3.8 WIND SHEAR DISPERSION AND CROSSWIND SPREAD OF THE FALLOUT PATTERN

Following in principle, but not in detail, the procedure of Pugh and Galiano⁴, we account for the effect of vertical wind shear on crosswind dispersion variance by an added variance increment, σ_s^2 (m^2), given by

$$\sigma_s^2 = \left[S_Y(z_T - z_B)t_a/10 \right]^2 \quad (28)$$

Here S_Y is an approximation to the crosswind component of vertical wind shear, determined as described in section 4.3, and the other quantities are as defined by eqs. (3), (4) and (20). In addition to being a very rough approximation, this equation is somewhat arbitrary in that some height difference other than $z_T - z_B$ could have been used. The divisor 10 was

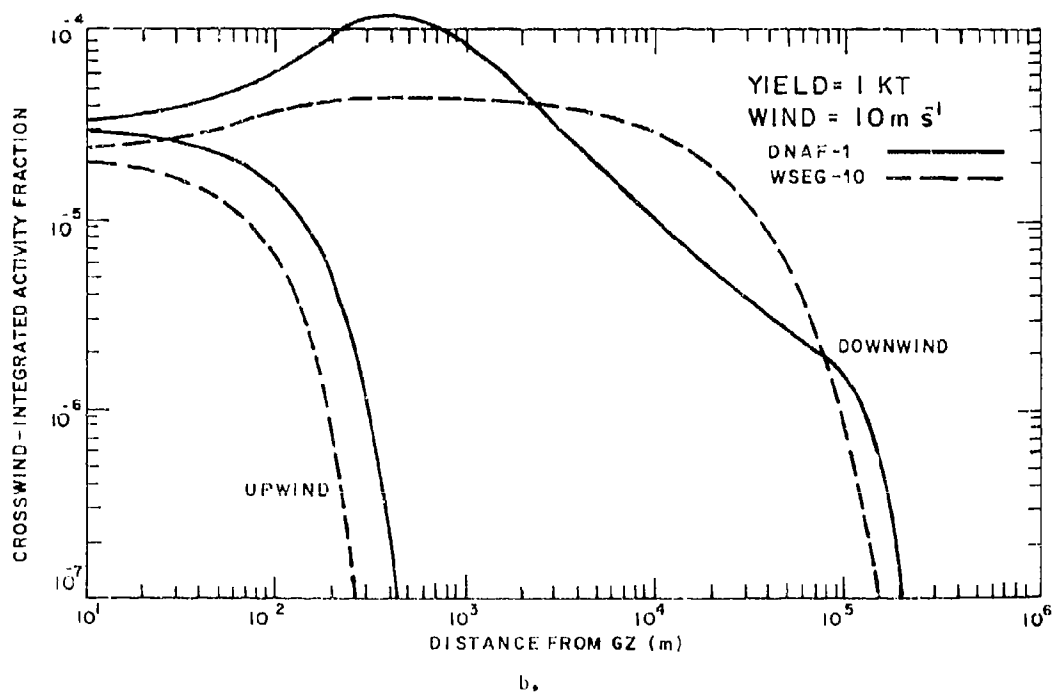
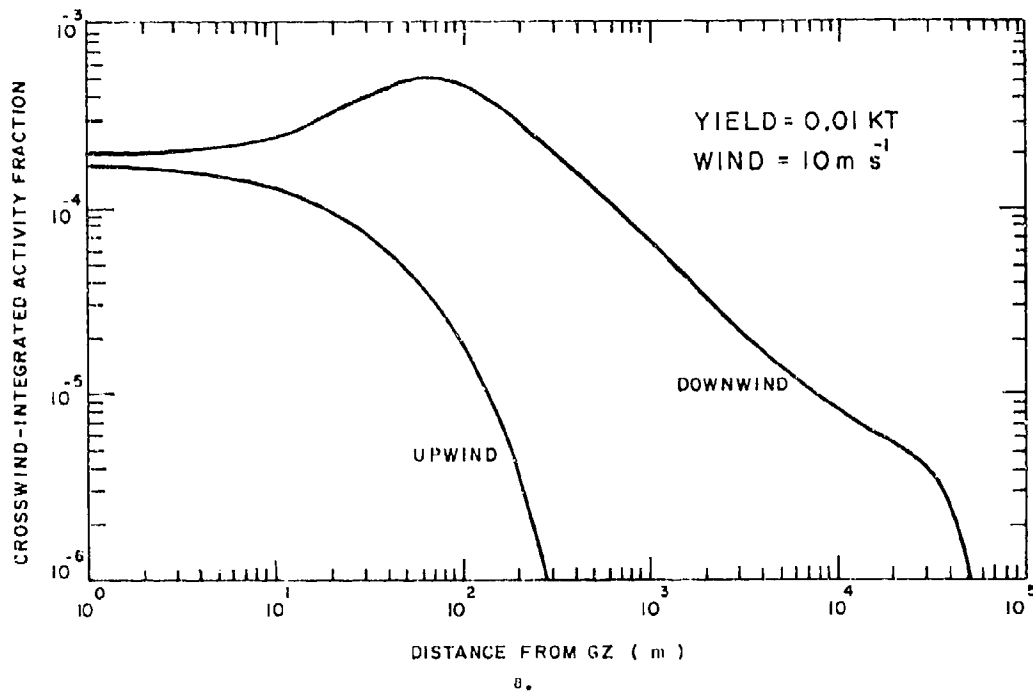


Figure 8. Crosswind-integrated activity fraction, $D(X)_F$ and $D(X)_U$, vs. distance from ground zero along the hotline.

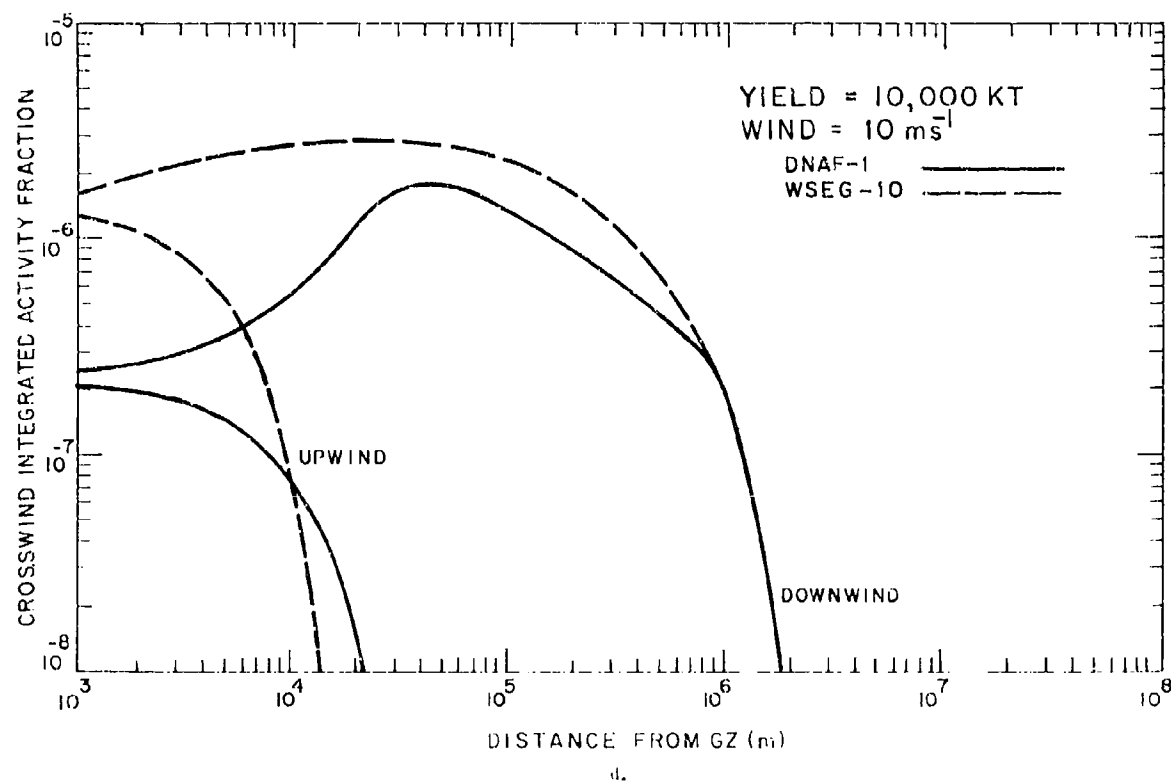
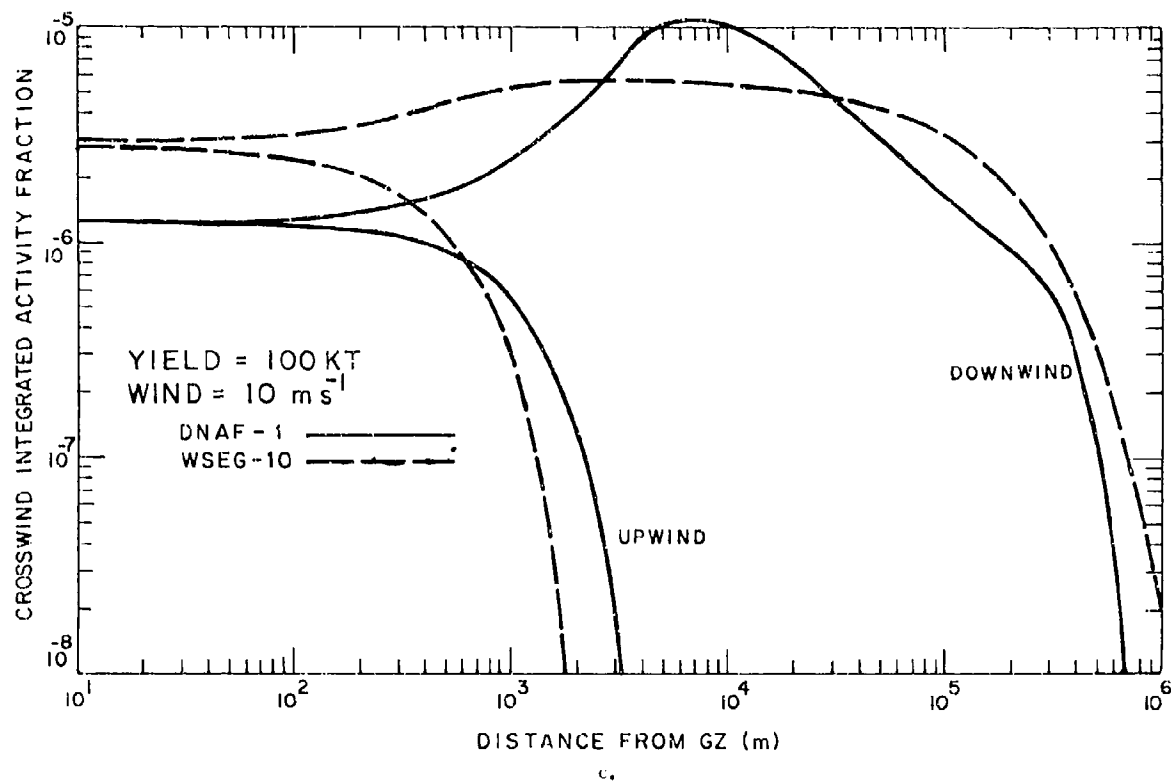


Figure B. Crosswind-integrated activity fraction, $D(X)_f$ and $D(X)_u$, vs. distance from ground zero along the hotline. (continued)

chosen by numerical experimentation to give good comparisons between observed and calculated test shot fallout patterns.

Crosswind (i.e., Y axis) dispersion of the fallout pattern is provided by multiplication of eqs. (15) and (18) by a Gaussian function

$$G(Y) = \frac{1}{\sqrt{2\pi}\sigma_Y} \exp \left[-\frac{1}{2} \left(\frac{Y}{\sigma_Y} \right)^2 \right] \quad (29)$$

where

$$\sigma_Y^2 = \sigma^2 + \sigma_S^2, \quad (30)$$

and σ^2 and σ_S^2 are given by eqs. (27) and (28) (m^2).

3.9 GAMMA RAY EXPOSURE RATE AND MAXIMUM EFFECTIVE BIOLOGICAL DOSE

If we define, as usual, X to be the distance from ground zero along the direction of the effective fallout wind vector, positive in the downwind direction, and Y to be perpendicular distance to the X axis in the ground plane, then the H + 1 hour normalized* gamma ray exposure rate (Roentgens per hour) at a height of one meter above a point X, Y on the ground is

$$A(X,Y) = CKW_F G(Y) D(X)_{\eta} \quad (31)$$

where C is a scale factor (for example, see Appendix B), W_F is fission yield (KT), $K = 6.9733 \times 10^9$ (Roentgens - m^2)/(hr - KT)**, and $G(Y)$ is given by eq. (29). $D(X \geq 0)_{\eta=f}$ is given by eq. (15), while $D(X < 0)_{\eta=u}$ is given by eq. (18). Fallout maps are symmetrical across the X axis (i.e., $A(X,Y) = A(X,-Y)$).

*The "normalized" H + 1 hour exposure rate assumes that all fallout is deposited at H + 1 hour, regardless of whether this is actually the case or not.

**In the older, more familiar units, $K = 2692.4$ (Roentgens - mi^2)/(hr - KT)

To estimate radiation damage to people, in terms of short-term survivability for damage assessment/vulnerability analysis studies, a quantity here called "maximum effective biological dose" is conventionally used⁵. This quantity is designed to allow for effects of a continuing exposure of ever decreasing intensity, and to account for some coincident repair of radiation damage by the human body. Following a theory postulated by Blair¹⁶, Davidson¹⁷ assumes that 90 percent of total radiation injury is reparable, while the remaining 10 percent is irreparable. Further, he estimates that for humans the repair rate is about 0.1 percent per hour of the residual reparable injury. Taking fallout gamma radiation exposure rate to vary with time according to the usual $t^{-1.2}$ approximation¹⁸, Davidson derives an equation for the ratio of biological effective dose to $H + 1$ hour exposure rate that is a function of two variables: time of arrival of fallout (or time of entry into the fallout field), and time of exit from the fallout field. This equation has been evaluated numerically, and when plotted against exit time for specified t_a , the curve is found to have a maximum: the late-time falloff in effective biological dose being caused by combined effects of damage repair and decay of exposure rate intensity. The maximum in this curve gives the quantity called maximum effective biological dose, $M(X,Y)$, and if we assume that residence in the fallout field is from t_a to at least the time of the maximum, it is a function only of $A(X,Y)$ and t_a , where $A(X,Y)$ is a simple multiplier.

The numerical calculations necessary to define the ratio $M(X,Y)/A(X,Y)$ as a function of t_a have been done by the DoD Command and Control Technical Center and simple functions have been fitted to the results to give the following "quick approximation" equations:⁵

$$M(X,Y) = A(X,Y)(a_0 + a_1\beta + a_2\beta^2) \quad (32)$$

where

$$\begin{array}{lcl}
 \beta & = & 0.8685833 \ln(t_a) \\
 a_0 & = & 15.2891 \\
 a_1 & = & -2.903225 \\
 a_2 & = & 0.1662315 \\
 & & \left. \vphantom{\begin{array}{l} \beta \\ a_0 \\ a_1 \\ a_2 \end{array}} \right\} t_a < 1157.9 \text{ s} \\
 \\
 \beta & = & 2 \ln(t_a) \\
 a_0 & = & 4.6182 \\
 a_1 & = & -0.53587 \\
 a_2 & = & 0.016923 \\
 & & \left. \vphantom{\begin{array}{l} \beta \\ a_0 \\ a_1 \\ a_2 \end{array}} \right\} t_a \geq 1157.9 \text{ s.}
 \end{array}$$

As discussed in sections 3.1 and 3.2, a Gaussian dispersion function for deposited fallout is preferred for both the alongwind and crosswind directions. In this model a Gaussian crosswind function, $G(Y)$, is used, but the alongwind function, $F(X,t)$ (eq. (10)), is non-Gaussian. These functions are compared in Figure 4. A consequence of this inconsistency is that the fallout pattern is always asymmetric, even for zero wind, in which case all activity contours should be circles centered at ground zero. Specifically for $\vec{v} = 0$, eq. (31) becomes, if we omit the upwind and farfield corrections,

$$\Lambda(X,Y)_{\vec{v}=0} = KW_F \frac{\exp \left[-\frac{1}{2} \left(\frac{Y}{\sigma} \right)^2 \right]}{\sigma^2 \sqrt{2\pi}^3 \left[1 + \left(\frac{X}{\sigma} \right)^2 \right]},$$

which obviously cannot give circular contours for $\Lambda = \text{constant}$.

In practical terms this defect in the model is of little consequence. This is because a zero effective fallout wind is physically unacceptable. Indeed, it has been found that for other reasons (see sec. 4.2), the minimum acceptable value of v is about 0.5 m s^{-1} .

4. USE OF WIND DATA

4.1 GENERAL CONSIDERATIONS

Wind data are used to determine two essential model parameters: the effective fallout wind vector, \vec{V} , and the crosswind shear parameter, S_Y . Use of the magnitude of the effective fallout wind vector, v , is described throughout section 3, and use of S_Y is explained in section 3.8.

The code accepts wind data in two forms: either the user can specify \vec{V} and S_Y directly or he can supply a single vertical profile of wind vector data, in which case, the code computes \vec{V} and S_Y from these data. In this chapter we describe these computations.

4.2 EFFECTIVE FALLOUT WIND

The code accepts a single vertical profile of wind vectors, each vector representing the wind speed and direction at a specified altitude. As is described in detail in section 6.3, considerable flexibility is allowed in terms of form and format of the input data.

After some preprocessing (subroutine INWIND), the data are stored in tabular form. There are four tables which contain the following data: z_i , $U_{E,i}$, $U_{N,i}$ and $z_{b,i}$. Here z_i is the altitude (m above ground) at which wind vector components $U_{E,i}$, $U_{N,i}$ are defined*, i is the table entry (i.e., wind stratum) index ($i = 1, 2, \dots, I$), and $z_{b,i}$ is the base altitude (m above ground) of the i^{th} wind stratum defined as

$$z_{b,i} = \frac{1}{2} (z_{i-1} + z_i) \quad (33)$$

*Note that it is standard practice to measure surface wind at an elevation of 10 meters.

with $z_{b,1}=0$. $U_{E,i}$ is the wind component along the west-east axis, positive toward the east, and $U_{N,i}$ is the wind component along the south-north axis, positive toward the north ($m s^{-1}$).

Strictly speaking, altitude should be relative to mean sea level (MSL). However, in most cases MSL can be replaced by ground level (GL) without substantial error, and in practice this substitution will be implicit in most land surface burst predictions, as it is in the cases of the predictions of the Nevada Test Site shots discussed in section 5. The code provides for adjustment of altitudes to be relative to GL even though they may be input relative to some other origin.

Effective fallout wind is a weighted-average wind, the average being taken between the stabilized cloud cap center height and the surface, and the weighting being taken according to settling time of the nominal particle (sec. 2.4) through each wind stratum. The calculations are done in subroutine EFWIND.

Define \vec{U}_i to be the wind vector in the i^{th} stratum. Then the effective fallout wind is

$$\vec{v} = \frac{\sum_{i=1}^{J-1} \vec{U}_i (z_{b,i+1} - z_{b,i})/f(z_i) + \vec{U}_{z_J'} (z_c - z_{b,J})/f(z_J')}{\sum_{i=1}^{J-1} (z_{b,i+1} - z_{b,i})/f(z_i) + (z_c - z_{b,J})/f(z_J')} \quad (34)$$

where the summation begins at the ground, z_i and $z_{b,i}$ are as defined above, but

$$z_c = (z_T + z_B)/2$$

$$z_J' = (z_c + z_{b,J})/2 \quad ; \quad z_{b,J} \leq z_c$$

and \vec{U}_{z_j} is the wind vector at altitude z_j as determined by linear interpolation. $f(z)$ is the settling speed of the nominal particle at altitude z determined by linear interpolation in Table 1.

Actually, the code uses the magnitude of the effective fallout wind,

$$v = \sqrt{v_E^2 + v_N^2} \quad , \quad (35)$$

and the sine and cosine of its direction angle ϕ defined as

$$\begin{aligned} \sin \phi &= v_E / v \\ \cos \phi &= v_N / v \end{aligned} \quad (36)$$

where v_E and v_N are the easterly and northerly directed components of \vec{v} .

Theoretical and practical considerations impose a lower limit on the acceptable value of v . While occasionally a calm condition may be observed at the surface, this is never the case throughout the transport air space, and therefore a zero value for v is never acceptable. Very low values of v may cause certain unrealistic results to appear: for example, the upwind hotline activity may fall off less rapidly than the downwind activity.*

Accordingly, the code will not accept a value of v less than 0.5 m s^{-1} . An input value of $v = 0$ is used as a flag to signal input of a vertical profile of wind data. When the code encounters a value v less than 0.5 m s^{-1} (which is not interpreted as the value 0.0 used to signal input of the vertical profile) this value is printed along with a comment, and v is reset to 0.5 m s^{-1} .

*This anomalous behavior is caused by interaction of several features of the code. First, the horizontal variance of deposited fallout, σ^2 (secs. 3.6 and 3.7) is held constant upwind of ground zero, whereas it increases downwind. Second, the upwind correction (sec. 3.4) is, unfortunately, not a function of v , but was determined from test shot results for which v is always substantially greater than zero. Consequently, both of these features depend on use of realistically large values of v to give realistic results.

4.3 SHEAR PARAMETER

Vertical wind shear is defined as

$$\vec{S} = \frac{d\vec{U}}{dz}, \quad (37)$$

where \vec{U} is wind and z is the vertical coordinate. We make the customary assumption that advective transport will overwhelm effects of shear dispersion in the alongwind direction, and, therefore, we are interested only in the crosswind component of \vec{S} , S_Y .

In this model, S_Y is taken to be the root-mean-square value of the crosswind components of $\Delta\vec{U}/\Delta z$ computed at intervals of $\Delta z = (z_T - z_B)$ from the cloud top to the ground. The final Δz value is adjusted as required to avoid reaching below the ground.

In terms of the variables defined in the preceding section,

$$S_Y = \left[\frac{1}{K-T} \sum_{j=1}^{K-1} \left\{ \left[\sin\phi \left(U_{N,z_j} - U_{N,z_{j+1}} \right) - \cos\phi \left(U_{E,z_j} - U_{E,z_{j+1}} \right) \right] / \left(z_j - z_{j+1} \right) \right\}^2 \right]^{1/2} \quad (38)$$

Here the summation begins at the cloud top such that we have

$$z_j = z_T - (j-1)(z_T - z_B) \quad ; \quad j = 1, 2, \dots, K-1$$

and

$$z_K = 0.$$

Wind components for arbitrary z are determined by linear interpolation in the wind data tables. The calculations are done in function SYWIND.

5. VALIDATION

5.1 DISCUSSION OF RESULTS

Predictions are compared with observed H + 1 hour normalized* exposure rate maps for the first five test shots described in Table 2. For the sixth shot, Bravo, there are not enough observed data to construct a complete fallout map. Thus, for this case we compare our prediction against a special "reconstruction" calculation made by the Naval Radiological Defense Laboratory shortly after the event¹⁹.

Three methods of comparison of fallout patterns are used:

1. Visual comparison of contour maps.
2. Comparison of contour areas, and hotline lengths and azimuths.**

TABLE 2
TEST SHOT DATA

<u>Shot</u>	<u>Total Yield (KT)</u>	<u>Fission Yield (KT)</u>	<u>HOB (m)</u>	<u>Altitude of GZ (m)</u>	<u>Site</u>
Johnie Boy	0.5	0.5	-0.584	1570.6	NTS ⁺
Jangle-S	1.2	1.2	1.067	1284.7	NTS
Small Boy	low	-	3.048	938.2	NTS
Koon	150.	-	4.145	0.0	Bikini
Zuni	3380.	-	2.743	0.0	Bikini
Bravo	15000.	-	2.134	0.0	Bikini

⁺ Nevada Test Site

* A "normalized" exposure rate map is constructed on the assumption that all local fallout is down at the specified time, regardless of its actual deposition time.

** Hotline length is defined as the furthest distance from ground zero on a contour, and hotline azimuth is the angle, measured clockwise from north, to the point of furthest distance from ground zero on a contour.

3. The Rowland-Thompson Figure-of-Merit (FM)²⁰ which is a measure of contour overlap. (See Appendix C.)

These are roughly in order of importance.

Statistical data are in Table 3 and the contour plots are on pp. 58 through 80. Contours were drawn by a 30-inch Calcomp plotter, and each observed-predicted pair are to the same scale. Contour maps and statistical data are included for predictions by DELFIC and WSEG-10 as well as by DNAF-1.

Prediction accuracy is seen to be good. Perhaps the best quantitative measure of accuracy is provided by the mean absolute percent error, E, which for n observed-predicted data pairs is

$$E = \frac{100}{n} \sum_{i=1}^n |x_{\text{obs},i} - x_{\text{pred},i}| / x_{\text{obs},i} \quad .$$

Values of E for each prediction (excluding Bravo) by each of the three models are given under the solid lines in Table 3. The values in parentheses are computed with the data for the highest level contours excluded. The highest level contours are particularly difficult to predict since usually they are dominated by the region most affected by induced activity in the ground and throwout from the crater, neither of which are addressed by the fallout models. Overall mean absolute percent errors are given in Table 4. (Bravo prediction data are excluded.) As one might expect, DNAF-1 errors are intermediate between those of DELFIC, which are best, and WSEG-10, which are worst, though the differences between the DNAF-1 and DELFIC errors are less than between DNAF-1 and WSEG-10. Note that the most obvious problem with the WSEG-10 predictions is a tendency to overpredict the low level contours at the expense of the higher levels, to the extent that frequently the higher level contours are completely absent.

TABLE 3
COMPARISON OF OBSERVED AND PREDICTED FALLOUT PATTERN STATISTICS
Observed/DNAF-1/DIELFIC*/WSLG-10⁴

Test Shot	FM DNAF-1 DIELFIC WSLG-10	Contour (Roentgen hr ⁻¹)	Area (km ²)	HotLine Length (km)	Azimuth (deg.)
Johnie Boy	0.245	1000	0.278/0.038/0.029/----	1.38/0.38/0.037/----	359/351/ 0/---
	0.182	100	0.539/1.00 /0.77 /1.17	2.73/2.18/2.58 /3.7	345/351/344/344
	0.187	50	1.27 /1.90 /1.79 /4.57 74(68)/68(42)/159(188)**	4.10/3.21/4.13 /8.9 38(21)/28(3)/84(76)	343/351/343/344
Jangle-S	0.70	500	0.117/0.390/0.144/----	0.69/1.64/1.00 /----	347/ 15/353/---
	0.483	300	0.386/0.821/0.316/---	1.50/2.49/1.22 /----	346/ 15/354/ - -
	0.080	100	1.44 /2.64 /2.24 /0.55	3.74/4.97/5.87 /2.8	1/ 15/355/ 10
		35	3.11 /6.99 /5.08 /5.45 138(106)/40(46)/84(79)	5.06/9.07/7.68/10.2 79(59)/43(42)/82(76)	6/ 15/355/ 10
Small Boy †	0.582	1000	0.216/0.302/0.047	1.00/0.92/0.25	71/ 64/ 66
	0.308	500	0.528/0.703/0.135	1.62/1.49/0.56	73/ 64/ 80
	-----	200	0.942/1.75 /0.564	2.22/2.62/1.69	72/ 64/ 73
		100	3.75 /3.35 /1.10	5.66/3.90/3.72	72/ 64/ 74
		50	9.03 /6.45 /4.38 40(40)/63(59)	8.10/5.69/6.47 19(22)/44(36)	75/ 64/ 72
Koon	0.515	500	32.0 /55.9 /26.0 /5.7	10.2/14.8/12.5 /5.0	18/11.3/ 0/ 9
	0.287	250	122 /13.8 /8/ /70	17.3/22.7/24.2 /18.4	15/11.1/ 4/ 9
	0.340	100	550 /387 /261 /384 39(21)/33(41)/52(36)	41.0/39.8/39.5 /45.6 26(17)/22(22)/23(9)	17/11.3/ 3/ 9
Zuni	0.163	150	474 /537 /2239 /2659	98 /32 /78 /82	12/340/337/349
	0.105	100	2761 /1088 /3619 /4684	125 /44 /96 /110	17/340/337/349
	0.180	50	5187 /3055 /6660 /10760	138 /74 /121 /168	27/340/338/349
		30	10950/5791 /9913 /18200 43(53)/105(16)/168(70)	177 /103 /153 /216 55(51)/17(16)/18(19)	33/ 340/340/349
Bravo (NRMI)	0.054	3000	5373 /-----/188 /----	177 /----/31 /----	72/----/ 90/---
	0.069	2000	13520/122 /413 /219	198 /24 /43 /30	69/ 94/ 90/ 89
	0.070	1000	23660/1074 /1798 /2613	237 /46 /73 /121	78/ 94/ 90/ 89
		500	40480/4113 /5444 /9056	298 /103 /112 /259	75/ 94/ 90/ 89
		100	76320/41590/27550/41620	559 /445 /268 /597	90/ 94/ 92/ 89

*Data taken from reference 1.

†Data taken from reference 7

‡A comparable Small Boy prediction by WSLG-10 is not available.

**Mean absolute percent errors: DNAF-1/DIELFIC*/WSLG-10. The values in parentheses are calculated without including the data for the highest activity level contours. See p. 53.

TABLE 4
OVERALL MEAN ABSOLUTE PERCENT ERRORS*

	<u>Contour Area</u>	<u>Hotline Length</u>
DNAF-1	66(58)	43(35)
DELFIG	62(42)	32(26)
WSEG-10	117(90)	51(45)

The Figure-of-Merit (FM) results do not show a consistent order of capabilities for the models. This is typical of past experience as well, and we have concluded that in its present form, FM does not provide a very useful measure of prediction capability. Details are given in Appendix C.

5.2 DISCUSSION OF THE TEST SHOT DATA AND PREDICTIONS

The three low yield shots were executed at the Nevada Test Site, and their fallout patterns were measured over land. For this reason, observed patterns for these shots, though not highly accurate, may be considered to be superior to the patterns of the high yield shots which were executed on Bikini Atoll in the South Pacific. Not only are the fallout fields of the high yield shots very large, which adds to measurement problems, but most of the fallout from these shots fell into water. Even so, most of the Koon pattern area was covered by an array of fallout collection stations, so this pattern is probably reasonably accurate. Zuni, on the other hand, is a special case. The fallout pattern used here is exclusively downwind of the atoll and was determined by an oceanographic survey method that was known to be inaccurate. The close-in pattern in the region of the atoll is available, but contains no closed contours so it could not be used here; thus the high-activity portion of the observed pattern for this shot is ignored

*Values in parentheses are calculated with data for the highest level contours excluded.

and this alone must account for a substantial portion of the disagreement between observation and prediction for this shot, particularly with regard to contour areas and contour overlap (Table 3). As already mentioned, we have no observed pattern for the Bravo shot. In addition, we have the following problem.

DNAF-1 and DELFIC predictions for the high yield shots are expected to be inferior to those for the low yield shots. This is because the high yield shots were detonated over coral soil, and in the cases of Zuni and Bravo, large but uncertain amounts of sea water were lifted by the clouds. The particle size distribution used for these predictions is typical of fallout produced from the siliceous soil found at the Nevada Test Site. We have not succeeded in developing a distribution appropriate for coral and coral-sea water mixtures.

DNAF-1 predictions were made using the H hour winds tabulated in reference 7. DELFIC predictions were made using all of the reference 7 wind profiles, from H hour onward in time. WSEG-10 calculations were done using \vec{V} and S_y values supplied by the DoD Command and Control Technical Center as determined by them from the H hour wind profiles; these data also are tabulated in reference 7 (Appendix A.3). For shots Small Boy and Bravo, the published wind data have been found to be not pertinent to transport of the nuclear clouds. For both of these cases, we have used reconstructed wind data: for Small Boy the reconstruction is described in Appendix B of reference 7, and for Bravo we have used the winds developed by Dean and Olmstead. Values of \vec{V} , ϕ and S_y computed for the DNAF-1 predictions are given in Table 5.

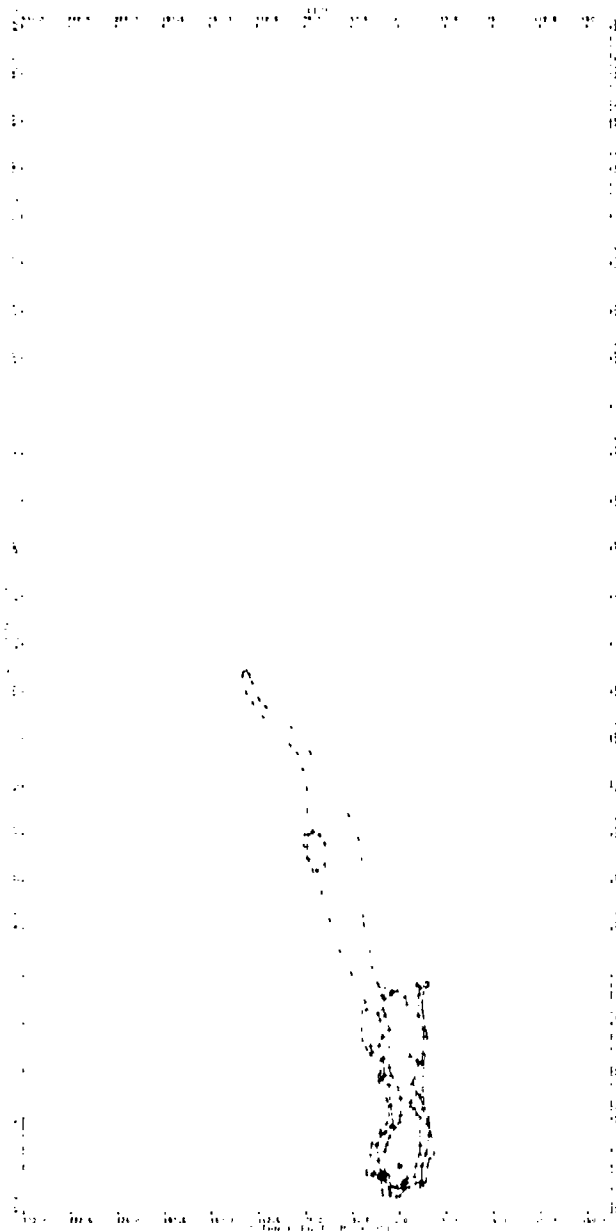
TABLE 5
EFFECTIVE FALLOUT WINDS AND SHEAR PARAMETERS
COMPUTED FROM H HOUR WIND PROFILES FOR USE BY DNAF-1

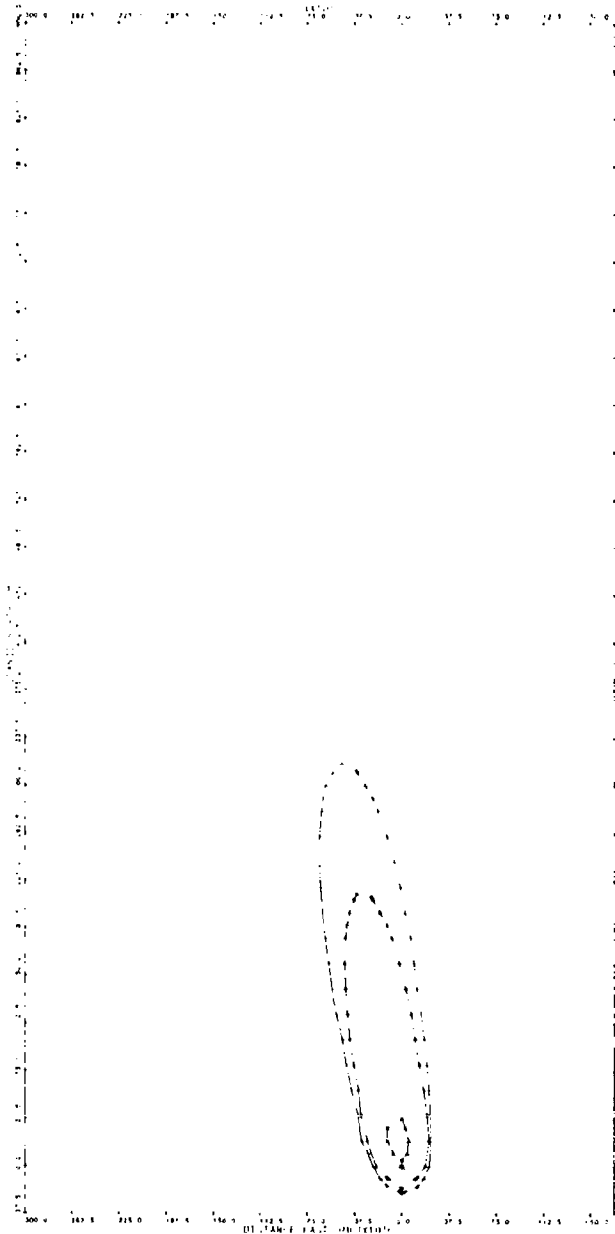
<u>Test Shot</u>	<u>V (m s⁻¹)</u>	<u>ϕ (deg.)</u>	<u>S_{Y1} (s⁻¹)</u>
Johnie Boy	6.0	- 8.6	0.00323
Jangle-S	13.1	14.6	0.00311
Small Boy	3.8	64.0	0.00066
Koon	6.2	11.3	0.00133
Zuni	4.9	-20.0	0.00225
Bravo	5.8	93.6	0.00044

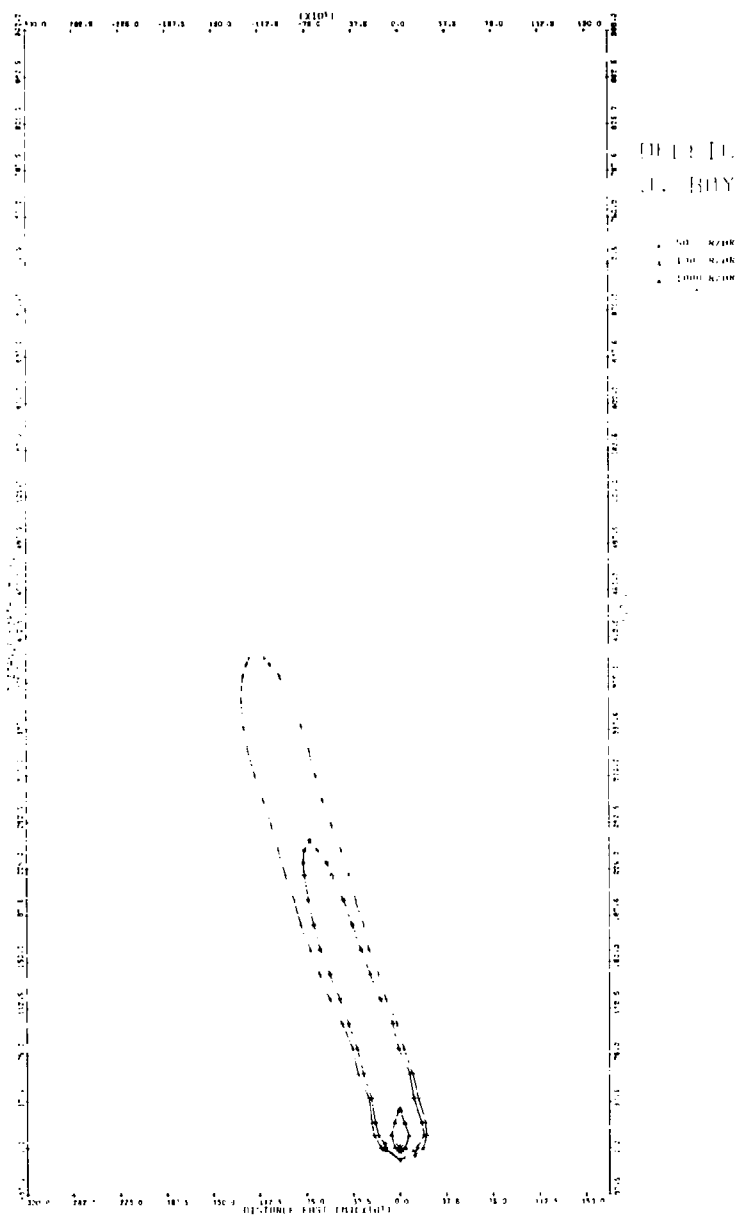
5.3 OBSERVED AND PREDICTED FALLOUT PATTERNS

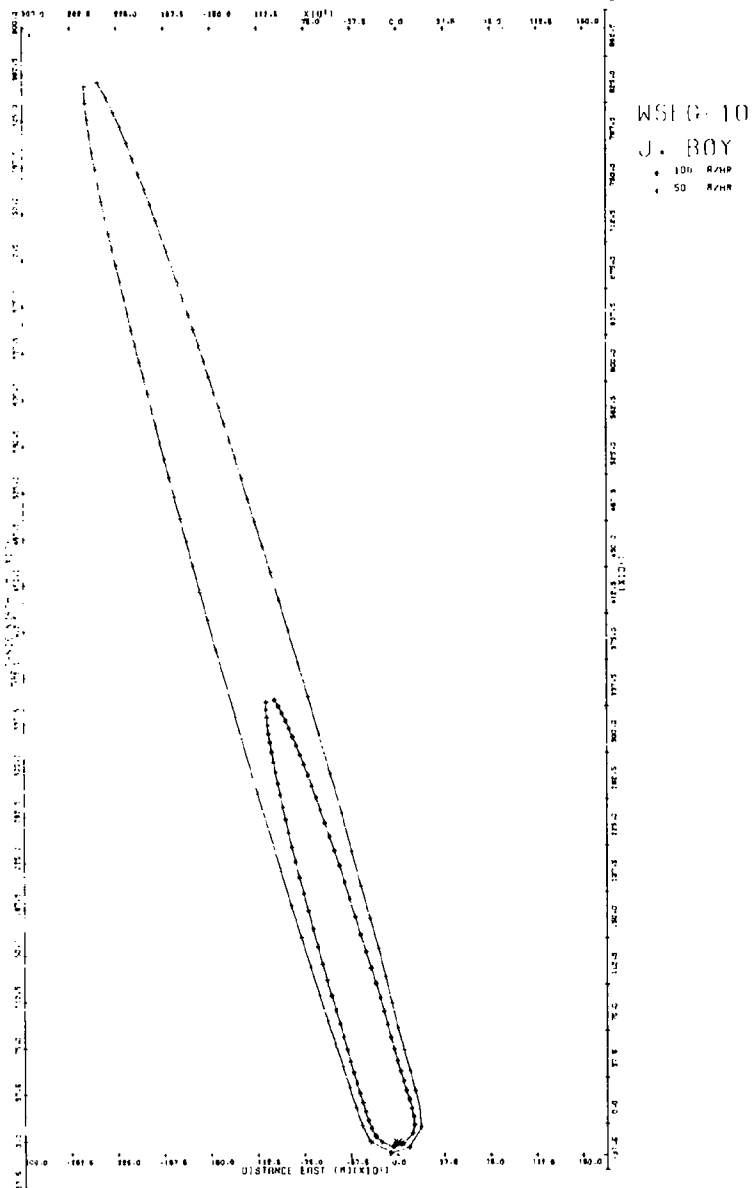
Contours are in units of Roentgens per hour for gamma radiation at a height of one meter above ground at H + 1 hour. All activity is assumed to be deposited at H + 1 hour. For all but the Zuni shot, for which fall-out activity was measured by an oceanographic method, predicted activities are multiplied by a combined ground roughness-instrument response correction factor of 0.5. (See Appendix B.)

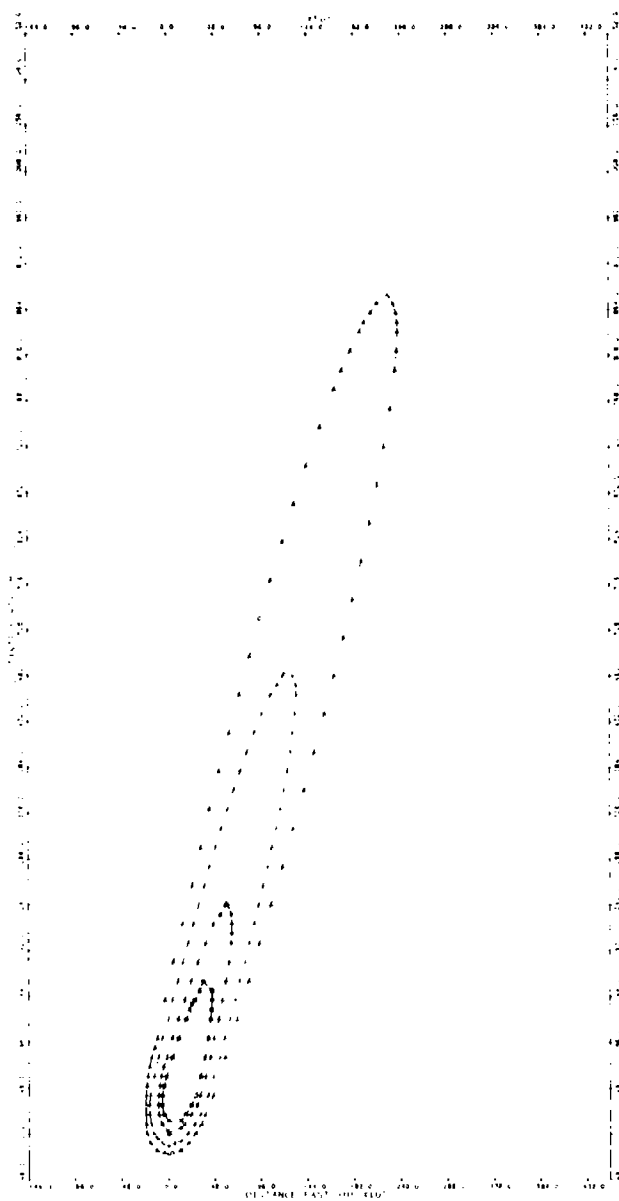
Observed and predicted patterns for each case are plotted to the same scale. North is up the pages and east is across the pages toward the right. Visual comparisons are best made by superimposing electrostatic copies of the plots.





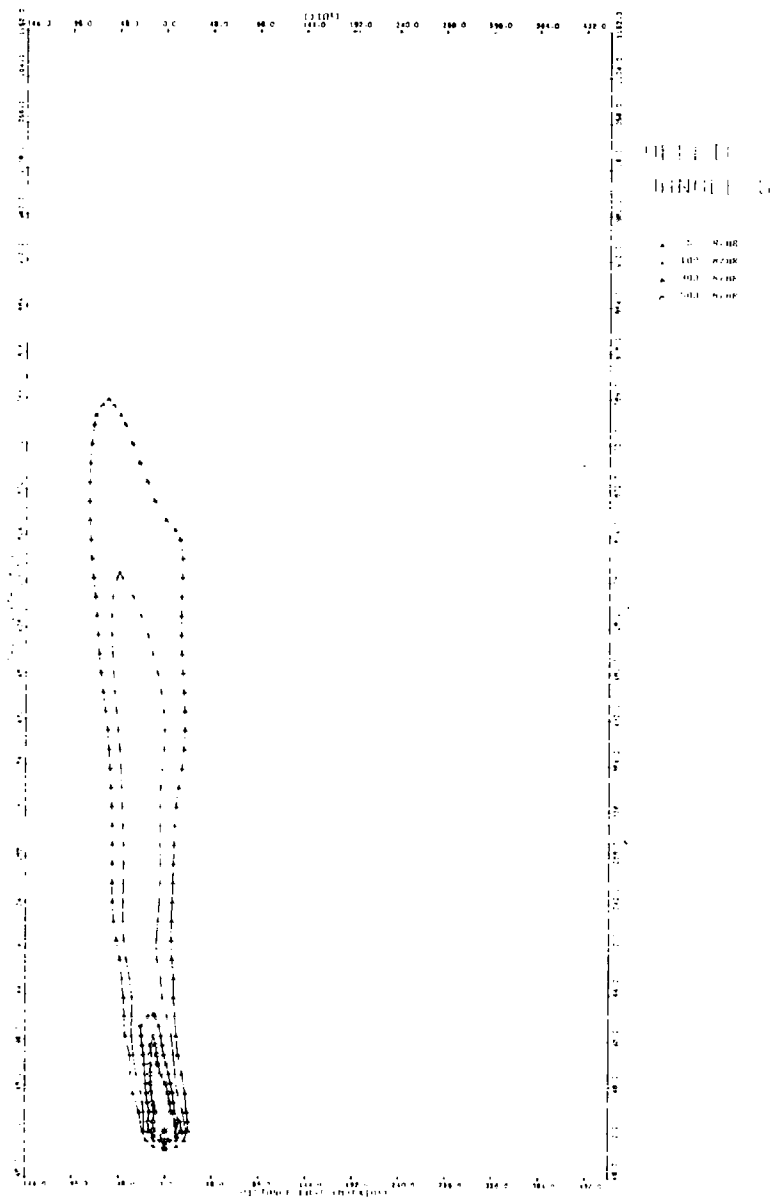


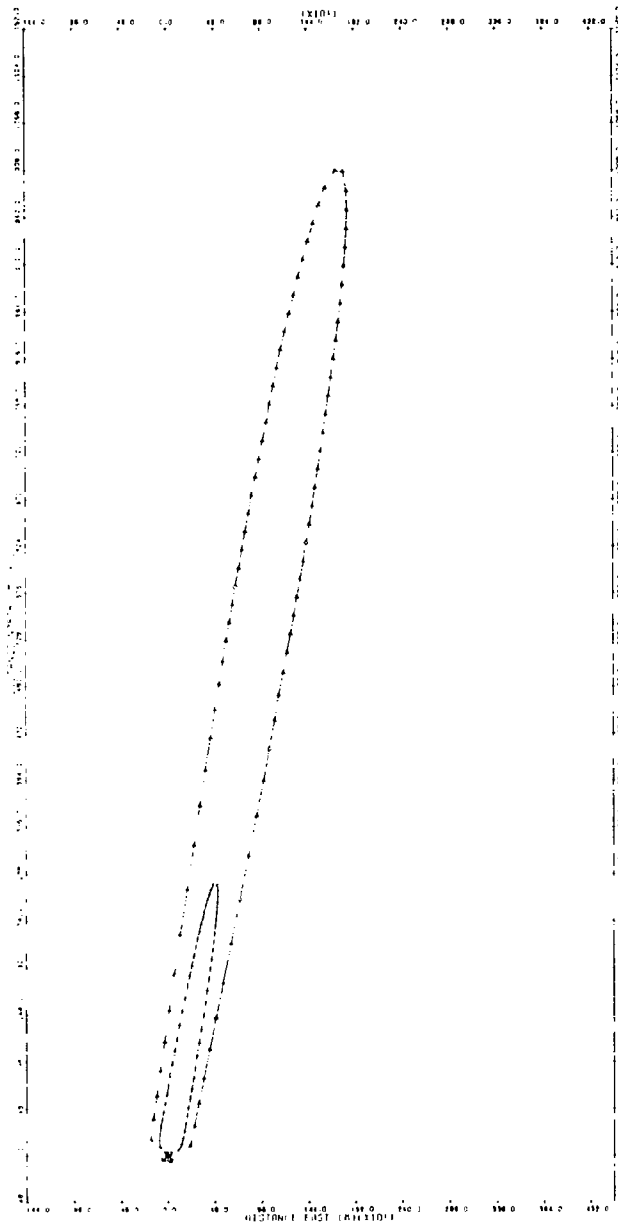


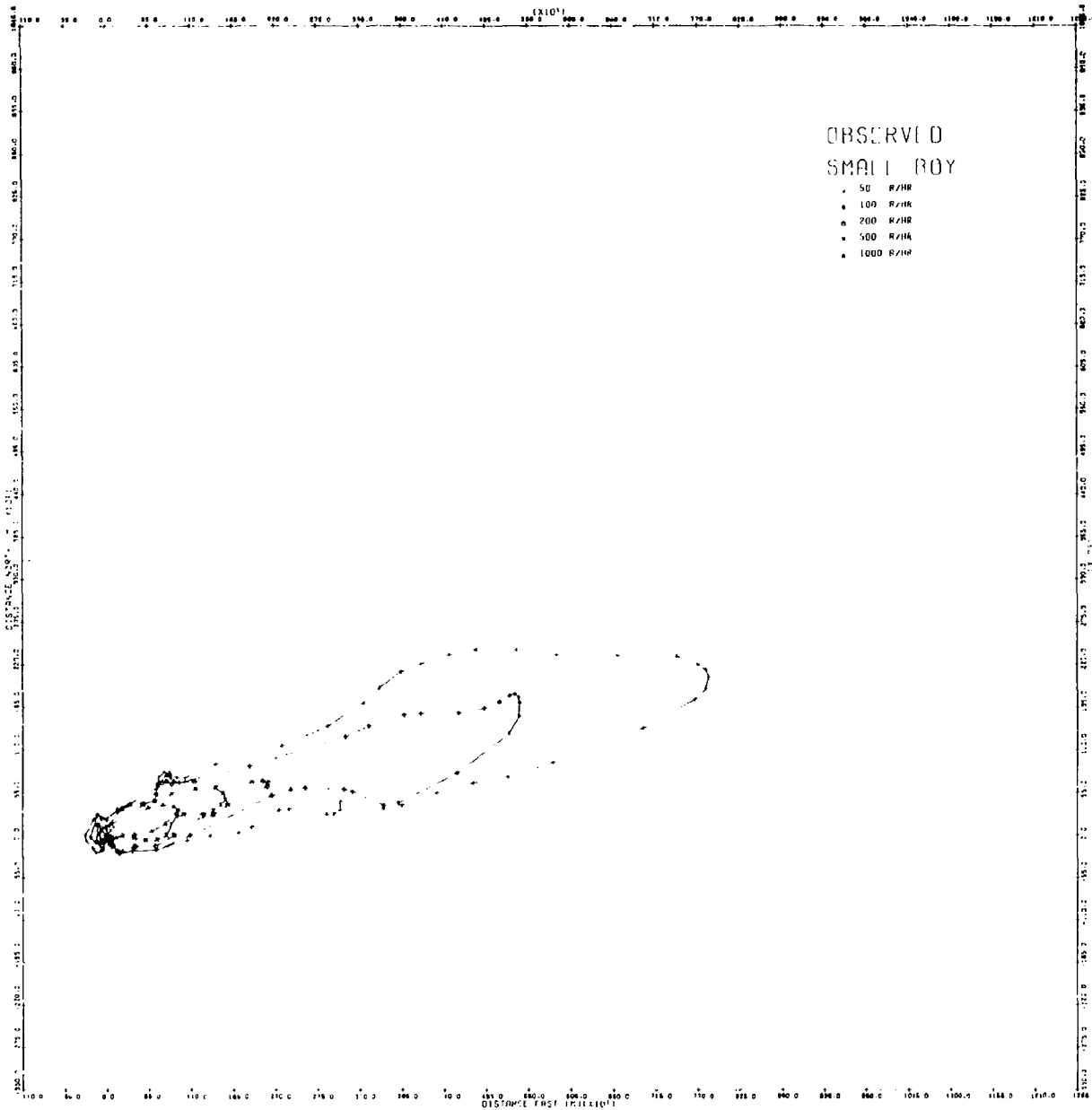


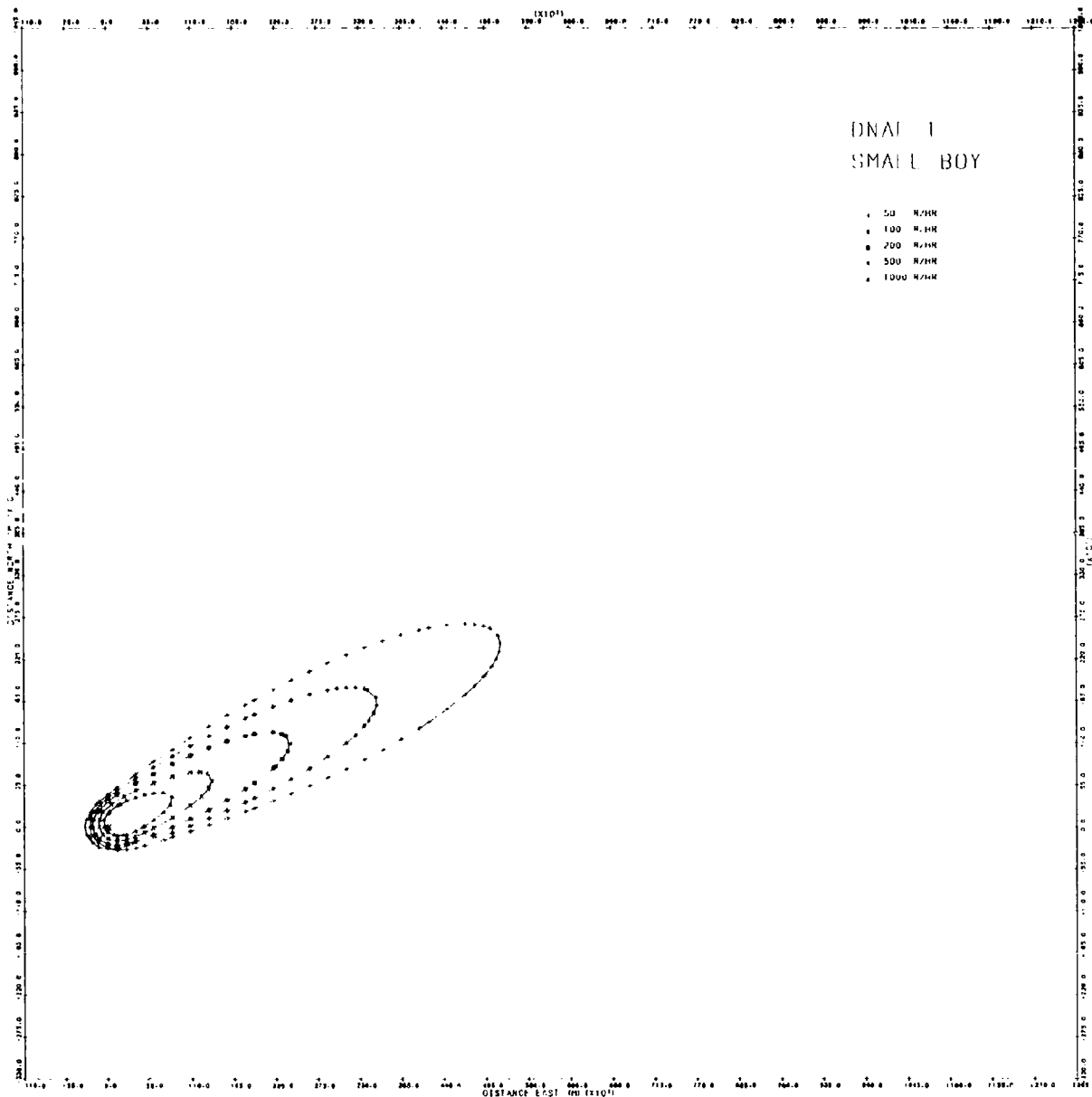
DATA
LANGUAGE

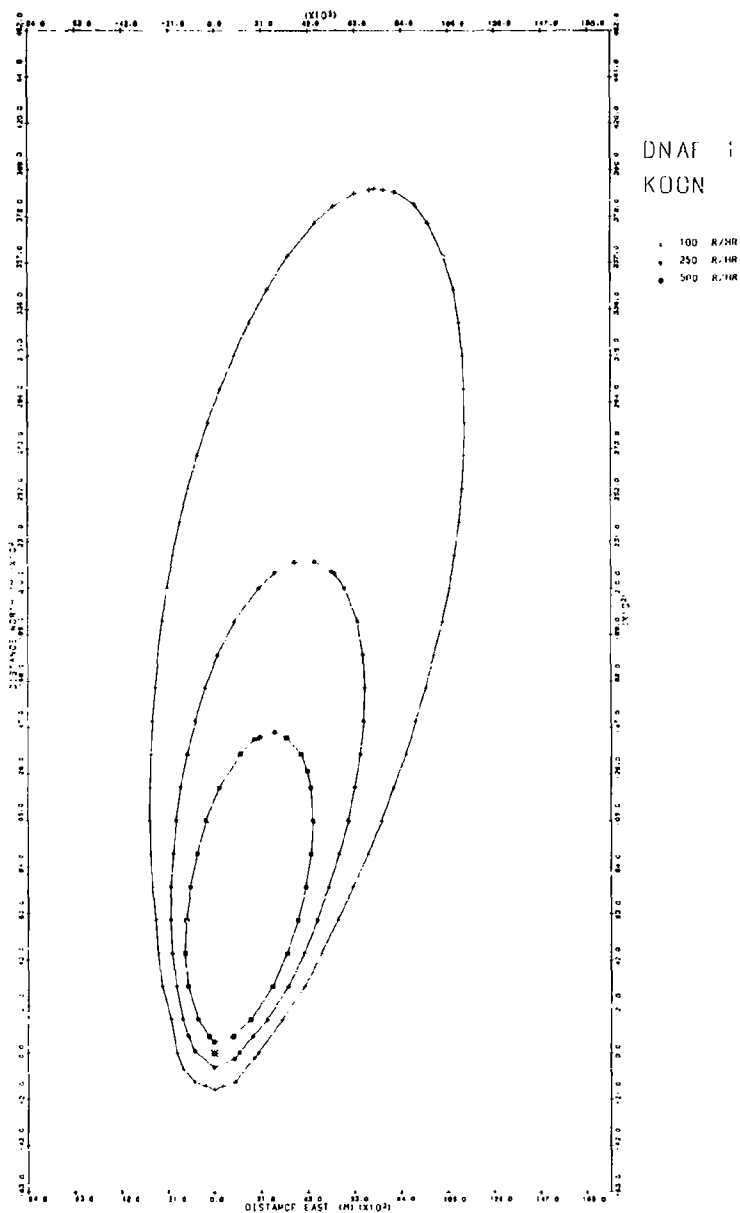
- 1000000
- 1000000
- 1000000
- 1000000

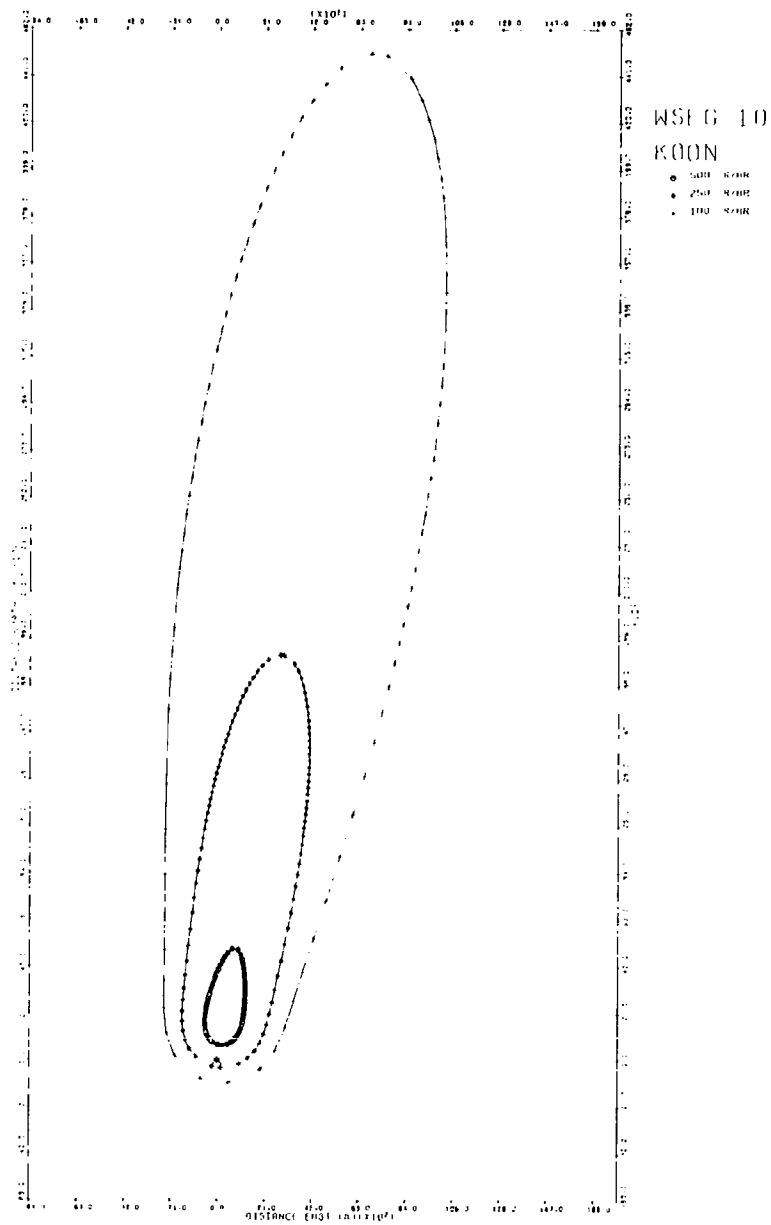


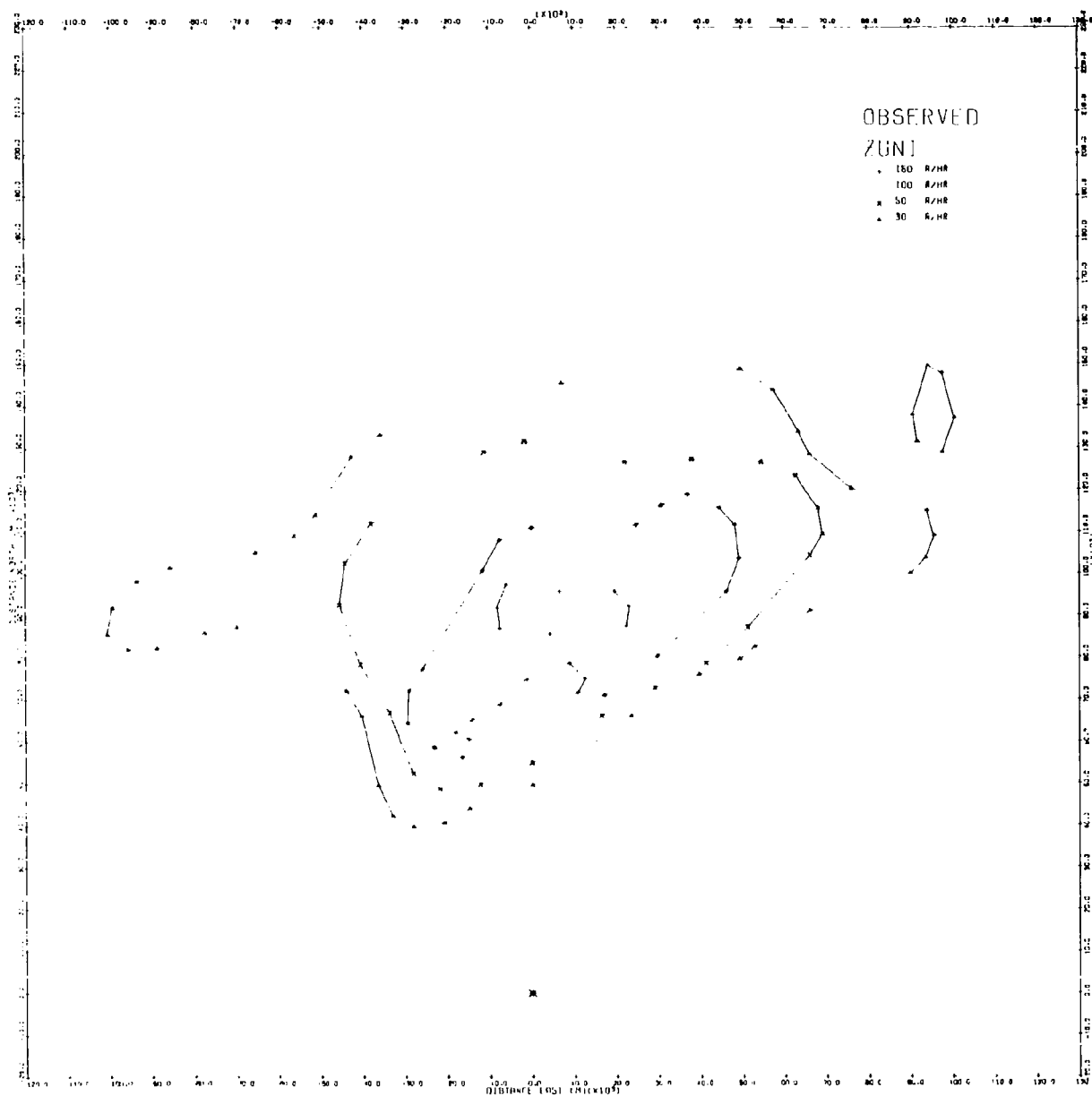


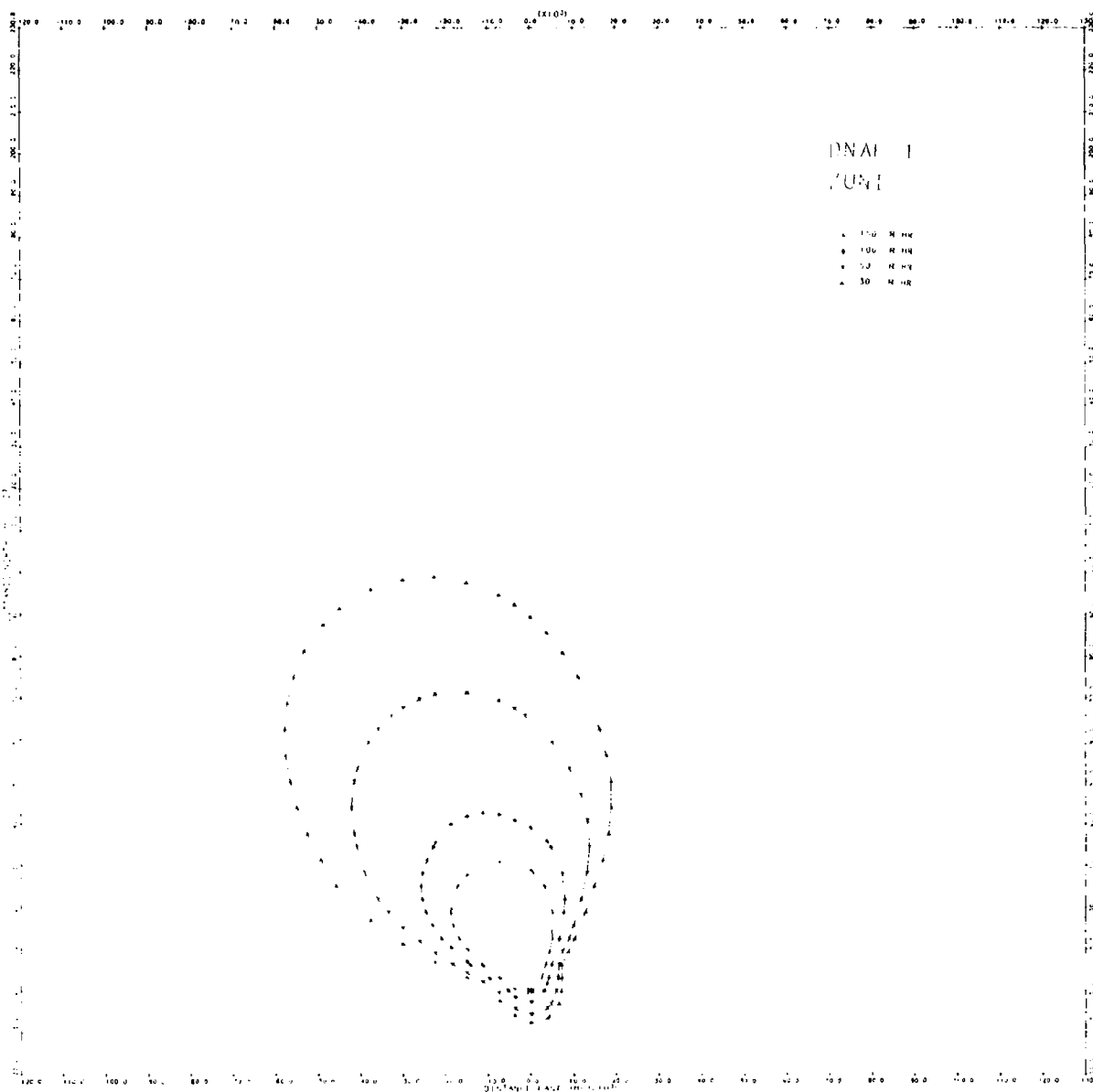


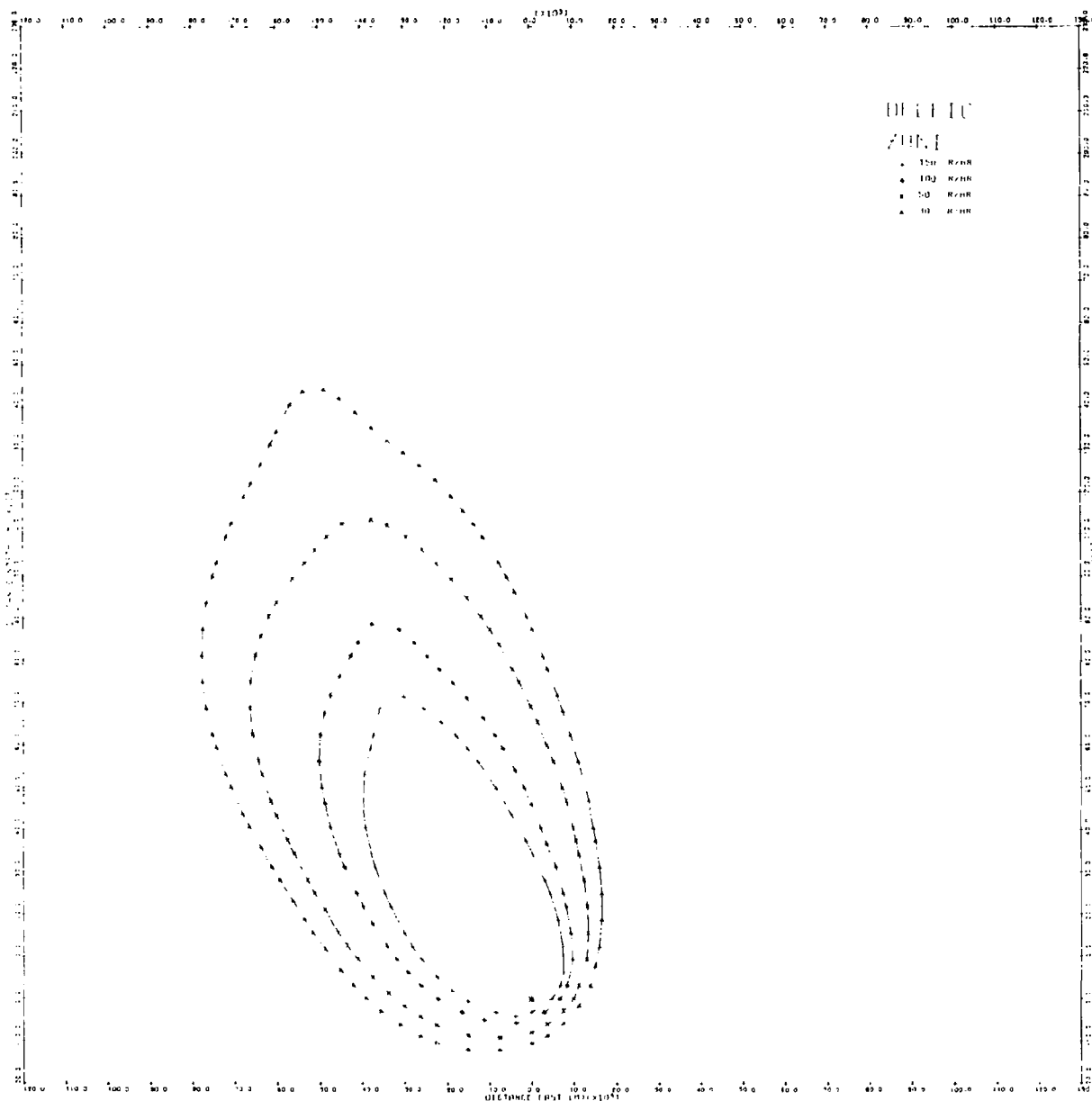


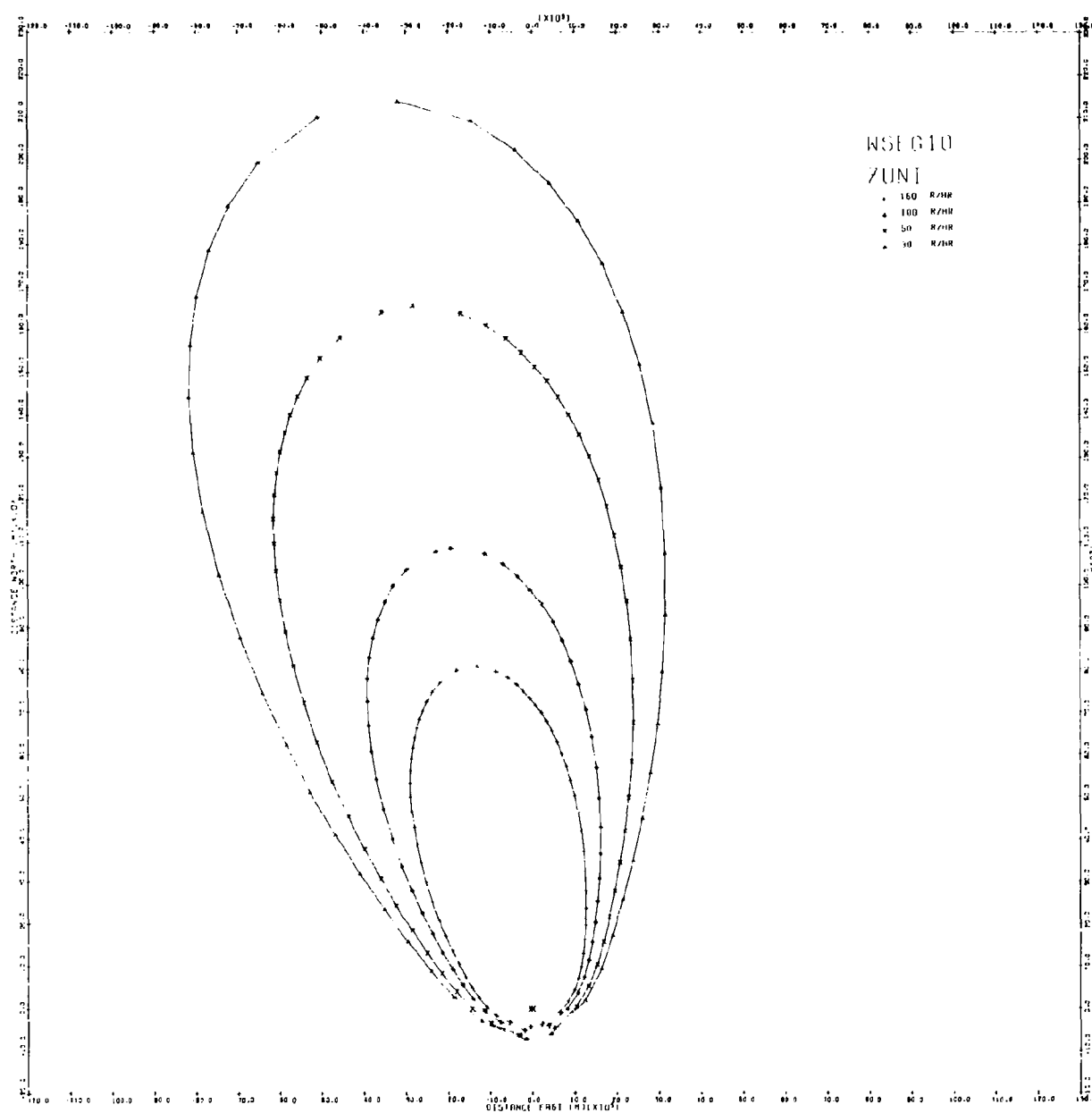


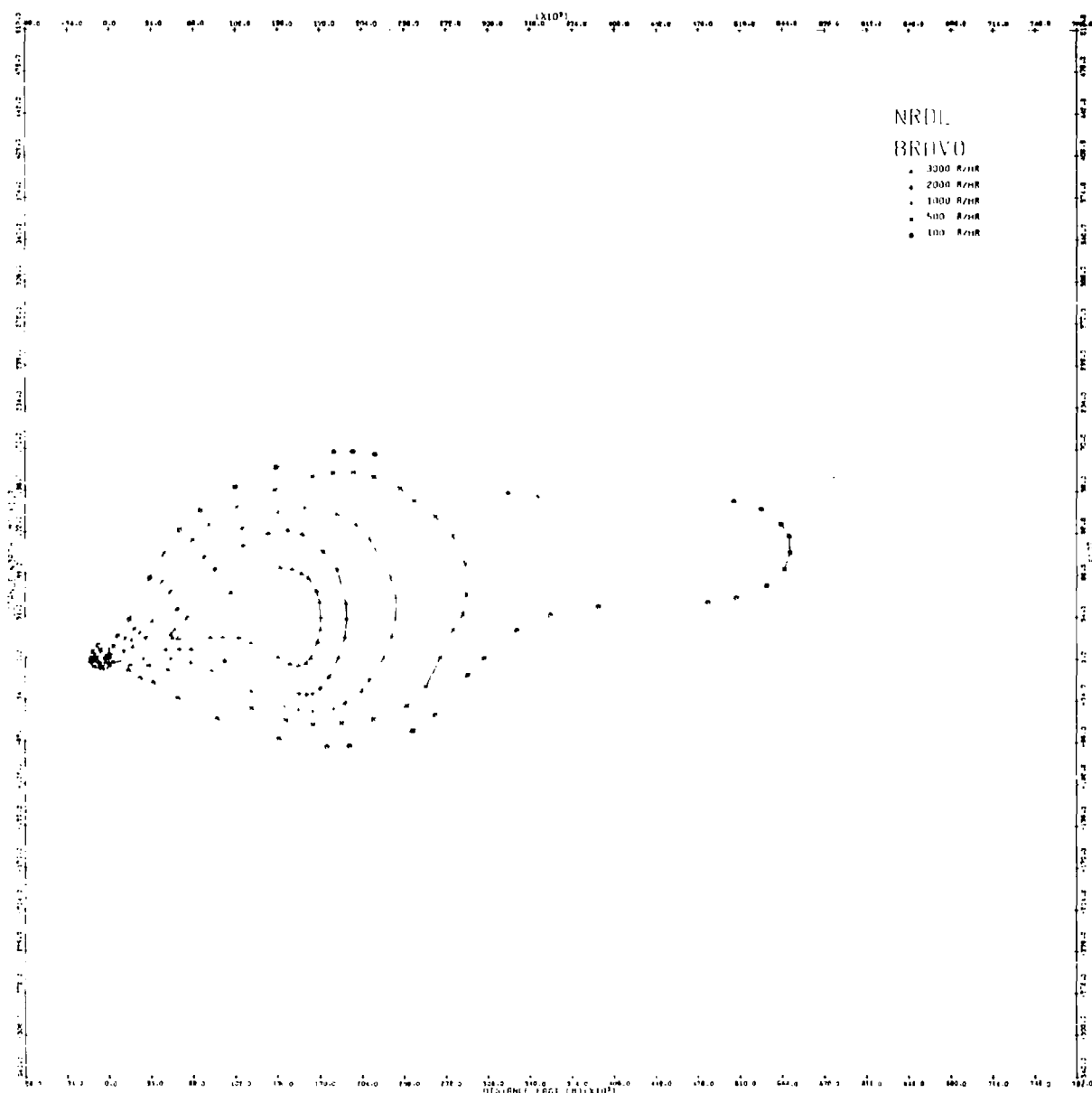


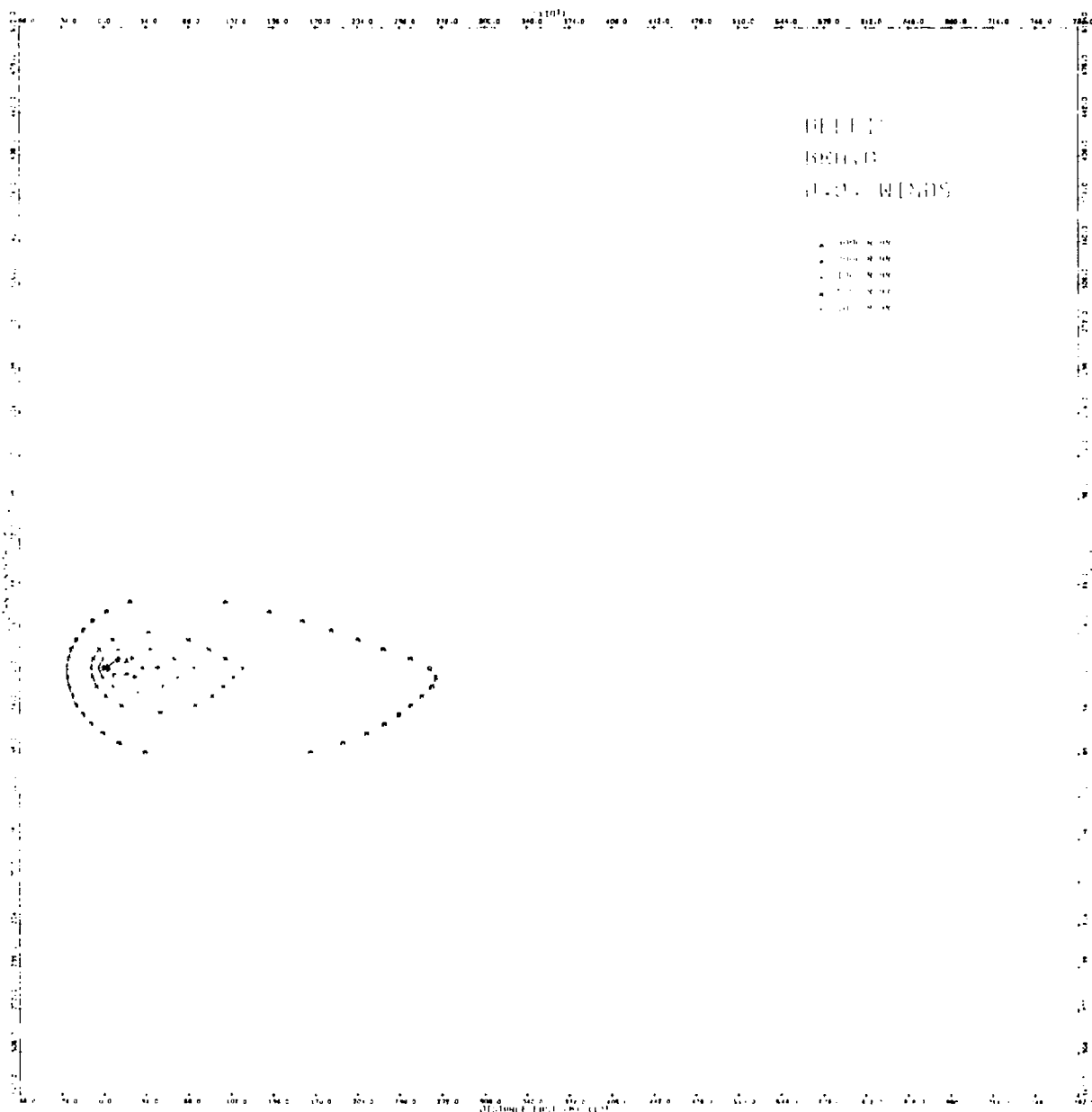


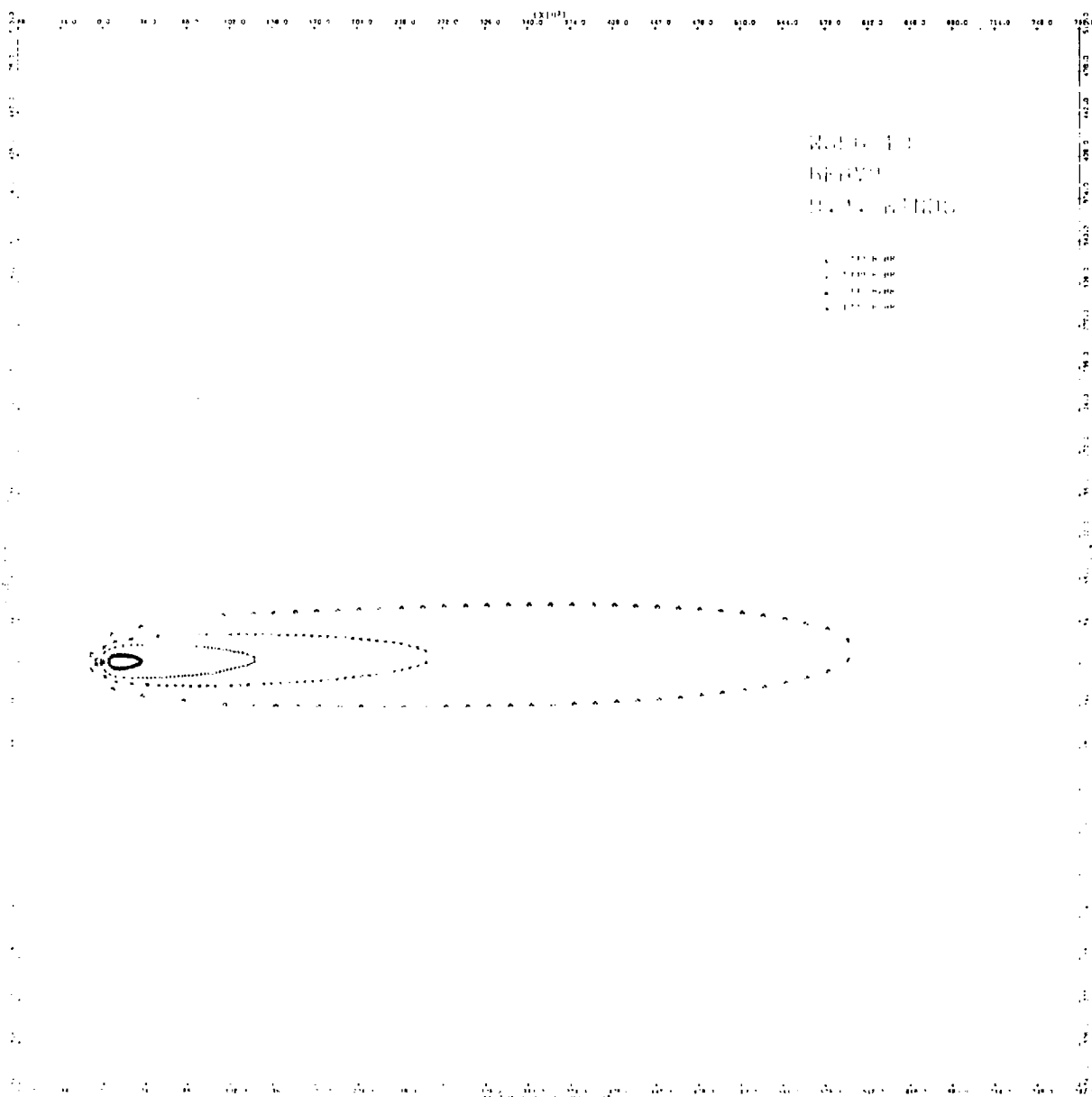












6. COMPUTER CODE

6.1 GENERAL DISCUSSION

Coding is entirely in ANSI FORTRAN and complete listings are presented in Appendix D. Glossaries of mnemonics are in subroutines DNAF and INWIND, and the Appendix A glossary relates symbols used in the report text to the FORTRAN mnemonics. The code was originally developed and exercised on the CDC 6600 computer, but also has been extensively tested and exercised on the Honeywell Information Systems 6080 computer used by the DoD Command and Control Technical Center.*

Data is input via system unit 5 and output via unit 6. These unit specifications can be changed by changing the values of parameters IN and IO (lines 69 and 70, subroutine DNAF). No other peripheral storage units are addressed.

All subroutine and function names are listed, with a brief description, in Table 6.

There are two optional modes of code operation:

- Mode 1. H + 1 hour exposure rate map preparation
- Mode 2. H + 1 hour exposure rate, and maximum effective biological dose at user specified points.

Map calculation is discussed in detail in section 6.2. For the Mode 2 calculation, the user simply specifies ground points in terms of X,Y coordinates relative to ground zero, and the H + 1 hour normalized exposure rates (Roentgens hr⁻¹) and maximum effective biological doses (Roentgens), at a height of one meter above the point are printed.

Wind data may be specified in either of two ways:

1. Effective fallout wind speed, v (m s⁻¹), wind direction, ϕ (degrees clockwise from north in the direction of the wind vector), and crosswind shear parameter, S_y (s⁻¹), are input directly.

*In addition to the FORTRAN code, the Texas Instruments TI 59, a sophisticated pocket calculator, has been programmed to compute $A(X,0)$ (see eq. 31)).

TABLE 6

DESCRIPTION OF DNAF-1 CODE SUBROUTINES AND FUNCTIONS

Subroutine or Function	Description
DNAF	Executive. Controls calculation flow and calls most of the following programs.
SCLOD	Computes stabilized cloud heights and radius plus fireball radius: Z_B, Z_T, R_S, R_i .
INWIND	Reads in and processes a vertical profile of wind data if the effective fallout wind speed, v , is not specified by input.
EWIND	Computes effective fallout wind, \bar{v} , from data input via subroutine INWIND.
SWIND	Computes the wind shear parameter, S_y , from the wind data input via subroutine INWIND.
ONSET	Computes fallout onset time, t_0 .
DOSE	Computes the factor which when multiplied by H + 1 hour exposure rate gives the maximum effective biological dose, $M(X,Y)$.
DNAFI	Computes crosswind-integrated H + 1 hour activity fraction deposited at distance X along the hotline from ground zero.
SIGTA	Computes deposition variance, σ^2 , crosswind pattern standard deviation, σ_y , and fallout arrival time, t_a , all at alongwind distance X from ground zero.
MAPP	Prints a two-dimensional map of H + 1 hour exposure rate.
SETMP	Sets fallout map boundaries and grid intervals for the user. This subroutine is called only if parameter \$SETMP is false, and the resulting map is intended to provide the user with a preliminary look at the fallout pattern.
TRPI	Linear interpolation between table entries.
ERROR	Error condition printout.

2. A vertical profile of winds are input from which the code computes v and S_y as described in sections 4.2 and 4.3.

The effective fallout wind speed is limited to values greater than or equal to 0.5 m s^{-1} . A zero input value is used to signal input of a vertical profile of wind data. If a value of $v < 0.5 \text{ m s}^{-1}$, other than the signal value of 0.0, is encountered, a comment is printed and v is reset to 0.5 m s^{-1} . (See the end of section 4.2.)

6.2 FALLOUT MAPS

Selection of the mode 1 calculation option (logical parameter IFMAP, card 3, is true) causes calculation of $H + 1$ hour normalized exposure rates (Roentgens hr^{-1}) at a height of one meter above a two-dimensional array of points on the ground. The points are spaced at grid intervals DGX and DGY (meters) in the x and y coordinate directions. Here the x axis is in the west-to-east direction (positive east of ground zero), and the y axis is in the south-to-north direction (positive north of ground zero).

Ordinate values are output in rectangular arrays, and it is assumed that the arrays are printed by a standard line printer. The x axis is across the printed page, west-to-east from left-to-right, and the y axis is up the page, south-to-north from bottom-to-top. A two-line, power of ten format is used. Thus, the activity for each point appears as

```

+NNNNN
V.VVV

```

which is interpreted as

$V.VVV \times 10^{+NNNNN} \text{ (Roentgens hr}^{-1}\text{)}.$

Printing is done in units of map strips, each strip consisting of a sufficient number of connected printer sheets to cover the entire y axis range.

Each row (across the page) of each strip contains a maximum of nineteen ordinate points in the x direction. Enough strips are produced to cover the entire x axis range. These strips can be attached side-by-side such as to construct the complete map, and contours may then be drawn by hand. x and y values are printed at regular intervals on each strip.

If logical parameter USETMP is true (card 3), the user must specify boundaries and grid increments for the map. Otherwise, the code sets these parameters (via subroutine SETMP) automatically, using both yield and wind as criteria. The result is a small, rather poorly resolved map which may not satisfy the particular needs of the user. It is intended to provide the user with a preliminary view of the map. From the information gained from this quick look, the user may devise his own map specifications as described next.

To specify his own map, the user must supply the following information:

1. Logical parameter USETMP = .TRUE. (card 3, sec. 6.5)
2. Coordinates (x_{\min} , y_{\min} or XMIN, YMIN) of the southwest corner of the map, and (x_{\max} , y_{\max} or XMAX, YMAX) of the northeast corner of the map. (card 6)
3. Grid increments DGX, or DGX and DGY, in the x and y axis directions. (card 6)

If only DGX is specified, the code computes DGY such as to produce a spatially undistorted map on a standard line printer: that is, one with 10 characters per inch across the page and 6 characters per inch down the page. To adjust for nonstandard character spacing, parameters IH and IV (lines 69 and 70 in subroutine DNAF and 13 and 14 in subroutine SETMP) must be changed.

The values of XMIN and YMIN specified on card 6 should be one grid increment less than the values actually expected on the printed map.

The code presented in Appendix D provides for a maximum of 5000 map points. If the map specified by card 6 input requires more than this number of points, DGX and DGY are adjusted such that no more than 5000 map points are required, a comment to the effect that the adjustment has been made is printed, and calculation then proceeds. Map point ordinates are stored in array OMAP, and parameter NMAP is used as a variable dimension for OMAP. To change the maximum number of points, change the dimension of the OMAP array and the value of NMAP as desired (lines 67, 69 and 70 of subroutine DNAF).

6. INPUT OF WIND PROFILE DATA

If parameter WIND (which is the effective fallout wind speed, v) on card 2 is zero, the code calls subroutine INWIND which reads in a vertical profile of wind data as described by cards 4a-4n (sec. 6.5). This input is designed for maximum versatility.

Card 4a is used to specify whether the wind data are input in resolved form (i.e., vector components in the easterly and northerly directions), or in terms of speed and direction angle.

Card 4b is an object-time format to be used to read the data.

Card 4c contains scale and translation factors, and card 4d contains data field pointers. Cards 4e to 4n-1 each contain altitude and wind vector data for a wind stratum, and the last card, 4n, is the data set terminator.

Use of the scale-translation data and the field pointers deserves some explanation.

In combination with the object-time format, the field pointers, N1, N2, N3, allow any arrangement of the data on the cards; the only restriction being that all of the data cards have the same arrangement. Each card contains three items of data:

- | | | |
|-------------------------------------|---|-------------|
| 1. Altitude of the wind measurement | } | FORM = RESO |
| 2. x component of the wind vector | | |
| 3. y component of the wind vector | | |

or

- | | | |
|-------------------------|---|-------------|
| 2. Wind direction angle | } | FORM = METE |
| 3. Wind speed | | |

Pointer N1 is associated with the altitude, N2 with the x wind component or direction angle, and N3 with the y wind component or wind speed. Collectively N1, N2, N3 consist of some permutation of the integers 1, 2, 3. The object-time format specifies three data fields, and N1 specifies which of the three contains the altitude, N2 specifies which contains the x wind component or the direction angle, etc. For example, if we have $N1 = 1$, $N2 = 3$, $N3 = 2$, then the altitude is in the first field (from the left), the x wind component or direction angle is in the third field, and the y wind component or wind speed is in the second field.

The scale and translation data input via card 4c allows input of data in any units, and allows certain common data translations to be made. Scale factors are in fields 1-3 and translations are in fields 4-5 of card 4c. After application of these translations and scale factors, altitude must be in meters with origin at the ground, and the wind must be expressed in terms of components ($m s^{-1}$) in the x (easterly) and y (northerly) directions. If it is used, the wind direction angle must be, after scaling and translating, the angle of the wind vector measured clockwise from north.

Scale and translation data are read from card 4c into array SCALE(). The three data items on each wind data card are read into array AP(). For the altitude, SCALE(4) is a translation, which is applied before scaling, to adjust the origin to be at ground level, and SCALE(1) is a scale factor used to adjust the units to meters. Thus the altitude, ZCH, is

$$ZCH = (AP(N1) + SCALE(4)) * SCALE(1).$$

If FORM = RESO (card 4a), the wind vector data are input in component form. In this case, the only other card 4c datum used is SCALE(2), which is a scale factor applied to both components to adjust units to meters per second. Specifically, we have for the x and y wind components, WX and WY,

$$WX = AP(N2) * SCALE(2)$$

$$WY = AP(N3) * SCALE(2).$$

If FORM = METE (card 4a), the wind vector data are input in terms of direction angle and speed. As with the previous case, SCALE(2) is used to scale the wind speed to units of meters per second. SCALE(3) is a scale factor used to convert the direction angle to degrees. SCALE(5) is an angle translation (i.e., rotation) which is input in the same units as is the direction angle. The angle translation calculation is set up to convert the angle from the conventional meteorological specification of direction from which the wind is blowing, to direction toward which the wind is blowing; in other words, the code automatically rotates the wind angle through 180° unless this is circumvented by appropriate specification of SCALE(5). Specifically we have

$$WX = AP(N3) * SCALE(2) * \sin\left(\frac{\pi}{180} (AP(N2) * SCALE(3) + TRNS)\right)$$

$$WY = AP(N3) * SCALE(2) * \cos\left(\frac{\pi}{180} (AP(N2) * SCALE(3) + TRNS)\right)$$

where

$$TRNS = SCALE(5) * SCALE(3) - 180.$$

Default values for the scale factors, SCALE(1) through SCALE(3), are unity. That is, if any or all of the first three fields on card 4c are left blank, the code sets the corresponding scale factors to unity.

The wind data should extend at least up to the cloud top height, z_T (eq. (4)), but if it does not, the code simply assumes that the data in the highest wind stratum is constant up to z_T .

The wind data are sorted by the code and arranged in sequence of increasing altitude; thus it is not necessary that they be input in any particular order.

An example of a common situation will illustrate how to set up the data cards. Suppose the wind data are available in the form shown in Table 7. Ground zero is at an altitude of 4215 feet, and we assume that the surface wind was measured at a height of 10 meters above the ground. Thus, the actual altitude of the surface wind is 4248 feet. Figure 9 shows how cards 4a-4n might be punched for this set of data.

TABLE 7
EXAMPLE WIND DATA LISTING
Site Elevation is 4215 Feet

<u>Altitude (kft relative to MSL)</u>	<u>Speed (mph)</u>	<u>Direction Angle* (degrees)</u>
Surface	2	190
6	15	170
8	30	180
10	37	200
.	.	.
.	.	.
.	.	.
30	80	210

*Direction from which the wind is blowing.

6.4 STORAGE AND COMPUTATION TIME REQUIREMENTS

Approximately 15,000 (decimal) storage cells are required by the CDC 6600 computer to contain the object codes compiled from the complete package of FORTRAN codes listed in Appendix D.

Computation is quite fast. A rough estimate of computation time is derived as follows. In a single run on the CDC 6600 computer, eight complete fallout maps were calculated and printed, and for each map a vertical profile of wind data was processed. In addition to the usual calculations, contour points were calculated, printed and punched for the maps shown on pp. 58 to 80. Activities for a total of 11,242 map points were calculated, and the total CPU time was 29.469 seconds. If we simply lump all of the accessory calculations, including print and punch times, in with the activity calculation time, we get 2.6 millisecond per activity calculation.

6.5 DESCRIPTION OF CARD INPUTS FOR THE DNAF-1 CODE

Card Number	Variables and Format	Data Description
1	HOLL(12), (12A6)	Run identification
2	W, FW, WIND, SY, ANG, GRUFF, (8F10.0)	<p>W = Total explosion energy yield (KT)</p> <p>FW = Fission yield (KT)</p> <p>WIND = Effective fallout wind speed ($m\ s^{-1}$) ($WIND \geq 0.0$) A blank field is used to signal input of card 4 data.</p> <p>SY = Wind shear parameter (s^{-1}). Required only if $WIND > 0.0$</p> <p>ANG = Effective fallout wind vector angle, or hotline angle, clockwise relative to north (degrees). Required only if $WIND > 0.0$.</p> <p>GRUFF = Scale factor for multiplication of all H + 1 hr exposure rate values. (See Appendix C.) Default value is unity.</p>
3	IFMAP, USETMP (5I1)	<p>IFMAP If true, a two-dimensional H + 1 hour exposure rate map is to be computed and printed. (See logical parameter USETMP and card number 6.) If false, H + 1 hour exposure rate and maximum biological dose are computed for user-specified points. (See cards number 5.)</p> <p>USETMP If true, the user must specify the fallout map boundaries and grid intervals via input of card 6. If false, the code sets these parameters via subroutine SETMP. In any case, USETMP is applicable only if IFMAP IS TRUE.</p>
4	Cards 4a-4n are input only if $WIND = 0.0$ on card 2. In that case, a wind profile in the vertical is specified as follows (see sec. 6.3)	
4a	FORM, (A4)	<p>Specifies whether wind data are input in meteorological format (i.e., speed and direction) or in resolved format (i.e., components resolved in the northerly and easterly directions).</p> <p>FORM METL specifies meteorological format</p> <p>FORM RESO specifies resolved format</p>

Card Number	Variables and Format	Data Description
4b	FMT, (12A6)	Wind data object-time format. (See cards number 4e-4n.)
4c	SCALE(5), (8F10.0)	Wind data scale factors and translations. Default values for SCALE(1) through SCALE(3) = 1. (See cards 4e-4n.)
4d	N1, N2, N3, (3I4)	Wind data input field pointers. N1, N2, N3 are some permutation of the integers 1, 2, 3. (See cards 4e-4n.)
4e	AP(3), (FMT, see card 4b)	Altitude (m above ground) = (AP(N1) + SCALE(4))*SCALE(1) For FORM : METE: Easterly wind component (m s ⁻¹) = AP(N3)*SCALE(2)*SIN(π /180.(AP(N2)*SCALE(3) + SCALE(5)*SCALE(5) - 180.))
4n	AP(N1) : 999999., (FMT)	Northerly wind component (m s ⁻¹) = AP(N3)*SCALE(2)*COS(π /180.(AP(N2)*SCALE(3) + SCALE(5)*SCALE(5) - 180.)) For FORM : RESO: Easterly wind component (m s ⁻¹) = AP(N2)*SCALE(2) Northerly wind component (m s ⁻¹) = AP(N3)*SCALE(2)
5	Cards 5a-5n are input only if parameter IFMAP = .FALSE. on card 3.	
5a	X, Y, (8F10.0)	X = Distance from GZ along the hotline. Positive X is in the downwind direction (m) Y = Distance normal to the hotline (m). Activity and maximum biological dose are calculated at each (X,Y) point input.
5n	End of record flag.	
6	XMIN, XMAX, YMIN, YMAX, DGX, DGY, (8F10.0)	Card 6 is input only if parameters IFMAP and USETMP both are true on card 3. Map boundaries and grid increments are specified as: XMIN, XMAX = minimum and maximum map coordinates relative to GZ along the easterly directed axis (m). YMIN, YMAX = minimum and maximum map coordinates relative to GZ along the northerly directed axis (m). DGX, DGY = map grid increments in the easterly and northerly axes directions (m). DGX must be specified, but DGY is optional. If DGY is not specified, it is computed by the program such as to provide a spatially undistorted map when printed by a standard line printer.

6.6 EXAMPLE PROBLEM AND PRINTOUT DESCRIPTION

To assist the user in getting the code running on his own computer, and to illustrate the card input and the printout for a mode 1 (fallout map) case, we provide here a simple test problem. The card input is given in Figure 10, and the complete printout is given below, which is largely self-explanatory.

The raw wind data are printed as well as the processed data. The processed data have been translated and scaled according to the data specified on card 4c. Wind layer base altitudes are in meters relative to the ground. When \vec{v} , ϕ and S_y are supplied directly, this output is omitted.

For a mode 2 (user supplied X, Y coordinates) calculation, the output is the same except that the map strips are replaced by a tabulation of X, Y, H + 1 hour exposure rate and maximum effective biological dose.

1 2 3 4 5 6 7 8 9 10 11 12 13 14 15 16 17 18 19 20 21 22 23 24 25 26 27 28 29 30 31 32 33 34 35 36 37 38 39 40 41 42 43 44 45 46 47 48 49 50 51 52 53 54 55 56 57 58 59 60 61 62 63 64 65 66 67 68 69 70 71 72 73 74 75 76 77 78 79 80

EXAMPLE	PROBLEM	DATA	EC
1	2	140	6
2	3	13	13
3	4	155	5
4	5	190	13
5	6	200	15
6	7	215	16
7	8	220	17
8	9	215	13
9	10	220	12
10	11	235	3
11	12	250	7
12	13	275	11
13	14	275	11
14	15	280	1
15	16	270	25
16	17	275	1800
17	18	51000	6000
18	19	13000	3000
19	20	99999	99999

1
2
3
4
5
6
7
8
9
10
11
12
13
14
15
16
17
18
19
20
21
22
23
24
25

LEAF - 1

THE FOLLOWING NUCLEAR ACTIVITY TEST RESULTS

PREDICTION SYSTEM

PREPARED BY
ATMOSPHERIC SCIENCE ASSOCIATES
REDDING, MASS.

*** FOR PREDICTION *** EXAMPLE TEST PROBLEM - DNAT-1

WINDS - DATA (KTS) 5.00000E+01 (5.00000E+01) KT
ORIGIN - SCALE FACTOR 5.10000E+01

RAW WIND DATA			FOLLOWS WIND DATA		
	VX	VY		VX	VY
2.10000E+02	1.40000E+02	5.10000E+00	7.70000E+01	-5.10000E+00	4.10000E+00
1.50000E+01	1.00000E+02	1.10000E+01	1.40000E+03	-5.40000E+00	1.10000E+01
5.00000E+03	1.00000E+02	5.10000E+00	2.00000E+03	5.10000E+01	4.10000E+00
5.00000E+03	2.00000E+02	1.50000E+01	5.50000E+03	5.10000E+00	1.40000E+01
7.10000E+03	2.00000E+02	1.00000E+01	7.10000E+03	1.00000E+01	1.50000E+01
9.10000E+03	2.00000E+02	1.00000E+01	9.10000E+03	1.00000E+01	1.20000E+01
1.00000E+01	2.10000E+02	1.00000E+01	1.00000E+01	2.00000E+00	5.00000E+00
1.10000E+01	2.00000E+02	1.00000E+01	1.10000E+01	2.00000E+00	5.00000E+00
1.20000E+01	2.00000E+02	1.00000E+01	1.20000E+01	2.00000E+00	5.00000E+00
1.30000E+01	2.00000E+02	1.00000E+01	1.30000E+01	2.00000E+00	5.00000E+00
1.40000E+01	2.00000E+02	1.00000E+01	1.40000E+01	2.00000E+00	5.00000E+00
1.50000E+01	2.00000E+02	1.00000E+01	1.50000E+01	2.00000E+00	5.00000E+00
1.60000E+01	2.00000E+02	1.00000E+01	1.60000E+01	2.00000E+00	5.00000E+00
1.70000E+01	2.00000E+02	1.00000E+01	1.70000E+01	2.00000E+00	5.00000E+00
1.80000E+01	2.00000E+02	1.00000E+01	1.80000E+01	2.00000E+00	5.00000E+00
1.90000E+01	2.00000E+02	1.00000E+01	1.90000E+01	2.00000E+00	5.00000E+00
2.00000E+01	2.00000E+02	1.00000E+01	2.00000E+01	2.00000E+00	5.00000E+00
2.10000E+01	2.00000E+02	1.00000E+01	2.10000E+01	2.00000E+00	5.00000E+00
2.20000E+01	2.00000E+02	1.00000E+01	2.20000E+01	2.00000E+00	5.00000E+00
2.30000E+01	2.00000E+02	1.00000E+01	2.30000E+01	2.00000E+00	5.00000E+00
2.40000E+01	2.00000E+02	1.00000E+01	2.40000E+01	2.00000E+00	5.00000E+00
2.50000E+01	2.00000E+02	1.00000E+01	2.50000E+01	2.00000E+00	5.00000E+00

WIND LAYER NAME ALTITUDES

LEVELS	1 THRU	2	3	4	5	6	7	8	9	10 THRU
LEVELS	1 THRU	15	15000	15000	15000	15000	15000	15000	15000	15000

WIND DIRECTION (CLOCKWISE FROM NORTH) 1.10000E+01 M/SEC
WIND VELOCITY (CLOCKWISE FROM NORTH) 1.10000E+01 M/SEC
WIND DIRECTION (CLOCKWISE FROM NORTH) 1.10000E+01 M/SEC

GRID LIMITS AND INTERVALS		XMIN	YMIN	XMAX	YMAX	DELTA X	DELTA Y
XMIN	YMIN	-9999	-9999	9999	9999	1000.00	1000.00

THE QUANTITY PRINTED IS
EXPOSURE RATE IS PRINTED TO TIME PER HOUR
UNITS ARE HOURS PER HOUR
GROUND LEVEL IS 1000 FT X = 0.0 Y = 0.0

[illegible]

REFERENCES

1. H. G. Norment, "DELFIC: Department of Defense Fallout Prediction System. Volume I - Fundamentals," Atmospheric Science Associates, DNA 5159F-1 (31 December 1979). AD A088 367.
2. H. G. Norment, "DELFIC: Department of Defense Fallout Prediction System. Volume II - User's Manual," Atmospheric Science Associates, DNA 5159F-2 (31 December 1979). AD A088 512.
3. H. G. Norment, "SIMFIC: A Simple, Efficient Fallout Prediction Model," Atmospheric Science Associates, DNA 5193F (31 December 1979). AD A089 187/9.
4. G. E. Pugh and R. J. Galiano, "An Analytical Model for Close-In Operational-Type Studies," Weapons Systems Evaluation Group, WSEG RM No. 10 (15 October 1959). AD 261 752.
5. R. B. Mason, L. Bragg and J. Sherby, "Description of Mathematics for the Single Integrated Damage Analysis Capability (SIDAC)," Command and Control Technical Center, TM 15-80 (13 June 1980).
6. H. G. Norment, "Analysis and Comparison of Fallout Prediction Models," Atmospheric Science Associates, unpublished.
7. H. G. Norment, "Evaluation of Three Fallout Prediction Models: DELFIC, SEER and WSEG-10," Atmospheric Science Associates, DNA 5285F (16 June 1978).
8. U.S. Standard Atmosphere, 1976, NOAA, NASA, NOAA-S/T 76-1562 (October 1976).
9. L. F. Shampine and R. C. Allen, Numerical Computing: An Introduction (W. B. Saunders Co., 1973).
10. E. F. Wilsey and C. Crisco, "An Improved Method to Predict Nuclear Cloud Heights," Ballistics Research Laboratory, unpublished.
11. G. K. Batchelor, "Diffusion in a Field of Homogeneous Turbulence. I. Eulerian Analysis," Australian J. Sci. Res. 2A, 437 (1949).
12. A. C. Best, "Empirical Formulae for the Terminal Velocity of Water Drops Falling Through the Atmosphere," Quart. J. Roy. Meteor. Soc. 76, 302 (1950).

REFERENCES, continued

13. J. J. Walton, "Scale Dependent Diffusion," J. Appl. Meteor. 12, 547 (1973).
14. E. M. Wilkins, "Decay Rates for Turbulent Energy Throughout the Atmosphere," J. Atm. Sci. 20, 473 (1963).
15. H. G. Norment, "Validation and Refinement of the DELFIC Cloud Rise Module," Atmospheric Science Associates, DNA 4320F (15 January 1977). AD A047 372.
16. H. A. Blair, "The Constancy of Repair Rate and of Irreparability During Protracted Exposure to Ionizing Radiation," Ann. New York Acad. Sci. 114, 150 (1964).
17. H. O. Davidson, Biological Effects of Whole-Body Gamma Radiation on Human Beings (Johns Hopkins University Press, 1957).
18. S. Glasstone and P. J. Dolan, The Effects of Nuclear Weapons, 3rd Edition (Department of Defense and Department of Energy, 1977). Sec. 9.146 ff.
19. R. L. Stetson, et. al., "Operation Castie, Proj. 2.5a. Distribution and Intensity of Fallout," U. S. Naval Radiological Defense Laboratory, unpublished.
20. R. H. Rowland and J. H. Thompson, "A Method for Comparing Fallout Patterns," DASIAC, G. E. - Tempo, DNA 2919F (April 1972).

APPENDIX A
GLOSSARY OF SYMBOLS AND FORTRAN MNEMONICS

Text Symbol	FORTRAN Mnemonic	Description
$A(X,Y)$	OMAP(),A	H + 1 hr normalized exposure rate (Roentgen hr ⁻¹) at three meters above point X, Y.
C	GRUFF	Scale factor to be applied to activity calculations.
$D(X)$	GOLF DNAF1 (Function)	Crosswind integrated activity fraction deposited at distance X from ground zero. (m ⁻¹)
$D(X)_F$		Farfield corrected, crosswind integrated activity fraction deposited at downwind distance X from ground zero. (m ⁻¹)
$D(X)_U$		Upwind corrected, crosswind integrated activity fraction deposited at upwind distance X from ground zero. (m ⁻¹)
$f(z)$	V()	Settling speed of the nominal fallout particle at altitude z. (m s ⁻¹)
$F(X,t)$		Factor to account for dispersion in the hotline axis direction of fallout being deposited at time t at point X. (m ⁻¹)
$g(t)$		Activity fraction deposition rate function. (s ⁻¹)
$G(Y)$	CROSS (Statement Function)	Crosswind fallout pattern dispersion factor. (m ⁻¹)
$M(X,Y)$	DMAX	Maximum effective biological dose (Roentgens)
R_i	RI	Early cloud radius. (m)
R_s	RS	Stabilized cloud cap radius. (m)
S_Y	SY	Wind shear parameter: approximation to the crosswind component of the vertical wind shear. (s ⁻¹)
t		Time. (s)
t_a	TA	Time of arrival of the first fallout at distance X from ground zero. (s)
t_B	TB	Time required for the nominal particle to settle from the stabilized cloud cap base to the ground. (s)
t_{max}	TM	Yield dependent time of maximum activity deposition rate according to the g(t) function. (s)
t_G	TO	Fallout onset time. (s)

Text Symbol	FORTTRAN Mnemonic	Description
T		Yield dependent constant in the $g(t)$ and $D(X)$ functions. (s)
$U_{E,i}$	WX(I)	Easterly directed component of the wind vector in the i th wind stratum. ($m\ s^{-1}$)
$U_{N,i}$	WY(I)	Northerly directed component of the wind vector in the i th wind stratum. ($m\ s^{-1}$)
v	WIND	Effective fallout wind speed. ($m\ s^{-1}$)
\vec{v}		Effective fallout wind vector. ($m\ s^{-1}$)
W	W	Energy yield of the explosion (KT). (The KT unit is the energy released by explosion of one kiloton of TNT.)
W_F	FW	Fission yield of the nuclear explosion. (KT)
x	XM	Coordinate, relative to ground zero, in the easterly direction. (m)
X	X	Hotline distance from ground zero, positive in the down- wind direction. (m)
y	YM	Coordinate, relative to ground zero, in the northerly direction. (m)
Y	Y	Perpendicular distance to the hotline in the ground plane. (m)
$z_{b,i}$	ZBH(I)	Altitude of the base of the i th wind stratum above ground. (m)
z_B	ZB	Height of the base of the stabilized cloud cap above ground. (m)
z_i	ZCH(I)	Altitude of the center of the i th wind stratum above ground. (m)
z_T	ZT	Height of the top of the stabilized cloud cap above ground. (m)
α	ALPHA	Yield dependent parameter in the $g(t)$ and $D(X)$ functions. (dimensionless)
δ_{nom}		Diameter (μm) of the nominal fallout particle.
ϵ		Turbulent energy density dissipation rate. ($m^2\ s^{-3}$)
σ^2	SIGE	Variance of the horizontal spread of the nuclear cloud at deposition time. (Does not include the wind shear dis- persion contribution.) (m^2)
σ_C		Standard deviation of horizontal spread of the cloud before atmospheric transport. (m)

<u>Text Symbol</u>	<u>FORTRAN Mnemonic</u>	<u>Description</u>
σ_s^2		Wind shear contribution to the crosswind fallout pattern variance. (m ²)
σ_Y	SIGY	Crosswind standard deviation of the fallout pattern. (m)
\angle	ANG	Direction angle (clockwise from north) of the effective fallout wind vector. (deg.)

APPENDIX B

GROUND ROUGHNESS AND INSTRUMENT RESPONSE CORRECTION FACTORS

To compare predicted H + 1 hour gamma exposure rates in a fallout field with values measured over land by radiation survey meters, it is necessary to make certain adjustments to either the observed or predicted values. Conventional practice is to adjust the predictions.

Predicted exposure rates are based on laboratory measurements of fission product yields and on factors called exposure rate multipliers that convert the fission yields for individual nuclides to exposure rates at one meter height above an infinite plane on which the fission products are assumed to be uniformly distributed. One correction, the ground roughness factor, is required to account for absorption of radiation by small irregularities, or roughness elements, in an actual ground surface. The other correction is necessary to account for variation of response of survey meters to radiation over the spectrum of wave lengths encountered. Ground roughness factors for Nevada Test Site terrains are estimated to be in the range of 0.70 to 0.75, and an instrument response factor of about 0.75 is appropriate for commonly used survey meters. The product of these two factors is approximately 0.5, and this factor is applied to dose rates throughout all of the predicted test shot patterns except for Zuni as noted in section 5.3.

PREVIOUS PAGE
IS BLANK



APPENDIX C

FALLOUT PATTERN COMPARISON BY THE FIGURE-OF-MERIT METHOD

Rowland and Thompson²⁰ developed this method for comparison of pairs of fallout contour maps by computation of a single index, the FM, that is a measure of contour overlap between them. For each contour common to the patterns, the area overlapped and the area not overlapped is calculated. The areas are weighted by the average radiation level between successive contours. Sums over all contours of weighted overlapped areas and weighted total areas are computed, and the FM is the ratio of the two sums. For completely overlapped, perfectly matched patterns, FM = 1; for no overlap, FM = 0.

Mathematically, FM is

$$FM = \frac{\sum_{i=1}^N \frac{(r_i + r_{i-1})}{2} (a_i - a_{i-1})}{\sum_{i=1}^N \frac{(r_i + r_{i-1})}{2} (A_i - A_{i-1})}$$

where

N is the number of contours in the patterns. The summations are from highest contour to lowest

r_i is activity of the i th contour (Roentgen hr^{-1}), $r_0 = 10 r_1$

a_i is common (i.e., overlapped) area for the i th contours.
 $a_0 = 0$.

A_i is total area of the i th contour. The summation in the denominator is computed for both patterns, and the largest sum is used. $A_0 = 0$.

The FM has been found to have limited utility as a measure of fallout prediction accuracy. This is mainly for two reasons. First, and most important, is that being a measure of overlap, the FM is strongly biased in favor of overprediction; that is, it favors predictions that cover a large area, and therefore overlap the observed pattern, regardless of other considerations. Second, the FM method imposes no penalty for missing or extra contours; contours not common to both patterns are simply ignored.

APPENDIX D

FORTRAN CODE FOR THE DNAF-1 FALLOUT MODEL

C	SUBROUTINE DNAF	DNAF	1
C		DNAF	2
C	EXECUTIVE PROGRAM FOR THE DNAF-1 FALLOUT PREDICTION MODEL	DNAF	3
C		DNAF	4
C	H. G. NORMENT, ATMOSPHERIC SCIENCE ASSOCIATES - AUGUST 1961	DNAF	5
C		DNAF	6
C	* * * * * GLOSSARY * * * * *	DNAF	7
C	A H+1 HOUR GAMMA EXPOSURE RATE (ROENTGENS/HR)	DNAF	8
C	ALPHA DNAF-1 MODEL PARAMETER	DNAF	9
C	ALT HEIGHTS (* ABOVE MSL) AT WHICH SETTLING SPEEDS OF THE	DNAF	10
C	NOMINAL PARTICLE ARE DEFINED	DNAF	11
C	ANG HOTLINE ANGLE (INPUT AS DEGREES CLOCKWISE FROM NORTH)	DNAF	12
C	B EXPONENT PARAMETER USED FOR APPROX. PARTICLE SETTLING	DNAF	13
C	SPEED CALCULATION	DNAF	14
C	CAY K FACTOR $(R-M**2)/(HR-KT)$	DNAF	15
C	COSA COSINE OF HOTLINE ANGLE = WINDY/WIND	DNAF	16
C	DSX,DGY MAP INCREMENTS (SEE XMAX, ETC) (M)	DNAF	17
C	DMAX MAXIMUM EFFECTIVE BIOLOGICAL DOSE (ROENTGENS)	DNAF	18
C	FW FISSION YIELD (KT)	DNAF	19
C	GRUFF SCALE FACTOR TO BE APPLIED TO ACTIVITY VALUES	DNAF	20
C	(E.G. GROUND ROUGHNESS + INSTRUMENT RESPONSE FACTOR)	DNAF	21
C	IFMAP LOGICAL FLAG WHICH WHEN TRUE SPECIFIES THAT A FALLOUT MAP	DNAF	22
C	BE PREPARED	DNAF	23
C	IN NUMBER OF CHARACTERS/INCH HORIZONTALLY ON THE PRINTED MAP	DNAF	24
C	IN SYSTEM INPUT UNIT	DNAF	25
C	INTL1,INTL2 FLAGS TO SIGNAL FIRST PASS THROUGH SIGTA & DNAF1	DNAF	26
C	IO SYSTEM PRINT UNIT	DNAF	27
C	IP SYSTEM PUNCH UNIT	DNAF	28
C	IV NUMBER OF CHARACTERS/INCH VERTICALLY ON THE PRINTED MAP	DNAF	29
C	NHODO NUMBER OF HEIGHTS AT WHICH WIND DATA ARE INPUT	DNAF	30
C	NMAP MAX. NO. OF POINTS ALLOWED IN A MAP. (DIMENSION OF DMAP)	DNAF	31
C	NXMAP NUMBER OF MAP INCREMENTS IN THE X DIRECTION (SEE XMAX ETC)	DNAF	32
C	NYMAP NUMBER OF MAP INCREMENTS IN THE Y DIRECTION (SEE XMAX ETC)	DNAF	33
C	DMAP FALLOUT MAP ORDNATE ARRAY	DNAF	34
C	RI FIREBALL RADIUS (M)	DNAF	35
C	RS STABILIZED CLOUD RADIUS (M)	DNAF	36
C	SIGZ GAUSSIAN VARIANCE OF CLOUD DISPERSION (M**2)	DNAF	37
C	SIGY CROSS-WIND GAUSSIAN STANDARD DEVIATION OF THE FALLOUT	DNAF	38
C	PATTERN (1)	DNAF	39
C	SINA SINE OF HOTLINE ANGLE = WINDX/WIND	DNAF	40
C	SY SHEAR PARAMETER OR RMS SHEAR PARAMETER FROM ZO TO GROUND	DNAF	41
C	TA TIME OF ARRIVAL OF FALLOUT (S)	DNAF	42
C	T4 ARRIVAL TIME OF FALLOUT FROM THE STABILIZED CLOUD BASE (S)	DNAF	43
C	TLL,TLS ARRIVAL TIMES AT WHICH RATE OF GROWTH OF CLOUD TURBULENT	DNAF	44
C	DISPERSION VARIANCE BECOMES CONSTANT (")	DNAF	45
C	TM TIME OF MAXIMUM ACTIVITY DEPOSITION RATE (S)	DNAF	46
C	TD FALLOUT ONSET TIME (S)	DNAF	47
C	USETMP LOGICAL FLAG WHICH WHEN TRUE REQUIRES THE USER TO SPECIFY	DNAF	48
C	MAP BOUNDRIES AND GRID	DNAF	49
C	V SETTLING SPEEDS (M/S) OF THE NOMINAL PARTICLE AT HEIGHTS	DNAF	50
C	ALT	DNAF	51
C	VJ SETTLING SPEED AT SEA LEVEL OF THE NOMINAL PARTICLE (M/S)	DNAF	52
C	W TOTAL YIELD (KT)	DNAF	53
C	WIND EFFECTIVE WIND SPEED (M/S)	DNAF	54
C	WL NAPERIAN LOGARITHM OF W	DNAF	55
C	WL10 BRIGGSIAN LOGARITHM OF W	DNAF	56
C	WX OBSERVED WIND COMPONENTS IN THE X DIRECTION (SEE XMAX ETC)	DNAF	57
C	WY OBSERVED WIND COMPONENTS IN THE Y DIRECTION (SEE XMAX ETC)	DNAF	58
C	XMAX,XMIN,YMAX,YMIN MAP LIMITING COORDINATES. (X IS POSITIVE	DNAF	59
C	TOWARD EAST AND Y IS POSITIVE TOWARD NORTH) (M)	DNAF	60

CALL	SCLOUD(W, RI, RS, ZT, ZB)	DNAF 121
COPY OUT BASIC DATA		DNAF 122
WRITE(10, 1500) HOLL		DNAF 123
WRITE(10, 1600) W, FW, GRUFF		DNAF 124
IF(WIND .GE. 0.0) GO TO 200		DNAF 125
COPY IN WIND PROFILE DATA		DNAF 126
CALL INWIND(IN, I)		DNAF 127
COMPUTE EFFECTIVE WIND, WIND		DNAF 128
CALL	EFWIND(ZT, ZB, WIND, SINA, COSA)	DNAF 129
COMPUTE WIND SHEAR PARAMETER, SY		DNAF 130
SY = SYWNO (ZT, ZB, SINA, COSA)		DNAF 131
CHECK WIND FOR THRESHOLD AND SET WIND=0.50 IF IT IS BELOW THE THRESHOLD		DNAF 132
200 IF(WIND .GE. 0.50) GO TO 205		DNAF 133
WRITE(10, 2000) WIND		DNAF 134
WIND = 0.50		DNAF 135
COMPUTE FALLOUT ONSET TIME, TO		DNAF 136
205 TO = ONSET(W)		DNAF 137
COPY OUT MODEL PARAMETERS		DNAF 138
WRITE(10, 1700) WIND		DNAF 139
IF(.NOT. IFMAP) GO TO 210		DNAF 140
DIR = DIRC * ATAN(SINA/COSA)		DNAF 141
IF(COSA .LT. 0.0) DIR = DIR - SIGN(180.0, DIR)		DNAF 142
WRITE(6, 1800) DIR		DNAF 143
210 WRITE(10, 1900) SY		DNAF 144
CHECK IF A MAP IS TO BE PREPARED		DNAF 145
IF(IFMAP) GO TO 300		DNAF 146
WRITE(10, 1300)		DNAF 147
COPY IN COORDINATES AT WHICH ACTIVITY IS TO BE COMPUTED		DNAF 148
250 READ(IN, 1000, END=100) X, Y		DNAF 149
C		DNAF 150
COMPUTE CLOUD DISPERSION PARAMETERS AND FALLOUT ARRIVAL TIME		DNAF 151
275 CALL	SIGTA((W, TO, WIND, SY, RI, RS, ZB, ZT, WL10,	DNAF 152
1 INTL1, SIGE, SIGY, TA)		DNAF 153
COMPUTE CROSSWIND-INTEGRATED ACTIVITY FRACTION ON THE HOTLINE AT X		DNAF 154
GOFX = DNAF1(X, WIND, SIGE, W, INTL2)		DNAF 155
COMPUTE H+1 ACTIVITY (R/HR) AT POINT (X,Y)		DNAF 156
A = CAYW * CROSS(Y, SIGY) * GOFX		DNAF 157
COMPUTE MAXIMUM EFFECTIVE BIOLOGICAL DOSE		DNAF 158
DMAX = A * DOSE(T1)		DNAF 159
COPY OUT RESULTS		DNAF 160
WRITE(10, 1200) X, Y, A, DMAX		DNAF 161
GO TO 250		DNAF 162
C		DNAF 163
CHECK IF MAP IS SPECIFIED BY THE USER OR BY THE PROGRAM		DNAF 164
300 IF(USETMP) GO TO 400		DNAF 165
CALL	SETMP(W, FW, WIND, SINA, COSA, GRUFF, XMIN, XMAX,	DNAF 166
1 YMIN, YMAX, DGX, DGY)		DNAF 167
GO TO 450		DNAF 168
400 READ(IN, 1000) XMIN, XMAX, YMIN, YMAX, DGX, DGY		DNAF 169
410 IF(DGY .EQ. 0.0) DGY = DGX*IH/IV/2.0		DNAF 170
450 NXMAP = (XMAX - XMIN)/DGX		DNAF 171
NYMAP = (YMAX - YMIN)/DGY		DNAF 172
MMAP = NXMAP*NYMAP		DNAF 173
IF(MMAP .LE. NMAP) GO TO 460		DNAF 174
WRITE(10, 47)		DNAF 175
DGX = SQRT(2.0*I/(MMAP*DGX*DGY/(NMAP*IH))		DNAF 176
DGY=0.0		DNAF 177
GO TO 410		DNAF 178
460 WRITE(10, 24) XMIN, XMAX, YMIN, YMAX, DGX, DGY		DNAF 179
COMPUTE ACTIVITY AT MAP POINTS		DNAF 180

Y1 = YMIN	ONAF 181
INDEX = 0	ONAF 182
DO 500 J=1,NYMAP	ONAF 183
YM = YM + DGY	ONAF 184
X1 = XMIN	ONAF 185
DO 500 I=1,NXMAP	ONAF 186
X1 = XM + DGX	ONAF 187
IF(WIND .GT. 1.0E+02) GO TO 470	ONAF 188
X = SQRT(XM**2 + (M**2)	ONAF 189
Y = 0.0	ONAF 190
GO TO 472	ONAF 191
470 X = XM*SINA + YM*COISA	ONAF 192
Y = -XM*COISA + YM*SINA	ONAF 193
COMPUTE CLOUD DISPERSION PARAMETERS AND FALLOUT ARRIVAL TIME	ONAF 194
472 CALL SIGTA(X, W, TO, WIND,SY, RI, RS, ZB, ZT, WL10,	ONAF 195
1 INTL1, SIGE, SIGY, TA)	ONAF 196
INDEX = INDEX + 1	ONAF 197
COMPUTE MAP ORDINATE - 4+1 HOUR EXPOSURE RATE (NORMALIZED)	ONAF 198
475 OMAP(INDEX) =CAYF*ONAF1(X, WIND, SIGE, W, INTL2) * CROSS(Y,SIGY)	ONAF 199
500 CONTINUE	ONAF 200
COPY OUT MAP	ONAF 201
600 CALL MAPP(IC, HOLL, DGX, DGY, NXMAP, NYMAP, OMAP,	ONAF 202
1 XMAX, XMIN, YMAX, YMIN)	ONAF 203
GO TO 100	ONAF 204
900 RETURN	ONAF 205
END	ONAF 206

SUBROUTINE SCLOC(W, RI, RS, ZT, ZB)	SCLOC 2
C	SCLOC 3
COMPUTES STABILIZED CLOUD PROPERTIES	SCLOC 4
C	SCLOC 5
C H. G. NORMENT, ATMOSPHERIC SCIENCE ASSOCIATES - AUGUST 1980	SCLOC 6
C	SCLOC 7
RI=199.9*W**(0.33)	SCLOC 8
WL=ALOG(W)	SCLOC 9
RS = EXP(6.7553 + WL*(0.32055 + WL*0.01137478))	SCLOC 10
IF(W .GT. 4.07) GO TO 10	SCLOC 11
ZB = 2223. * W**(0.3463)	SCLOC 12
GO TO 20	SCLOC 13
10 ZB = 2661. * W**(0.2198)	SCLOC 14
20 IF(W .GT. 2.29) IF(W - 19.0) 30,30,40	SCLOC 15
ZT = 3537. * W**(0.2553)	SCLOC 16
GO TO 50	SCLOC 17
30 ZT = 3170. * W**(0.4077)	SCLOC 18
GO TO 50	SCLOC 19
40 ZT = 6474. * W**(0.1650)	SCLOC 20
50 CONTINUE	SCLOC 21
RETURN	SCLOC 22
END	SCLOC 23

C	SUBROUTINE INWIN(IN, IO)	INWIN 2
C		INWIN 3
C	COPIES IN AND PROCESSES OBSERVED WIND DATA	INWIN 4
C		INWIN 5
C	H. G. NORMENT, ATMOSPHERIC SCIENCE ASSOCIATES - AUGUST 1980	INWIN 6
C		INWIN 7
C	*****	INWIN 8
C		INWIN 9
C	READS AND PROCESSES WIND DATA FOR A HORIZONTALLY	INWIN 10
C	HOMOGENEOUS FIELD. VERTICAL COMPONENTS ARE NOT CONSIDERED.	INWIN 11
C		INWIN 12
C	* * * * * GLOSSARY * * * * *	INWIN 13
C	FMT OBJECT-TIME FORMAT OF WIND DATA	INWIN 14
C	FORM INPUT PARAMETER TO INDICATE FORMAT OF WIND DATA TO FOLLOW-	INWIN 15
C	EITHER - 1ETEOR OR RESOLV	INWIN 16
C	N1,N2,N3 DATA FIELD POINTERS	INWIN 17
C	SCALE DATA SCALE FACTORS AND TRANSLATIONS	INWIN 18
C	SEE GLOSSARY IN PROSFAM DNAF FOR OTHER QUANTITIES	INWIN 19
C	*****	INWIN 20
C		INWIN 21
C	REAL METEOR	INWIN 22
C	COMMON /WIND/ NHO(0), ZBH(50), ZCH(50), WX(50), WY(50)	INWIN 23
C	DIMENSION SCALE(3), AF(3), FMT(12)	INWIN 24
C		INWIN 25
C	DATA ALIMIT , FMT , PROGRAM , METEOR , RESOLV	INWIN 26
C	1 / 999999 , 014532925, 6HINWIND, 4HMETE , 4HRESOL	INWIN 27
C	DATA IREC/8/	INWIN 28
C		INWIN 29
C	1 FORMAT(4X, 6HLEVELS,I4, 5H THRU,I4, 8F12.5)	INWIN 30
C	3 FORMAT(///33X, 25HWIND LAYER BASE ALTITUDES/)	INWIN 31
C	4 FORMAT(1H03X31HMAXIMUM WIND SPACE ALTITUDE IS E12.5,7H METERS)	INWIN 32
C	1000 FORMAT (12A6)	INWIN 33
C	1100 FORMAT (3F10.0)	INWIN 34
C	1200 FORMAT (20I4)	INWIN 35
C	1300 FORMAT(/// 26X, 13HRAW WIND DATA,33X,19HPROCESSED WIND DATA/18X,	INWIN 36
C	11HZ, 9X, 10HVX OR DIP., 3X, 11HVY OR SPEED, 14X, 1HZ, 12X,	INWIN 37
C	2 2HVX, 12X, 2HVV)	INWIN 38
C	1400 FORMAT (10X, 3(2X, 1F12.5))	INWIN 39
C	1500 FORMAT (1H+,57X, 3(2X, 1F12.5))	INWIN 40
C	1800 FORMAT(1H0, 5X, 34HWIND STRATA ALTITUDES INCONSISTENT)	INWIN 41
C	1900 FORMAT(A4)	INWIN 42
C		INWIN 43
C	COPY IN DATA SPECIFICATION	INWIN 44
C	READ(IN,1900) FORM	INWIN 45
C	CHECK FORM	INWIN 46
C	IF(FORM.EQ. METEOR) GO TO 25	INWIN 47
C	20 IF(FORM.NE. RESOLV)CALL ERROR(PROGRAM,-20,IO)	INWIN 48
C	COPY IN FORMAT, SCALE & FIELD POINTERS	INWIN 49
C	25 READ (IN , 1000)FMT	INWIN 50
C	READ (IN , 1100) SCALE	INWIN 51
C	READ (IN , 1200) N1, N2, N3	INWIN 52
C	DO 50 I = 1,3	INWIN 53
C	50 IF(SCALE(I).EQ. 0.0) SCALE (I) = 1.0	INWIN 54
C	IF(FORM.EQ. METEOR) TRNS=SCALE(5)*SCALE(3) - 180.	INWIN 55
C	WRITE (IO,1300)	INWIN 56
C	NH000=0	INWIN 57
C	COPY IN, PRINT RAW DATA, TRANSLATE AND SCALE DATA, AND PRINT PROCESSED	INWIN 58
C	DATA	INWIN 59
C	100 READ (IN , FMT) IF	INWIN 60
C	IF(AP(N1).GE.ALIMIT)GO TO 250	INWIN 61

WRITE(10,1400)AP(N1), AP(N2), AP(N3)	INWIN 62
NH000=NH000+1	INWIN 63
ZCH(NH000)=(AP(N1) + SCALE(4))*SCALE(1)	INWIN 64
IF(FORM.EQ.RESOLV) GO TO 150	INWIN 65
WX(NH000) =AP(N3)*SCALE(2)*SIN(RADC*(AP(N2)*SCALE(3) + TRNS))	INWIN 66
WY(NH000) =AP(N3)*SCALE(2)*COS(RADC*(AP(N2)*SCALE(3) + TRNS))	INWIN 67
GO TO 200	INWIN 68
150 WX(NH000) = AP(N2)*SCALE(2)	INWIN 69
WY(NH000) = AP(N3)*SCALE(2)	INWIN 70
200 WRITE(10,1500) ZCH(NH000),WX(NH000), WY(NH000)	INWIN 71
GO TO 100	INWIN 72
COMPILE DATA TO ARRANGE IT IN ORDER OF ASCENDING ALTITUDE	INWIN 73
250 NH00M1=NH000-1	INWIN 74
DO 255 I=1,NH00M1	INWIN 75
IP1=I+1	INWIN 76
DO 255 J=IP1,NH000	INWIN 77
IF(ZCH(I) .LE. ZCH(J)) GO TO 255	INWIN 78
TEMP= ZCH(I)	INWIN 79
ZCH(I)= ZCH(J)	INWIN 80
ZCH(J)=TEMP	INWIN 81
TEMP=WX(I)	INWIN 82
WX(I)=WX(J)	INWIN 83
WX(J)=TEMP	INWIN 84
TEMP=WY(I)	INWIN 85
WY(I)=WY(J)	INWIN 86
WY(J)=TEMP	INWIN 87
255 CONTINUE	INWIN 88
CONSTRUCT WIND LAYER BASE ALTITUDES IN ARRAY ZBH	INWIN 89
259 ZBH(1) = 0.0	INWIN 90
DO 260 I=2,NH000	INWIN 91
260 ZBH(I) = (ZCH(I-1) + ZCH(I))/2.0	INWIN 92
ZMAX=2.0*ZCH(NH000) - ZBH(NH000)	INWIN 93
COPY OUT WIND LAYER BASE DATA	INWIN 94
WRITE(10 ,3)	INWIN 95
DO 270 IGO=1,NH000,IREC	INWIN 96
ISTOP=IGO+IREC-1	INWIN 97
IF(ISTOP.GT.NH000) ISTOP=NH000	INWIN 98
270 WRITE(10 ,1)IGO,ISTOP,(ZBH(K),K=IGO,ISTOP)	INWIN 99
C WRITE(10 ,4)ZMAX	INWIN 100
RETURN	INWIN 101
END	INWIN 102

SUBROUTINE EFWIND(ZT, ZB, WIND, SINA, COSA)	EFWIN 2
C	EFWIN 3
COMPUTES THE EFFECTIVE WIND SPEED, WIND, AND ITS DIRECTION ANGLE FROM	EFWIN 4
C OBSERVED WIND DATA	EFWIN 5
C	EFWIN 6
C H. G. NORMENT, ATMOSPHERIC SCIENCE ASSOCIATES - JULY 1991	EFWIN 7
C	EFWIN 8
COMMON /WDAT/ NH000, ZBH(50), ZCH(50), WX(50), WY(50)	EFWIN 9
DIMENSION ALT(39), V(39)	EFWIN 10
DATA ALT/0.,1000.,2000.,3000.,4000.,5000.,6000.,7000.,8000.,	EFWIN 11
1 9000.,10000.,11000.,12000.,13000.,14000.,15000.,16000.,	EFWIN 12
2 17000.,18000.,19000.,20000.,21000.,22000.,23000.,24000.,	EFWIN 13
3 25000.,26000.,28000.,30000.,32000.,34000.,36000.,38000.,	EFWIN 14
4 40000.,42000.,44000.,46000.,48000.,50000./	EFWIN 15
DATA V/ 1.5638, 1.7124, 1.7744, 1.8401, 1.9097, 1.9836, 2.0621,	EFWIN 16
1 2.1453, 2.2350, 2.3303, 2.4324, 2.5419, 2.6446, 2.7489, 2.8551,	EFWIN 17
2 2.9630, 3.0723, 3.1831, 3.2951, 3.4082, 3.5222, 3.6322, 3.7422,	EFWIN 18
3 3.8243, 3.9994, 4.0806, 4.1746, 4.3565, 4.5326, 4.7063, 4.8517,	EFWIN 19
4 5.0023, 5.1767, 5.3910, 5.6632, 6.0155, 6.4727, 7.0776, 7.6819/	EFWIN 20
C	EFWIN 21
COMPUTE CLOUD CENTER HEIGHT, ZO	EFWIN 22
ZO = (ZT + ZB)/2.0	EFWIN 23
COMPUTE LOCATION OF ZO IN ZBH ARRAY	EFWIN 24
NH000 = NH000+1	EFWIN 25
DO 100 I=1,NH000	EFWIN 26
J = NH000 - I	EFWIN 27
IF(ZO.GT. ZBH(J)) GO TO 150	EFWIN 28
100 CONTINUE	EFWIN 29
150 Z = (ZO + ZBH(J))/2.0	EFWIN 30
CALL TRPL(Z, 39, ALT, V, VP)	EFWIN 31
WGT = (ZO - ZBH(J))/VP	EFWIN 32
SWGT = WGT	EFWIN 33
CALL TRPL(Z, NH000, ZCH, WX,WNDX)	EFWIN 34
CALL TRPL(Z, NH000, ZCH, WY,WNDY)	EFWIN 35
WNDX = WNDX*WGT	EFWIN 36
WNDY = WNDY*WGT	EFWIN 37
J = J - 1	EFWIN 38
IF(J.EQ. 0) GO TO 250	EFWIN 39
DO 200 I=1,J	EFWIN 40
CALL TRPL(ZCH(I), 39, ALT, V, VP)	EFWIN 41
WGT = (ZBH(I+1) - ZBH(I))/VP	EFWIN 42
SWGT = SWGT + WGT	EFWIN 43
WNDX = WNDX + WX(I)*WGT	EFWIN 44
WNDY = WNDY + WY(I)*WGT	EFWIN 45
200 WIND = SQRT(WNDX**2 + WNDY**2)	EFWIN 46
IF(WIND.EQ. 0.0) GO TO 300	EFWIN 47
SINA = WNDX/WIND	EFWIN 48
COSA = WNDY/WIND	EFWIN 49
WIND = WIND/SWGT	EFWIN 50
RETURN	EFWIN 51
300 SINA = 1.0	EFWIN 52
COSA = 0.0	EFWIN 53
RETURN	EFWIN 54
END	EFWIN 55

```

      FUNCTION DOSE(TA)
C
C COMPUTES THE FACTOR WHICH WHEN MULTIPLIED BY A PROVIDES MAXIMUM
C   EFFECTIVE BIOLOGICAL DOSE
C
      IF(TA .LT. 1157.9) GO TO 100
      ZEE = 2.0 * ALOG(TA/3600.0) + 4.0
      DOSE = 4.6182 - ZEE * (0.53587 - 0.016923 * ZEE)
      RETURN
100 ZEE = 0.4685833 * ALOG(TA)
      DOSE = 15.2891 - ZEE * (2.903225 - 0.16623215 * ZEE)
      RETURN
      END

```

```

DOSE 1
DOSE 2
DOSE 3
DOSE 4
DOSE 5
DOSE 6
DOSE 7
DOSE 8
DOSE 9
DOSE 10
DOSE 11
DOSE 12
DOSE 13

```

```

      FUNCTION SYWND(ZT, ZB, SINA, COSA)
C
C COMPUTES RMS SHEAR PARAMETER BETWEEN ZO AND THE GROUND
C
C   H. G. NORMENT, ATMOSPHERIC SCIENCE ASSOCIATES - AUGUST 1980
C
      COMMON /W0AT/ NH000, ZCH(50), ZCH(50), WX(50), WY(50)
      COMPUTE CLOUD CENTER HEIGHT AND HALF CLOUD THICKNESS
      ZO = (ZT + ZB)/2.0
      DH = (ZT - ZB)/2.0
      N = 0
      SY = 0.0
      ZU = ZO + DH
      ZL = ZO - DH
      COMPUTE SQUARE OF SHEAR PARAMETER AND INCREMENT SUM AND COUNTER
100 CALL TRPL(ZU, NH000, ZCH, WX, WXU)
      CALL TRPL(ZU, NH000, ZCH, WY, WYU)
      CALL TRPL(ZL, NH000, ZCH, WX, WXL)
      CALL TRPL(ZL, NH000, ZCH, WY, WYL)
      SY = SY + (((-COSA*(WXU - WXL) + SINA*(WYU - WYL))/(ZU-ZL))**2
      N = N + 1
      CHECK IF DONE
      IF(ZL .EQ. 0.0) GO TO 200
      ZU = ZL
      ZL = ZU - 2.0*DH
      CHECK IF THIS IS LAST SUMMATION
      IF(ZL .LT. ZBH(2)) ZL=0.0
      GO TO 100
200 SYWND = SQRT(SY/N)
      RETURN
      END

```

```

SYWND 2
SYWND 3
SYWND 4
SYWND 5
SYWND 6
SYWND 7
SYWND 8
SYWND 9
SYWND 10
SYWND 11
SYWND 12
SYWND 13
SYWND 14
SYWND 15
SYWND 16
SYWND 17
SYWND 18
SYWND 19
SYWND 20
SYWND 21
SYWND 22
SYWND 23
SYWND 24
SYWND 25
SYWND 26
SYWND 27
SYWND 28
SYWND 29
SYWND 30
SYWND 31
SYWND 32

```

FUNCTION ONSET(W)	ONSET 2
C	ONSET 3
COMPUTES FALLOUT ONSET TIME (S)	ONSET 4
C	ONSET 5
C H. G. NORMENT, ATMOSPHERIC SCIENCE ASSOCIATES - AUGUST 1981	ONSET 6
C	ONSET 7
IF(W .LT. 1.014) GO TO 100	ONSET 8
ONSET = 1147.54	ONSET 9
RETURN	ONSET 10
100 WL = ALOG(W)	ONSET 11
ONSET = EXP(1.527667 + WL*(0.4089466 + WL*2.064322E-2))	ONSET 12
RETURN	ONSET 13
END	ONSET 14

SUBROUTINE SIGTA(X, W, TO, WIND, SY, PI, RS, ZB, ZT, WL10,	SIGTA 2
1 INTL1, SIGF, SIGY, TF)	SIGTA 3
C	SIGTA 4
COMPUTES GAUSSIAN VARIANCE SIGF AND STANDARD DEVIATION SIGY, AND TIME	SIGTA 5
C OF ARRIVAL OF FALLOUT AT DISTANCE X FROM GZ ALONG THE HOTLINE	SIGTA 6
C	SIGTA 7
C H. G. NORMENT, ATMOSPHERIC SCIENCE ASSOCIATES - AUGUST 1981	SIGTA 8
C	SIGTA 9
DATA BXVO , R , EX	SIGTA 10
1 / 4.79602E-5 , 2.9E-5 , 0.66666666667 /	SIGTA 11
C	SIGTA 12
IF(INTL1 .GT. 0) GO TO 100	SIGTA 13
C * * * * *	SIGTA 14
COMPUTE INITIALIZATION PARAMETERS ON FIRST PASS	SIGTA 15
TF = (1.0 - EXP(-3*ZP))/BXVO	SIGTA 16
WTO = WIND * TO	SIGTA 17
TOPPIW = TO + RI/WIND	SIGTA 18
RSO2 = RS/2.0	SIGTA 19
IF(WL10 .GT. 1.0) IF(WL10-3.0)10,20,20	SIGTA 20
SIGOP = RI	SIGTA 21
GO TO 50	SIGTA 22
10 SIGOP = RI*(1.0 + 3.0*WL10)/4.0	SIGTA 23
GO TO 50	SIGTA 24
20 SIGOP = 2.5*RI	SIGTA 25
50 CINT = (RSO2-SIGOP)/(TF - TO)	SIGTA 26
SIGC1S = SIGOP**EX	SIGTA 27
SIGC1L = RSO2**EX	SIGTA 28
SIGC2S = 3.0E6*SIGC1S - 2.0E9	SIGTA 29
SIGC2L = 3.0E6*SIGC1L - 2.0E9	SIGTA 30
EPSC1 = 0.016522**(-0.10233)	SIGTA 31
EPSC2 = 3.0E6*EPSC1	SIGTA 32
TLS = (1000.0 - SIGC1S)/EPSC1	SIGTA 33
TLL = (1000.0 - SIGC1L)/EPSC1	SIGTA 34
SHEARC = SY*(ZT - ZB)/10.0	SIGTA 35
INTL1 = 1	SIGTA 36
C * * * * *	SIGTA 37
COMPUTE FALLOUT TIME OF ARRIVAL	SIGTA 38
100 XIM1 = X/WIND - TOPPIW	SIGTA 39
TA = TO + (XIM1 + SQRT(XIM1**2 + 0.01*TOPPIW))/2.0	SIGTA 40
COMPUTE CLOUD HORIZONTAL DISPERSION VARIANCE, SIGF	SIGTA 41
125 IF(X .GT. WTO) IF(TA - TF)300,200,200	SIGTA 42
IF(TA .GT. TLS) GO TO 150	SIGTA 43

SIGE = (SIGC1S + TA*EPSC1)**3	SIGTA 44
GO TO 500	SIGTA 45
150 SIGE = SIGC2S + TA*EPSC2	SIGTA 46
GO TO 500	SIGTA 47
200 IF(TA .GT. TLL) GO TO 250	SIGTA 48
SIGE = (SIGC1L + TA*EPSC1)**3	SIGTA 49
GO TO 500	SIGTA 50
250 SIGE = SIGC2L + TA*EPSC2	SIGTA 51
GO TO 500	SIGTA 52
300 SIGO = (SIGOP+ (TA - TO)*SINT)**EX	SIGTA 53
IF(TA.GT. (1000.0 - SIGO)/EPSC1) GO TO 350	SIGTA 54
SIGE = (SIGO + TA*EPSC1)**3	SIGTA 55
GO TO 500	SIGTA 56
350 SIGE = 3.0E6*SIGO + TA*EPSC2 - 2.0E9	SIGTA 57
CORRECT CLOUD HORIZONTAL DISPERSION VARIANCE FOR WIND SHEAR DISPERSION	SIGTA 58
C AND RETURN THE STANDARD DEVIATION	SIGTA 59
500 SIGY = SQRT(SIGE + (SHEARC*TA)**2)	SIGTA 60
RETURN	SIGTA 61
END	SIGTA 62

FUNCTION DNAF1(X, WIND, SIGE, W, INTL2)	DNAF1 2
C	DNAF1 3
COMPUTES TOTAL FALLOUT FRACTION (INTEGRATED IN THE CROSSWIND DIRECTION)	DNAF1 4
C DEPOSITED AT DISTANCE X FROM GZ ALONG THE HOTLINE (PER M)	DNAF1 5
C	DNAF1 6
C M. G. NORMENT, ATMOSPHERIC SCIENCE ASSOCIATES - AUGUST 1981	DNAF1 7
C	DNAF1 8
DATA PI/3.141592654/	DNAF1 9
IF(INTL2)10,10,500	DNAF1 10
C * * * * *	DNAF1 11
COMPUTE INITIALIZATION PARAMETERS ON FIRST PASS	DNAF1 12
10 INTL2 =1	DNAF1 13
WL = ALOG(W)	DNAF1 14
IF(W .GT. 10.0) GO TO 30	DNAF1 15
A = 570.0	DNAF1 16
B = 0.0175	DNAF1 17
GO TO 50	DNAF1 18
30 A = -3179.42 + 3800.0*WL	DNAF1 19
B = 0.03045*W**(-0.66)	DNAF1 20
50 IF(W .GT. 1.0E3) GO TO 200	DNAF1 21
IF(W .GT. 0.1) GO TO 60	DNAF1 22
ALPHA = 1.06	DNAF1 23
GO TO 100	DNAF1 24
60 ALPHA = 1.0375 + 0.0119431*WL	DNAF1 25
100 IF(W .GT. 1.0) GO TO 150	DNAF1 26
YM = 30. + W**(-0.1556)	DNAF1 27
GO TO 400	DNAF1 28
150 TM = 30. + W**(-0.1407)	DNAF1 29
GO TO 400	DNAF1 30
200 ALPHA = 1.17	DNAF1 31
IF(W .GT. 1.0E4) GO TO 300	DNAF1 32
TM = 933.516*W**(-0.18273)	DNAF1 33
GO TO 400	DNAF1 34
300 TM = 2437.18*W**(-0.05115)	DNAF1 35
400 X1 = TM*SQRT(ALPHA/(4.0 - ALPHA)) * WIND	DNAF1 36
COF = 2.0*SIN(PI*(3.0 - ALPHA)/2.0)/(3.0 - ALPHA)/PI**2	DNAF1 37
PIX1 = PI*X1	DNAF1 38
X1S = X1**2	DNAF1 39
FX1F = 4.0*X1S**2	DNAF1 40
FX1S = 4.0*X1S	DNAF1 41
TX1S = 3.0*X1S	DNAF1 42
VOK = WIND*W**(-0.26945)/0.267E-5	DNAF1 43

VTAU = 3160.0*W**(0.24E3) * WIND	DNAF1 44
IF(W - 38.7868)450,450,420	DNAF1 45
420 VATC = -1.443*WIND*EXP(10.124706 + WL*(0.1861768 -	DNAF1 46
1 8.66044E-3*WL))	DNAF1 47
GO TO 500	DNAF1 48
450 VATC = -1.443*WIND*14667.0*W**(0.26203)	DNAF1 49
C *****	DNAF1 50
COMPUTE G(X)	DNAF1 51
500 XS = X**2	DNAF1 52
X2S = X3 + SIGF	DNAF1 53
X3S = X2S - X1S	DNAF1 54
X3F = X3S**2	DNAF1 55
SRSIG = SQRT(SIGE)	DNAF1 56
XDSIG = X/SRSIG	DNAF1 57
FXSX1S = XS*FX1S	DNAF1 58
FXSX1F = XS*FX1F	DNAF1 59
IF(X3F GT. 1.0) GO TO 510	DNAF1 60
F1 = X3S	DNAF1 61
F2 = X3F	DNAF1 62
GO TO 550	DNAF1 63
510 F1 = 1.0/X3S	DNAF1 64
F2 = 1.0	DNAF1 65
FXSX1S = FXSX1S/X3F	DNAF1 66
FXSX1F = FXSX1F/X3F	DNAF1 67
550 DNAF1 = SRSIG * CGF*(-X*PIX1*((3.0*X2S + X1S)*F1 + FXSX1S) -	DNAF1 68
1 (F2 + FXSX1S)*X3S + (Y2S*F2 - FXSX1F)*ALOG(X2S/X1S) +	DNAF1 69
2 XDSIG*((X2S + FX1S)*Y2S*F1 + FXSX1F)*(PI + 2.0*ATAN(XDSIG)))/	DNAF1 70
3 ((F2 + 2.0*FXSX1S)*X3F + 4.0*X3F*FXSX1F)	DNAF1 71
CHECK FOR UPWIND OR DOWNWIND CORRECTION	DNAF1 72
IF(X)600,600,700	DNAF1 73
COMPUTE UPWIND CORRECTION	DNAF1 74
600 DNAF1 = DNAF1 * EXP(R*X*(1.0 - EXP(X/A)))	DNAF1 75
RETURN	DNAF1 76
COMPUTE DOWNWIND CORRECTION	DNAF1 77
700 DNAF1 = DNAF1 * EXP(-(ALOG(VOK*DNAF1) + (X/VTAU)**2) +	DNAF1 78
1 (1.0 - EXP(X/VATC)))	DNAF1 79
800 RETURN	DNAF1 80
END	DNAF1 81

SUBROUTINE SETMP(W, FW, WIND, SINA, COSA, GRUFF, XMIN, XMAX,	SETMP 2
1 YMIN, YMAX, DGX, DGY)	SETMP 3
C	SETMP 4
C AUTOMATIC MAP SETUP FOR PURPOSE OF PRELIMINARY LOOK AT PATTERN	SETMP 5
C	SETMP 6
C H. G. NORMINT, ATMOSPHERIC SCIENCE ASSOCIATES - AUGUST 1981	SETMP 7
C	SETMP 8
C THIS CODE ESTIMATES UPWIND AND DOWNWIND HOTLINE DISTANCES TO THE	SETMP 9
C 1 R/HR CONTOUR LEVEL, AND SETS UP THE MAP ACCORDINGLY.	SETMP 10
C THE MAP IS SPATIALLY UNDISTORTED.	SETMP 11
C	SETMP 12
DATA NGRIDX , NGRIDY , IH , IV	SETMP 13
1 / 37 , 44 , 10 , 6 /	SETMP 14
C	SETMP 15
COMPUTE APPROXIMATE HOTLINE DISTANCES TO THE 1 R/HR CONTOUR LEVEL	SETMP 16
TENWND = 10.0*WIND	SETMP 17
XDN = (2.5193 * TENWND**(.6834)) * (W**(.027125 + 0.031124 * 1 ALOG(TENWND)))	SETMP 18
IF(W.GT.10.0) GO TO 100	SETMP 19
XUP = -340.0 * (TENWND**(.1062)) * (W**(.015))	SETMP 20
GO TO 200	SETMP 21
100 XUP = -125.3 * (TENWND**(.1062)) * (W**(.05833))	SETMP 22
COMPUTE MAXIMUM AND MINIMUM MAP COORDINATES	SETMP 23
200 IF(SINA)300,400,400	SETMP 24
300 XMAX = XUP * SINA	SETMP 25
XMIN = XDN * SINA	SETMP 26
GO TO 500	SETMP 27
400 XMAX = XDN * SINA	SETMP 28
XMIN = XUP * SINA	SETMP 29
500 IF(COSA)600,700,700	SETMP 30
600 YMAX = XUP * COSA	SETMP 31
YMIN = XDN * COSA	SETMP 32
GO TO 300	SETMP 33
700 YMAX = XDN * COSA	SETMP 34
YMIN = XUP * COSA	SETMP 35
COMPUTE GRID INCREMENTS AND ADJUST MAP BOUNDARIES	SETMP 36
800 XLNGH = XMAX - XMIN	SETMP 37
YLNGH = YMAX - YMIN	SETMP 38
IF(XLNGH.GT.YLNGH) GO TO 900	SETMP 39
DGY = YLNGH/NGRIDY	SETMP 40
DGX = 2.0*DGY*IV/IH	SETMP 41
DG = (0.667*YLNGH - XLNGH)/2.0	SETMP 42
IF(DG)1000,1000,800	SETMP 43
850 XMAX = XMAX + DG	SETMP 44
XMIN = XMIN - DG	SETMP 45
GO TO 1000	SETMP 46
900 DGX = XLNGH/NGRIDX	SETMP 47
DGY = DGX*IH/IV/2.0	SETMP 48
DG = (0.667*XLNGH - YLNGH)/2.0	SETMP 49
IF(DG)1000,1000,900	SETMP 50
950 YMAX = YMAX + DG	SETMP 51
YMIN = YMIN - DG	SETMP 52
1000 XMIN = XMIN - DGX	SETMP 53
YMIN = YMIN - DGY	SETMP 54
RETURN	SETMP 55
END	SETMP 56
	SETMP 57

	SUBROUTINE MAPP(ISOUT, HOLL, DGX, CGY, NXMAP, NYMAP, OMAP,	MAPP	2
	1 XMAX, YMIN, YHAX, YMIN)	MAPP	3
C		MAPP	4
	COPIES OUT THE FALLOUT MAP FROM THE ARRAY OMAP	MAPP	5
C		MAPP	6
C	T. W. SCHWINKL 28 FEBRUARY 1967	MAPP	7
C	H. G. NORMENT, ATMOSPHERIC SCIENCE ASSOCIATES - JULY 1981	MAPP	8
C		MAPP	9
C	*****	MAPP	10
C		MAPP	11
C	DNAP-1 MAP PRINTER	MAPP	12
C		MAPP	13
C	*****	MAPP	14
C		MAPP	15
	DIMENSION JMAP(20), ABSSA(10), HOLL(12), OMAP(5*100)	MAPP	16
	DATA INC/ 13/, XGZ,YGZ/0.0,0.0/	MAPP	17
2	FORMAT(/12X,19I6)	MAPP	18
4	FORMAT(1X,F13.0,2X,19F6.3)	MAPP	19
6	FORMAT(/15X,25HTHE QUANTITY PRESENTED IS)	MAPP	20
10	FORMAT(15X,42H_XPOSURE RATE NORMALIZED TO TIME H+1 HOUR.)	MAPP	21
1	FORMAT(1H1,5HSTRIP13,5X, 12A6)	MAPP	22
16	FORMAT(/ 3X, 4H*** , 10F12.0, 3H **/)	MAPP	23
20	FORMAT(15X,31HGROUND ZERO IS LOCATED AT X = F10.1,6H , Y = F10.1	MAPP	24
1)		MAPP	25
25	FORMAT(15X,28HUNITS ARE PERCENTS PER HOUR)	MAPP	26
C		MAPP	27
	MAPPUN=0	MAPP	28
	TINC=2.0*DGX	MAPP	29
	XCOORD=YMIN+DGX	MAPP	30
	XCINC= INC*DGX	MAPP	31
	KKL=1	MAPP	32
	NX=NXMAP	MAPP	33
C	LEFT IS USED HERE AS A TEMPORARY STORAGE	MAPP	34
	LEFT=(XMAX-XMIN)/DGX	MAPP	35
C 102	PRINT ORIGINATE DESCRIPTION	MAPP	36
C		MAPP	37
102	WRITE (ISOUT,8)	MAPP	38
162	WRITE (ISOUT,10)	MAPP	39
	WRITE (ISOUT,25)	MAPP	40
C		MAPP	41
170	WRITE (ISOUT,20) XGZ,YGZ	MAPP	42
1702	IF(LEFT-NX) 1021,1022,1022	MAPP	43
1021	NX=LEFT	MAPP	44
1022	MM=NX/(INC)	MAPP	45
	MM=MM+1	MAPP	46
C	LEFT IS USED HERE AS THE NUMBER OF PRINT COLUMNS IN THE LAST	MAPP	47
C	PRINTER STRIP	MAPP	48
	LEFT=NX-MM*(INC)	MAPP	49
	IF (LEFT.NE.0) GO TO C 2023	MAPP	50
	H = MM	MAPP	51
	LEFT = INC	MAPP	52
C	STRIPS	MAPP	53
2023	DO 110 ISTRIP=1,M	MAPP	54
	MAPPUN=MAPPUN+1	MAPP	55
	ABSSA(1)=XCOORD	MAPP	56
	DO 3023 IAB=2,10	MAPP	57
3023	ABSSA(IAB)=ABSSA(IAB-1)+TINC	MAPP	58
	WRITE (ISOUT,1) MAPPUN,HOLL	MAPP	59
	WRITE (ISOUT,16) ABSSA	MAPP	60
1023	KL=KKL+(NYMAP-1)*NXMAP	MAPP	61

IF (ISTRIP-M) 103,104,103	MAPP 62
104 KINC=LEFT-1	MAPP 63
VLEFT=LEFT	MAPP 64
XCIN=VLEFT*OGX	MAPP 65
GO TO 1031	MAPP 66
103 KINC=INC-1	MAPP 67
XCIN=XCINC	MAPP 68
1031 CONTINUE	MAPP 69
C	MAPP 70
C ROWS	MAPP 71
YY=YMIN+OGY*FLOAT(NYMAP)	MAPP 72
DO 200 J=1,NYMAP	MAPP 73
KH=KL+KINC	MAPP 74
KDC=0	MAPP 75
C	MAPP 76
C NUMBERS WITHIN ROWS	MAPP 77
DO 300 K=KL,KH	MAPP 78
KDC=KDC+1	MAPP 79
C	MAPP 80
C 150 CODE FOR POWER OF TEN DISPLAY	MAPP 81
150 IF (OMAP(K)) 105,106,107	MAPP 82
105 ASSIGN 121 TO N3	MAPP 83
OMAP(K)=-OMAP(K)	MAPP 84
GO TO 109	MAPP 85
106 JMAP(KDC)=0	MAPP 86
GO TO 300	MAPP 87
107 ASSIGN 300 TO N3	MAPP 88
109 H = ALOG10(OMAP(K))	MAPP 89
H1=AMOD(H,1.0)	MAPP 90
JMAP(KDC)=H-H1	MAPP 91
1090 OMAP(K) = 10.0**H1	MAPP 92
IF (OMAP(K)-9.999) 115,115,1031	MAPP 93
1091 OMAP(K)=OMAP(K)/10.0	MAPP 94
JMAP(KDC)=JMAP(KDC)+1	MAPP 95
115 GO TO N3,(300,121)	MAPP 96
C 121 RESET SIGN OF MAP COORDINATE	MAPP 97
121 OMAP(K)=-OMAP(K)	MAPP 98
300 CONTINUE	MAPP 99
WRITE(ISOOT,2) (JMAP(K),K=1,KDC)	MAPP 100
WRITE(ISOOT,4) YY, (OMAP(K),K=KL,KH)	MAPP 101
YY=YY-OGY	MAPP 102
200 KL=KL-NYMAP	MAPP 103
WRITE (ISOOT,16) ARSSA	MAPP 104
XCOORD=XCOORD+XCIN	MAPP 105
110 KKL=KKL+INC	MAPP 106
111 RETURN	MAPP 107
END	MAPP 108

SUBROUTINE TRPL (TRPL	2
1 ARG, NPR, PARA, PARB, VRB)	TRPL	3
C *****	TRPL	4
C	TRPL	5
C	TRPL	6
C TRPL USES LINEAR INTERPOLATION TO LOCATE POSITION OF ARG WITHIN	TRPL	7
C THE ONE-DIMENSIONAL ARRAY PARA AND COMPUTES FOR THE CORRESPONDING	TRPL	8
C POSITION IN THE ONE-DIMENSIONAL ARRAY PARB, VRB, NPR IS THE	TRPL	9
C DIMENSION OF PARA AND PARB (WHOSE ELEMENTS CORRESPOND ONE TO ONE).	TRPL	10
C IF ARG IS OUTSIDE THE TABULATED VALUES OF PARA, VRB IS SELECTED	TRPL	11
C FROM THE CORRESPONDING END OF PARB.	TRPL	12
C PARA IS ORDERED FROM LEAST (PARA (1)) TO GREATEST (PARA (NPR))	TRPL	13
C *****	TRPL	14
C	TRPL	15
C	TRPL	16
C DIMENSION	TRPL	17
1 PARA (NPR), PARB (NPR)	TRPL	18
C *****	TRPL	19
C *****	TRPL	20
C *****	TRPL	21
C	TRPL	22
020 IF (ARG - PARA (1)) 022, 022, 040	TRPL	23
022 MB = 1	TRPL	24
024 VRB = PARB (MB)	TRPL	25
026 RETURN	TRPL	26
040 DO 054 MA =2, NPR	TRPL	27
IF (ARG - PARA (MA)) 042, 044, 054	TRPL	28
044 MB = MA	TRPL	29
GO TO 024	TRPL	30
048 VRB = (ARG - PARA (MA - 1)) * (PARB (MA) - PARB (MA - 1)) /	TRPL	31
1 (PARA (MA) - PARA (MA - 1)) + PARB (MA - 1)	TRPL	32
GO TO 026	TRPL	33
054 CONTINUE	TRPL	34
MB = NPR	TRPL	35
GO TO 024	TRPL	36
END	TRPL	37

	SUBROUTINE ERROR (PROGRAM,IPROR,ISOUT)	ERROR 2
C	T. W. SCHWENKE	ERROR 3
C	1 MARCH 1966	ERROR 4
C	*****	ERROR 5
C	*****	ERROR 6
C	THIS PROGRAM WRITES A GENERALIZED ERROR COMMENT OF THE FOLLOWING	ERROR 7
C	FORM ON TAPE ISOUT AND THEN RETURNS IF THE SIGN OF ERROR IS	ERROR 8
C	POSITIVE OR STOPS IF ITS SIGN IS NEGATIVE.	ERROR 9
C		ERROR 10
C	ERROR SENSED IN PROGRAM (PROGRAM) AT OR NEAR STATEMENT NUMBER	ERROR 11
C	(IPROR). PLEASE REFER TO THE PROGRAM LISTING.	ERROR 12
C		ERROR 13
C	PRIOR TO CALLING ERROR, THE PARAMETER PROGRAM MUST BE SET	ERROR 14
C	WITH THE 300 NAME OF THE CALLING	ERROR 15
C	PROGRAM AND PARAMETER IPROR MUST BE SET WITH THE NUMBER OF THE	ERROR 16
C	FORTRAN STATEMENT WHICH BEST IDENTIFIES THE ERROR CONDITION.	ERROR 17
C		ERROR 18
C	*****	ERROR 19
C	*****	ERROR 20
C	1 FORMAT(//26H ERROR SENSED IN PROGRAM A6,30H AT OR NEAR STATEMENT	ERROR 21
	1 NUMBER 16,40H . PLEASE REFER TO THE PROGRAM LISTING.)	ERROR 22
C		ERROR 23
C	*****	ERROR 24
C	*****	ERROR 25
C	*****	ERROR 26
C		ERROR 27
	IRR= IABS(IPROR)	ERROR 28
	WRITE(ISOUT,1)PROGRAM,IPR	ERROR 29
	IF (IPROR) 101,100,100	ERROR 30
100	RETURN	ERROR 31
101	STOP	ERROR 32
	END	ERROR 33

DISTRIBUTION LIST

DEPARTMENT OF DEFENSE

Armed Forces Radiobiology Resch Institute
ATTN: Director

Armed Forces Staff College
ATTN: Library

Assistant Secretary of Defense
Program Analysis & Evaluation
2 cy ATTN: Strat Programs
2 cy ATTN: Regional Programs

Assistant to the Secretary of Defense
Atomic Energy
ATTN: Exec Asst

Command & Control Technical Center
ATTN: C-315
ATTN: C-332
ATTN: C-320
5 cy ATTN: C-312, R. Mason

Commander-in-Chief, Pacific
ATTN: J-3

Defense Advanced Resch Proj Agency
ATTN: T10

Defense Communications Agency
ATTN: Code J300, M. Scher

Defense Intelligence Agency
ATTN: RDS-2C, Tech Svcs & Spt
ATTN: DB-4B
ATTN: DB-4C, P. Johnson
ATTN: DT, J. Vorona
ATTN: DB-4C, J. Burfening
5 cy ATTN: DB-4, Rch, Resources Div

Defense Nuclear Agency
ATTN: BAID
ATTN: SPSA
ATTN: SIRA
ATTN: SPSA
50 cy ATTN: T10

Defense Technical Information Center
12 cy ATTN: DD

Field Command Defense Nuclear Agency
Det 1
Lawrence Livermore Lab
ATTN: LC-1

Commander-in-Chief, Atlantic
ATTN: J5/J3

Field Command Defense Nuclear Agency
Det 2
Los Alamos National Lab/D51
ATTN: MS-605, FC-2

DRA PACOM Liaison Office
ATTN: CDR J. Bartlett

DEPARTMENT OF DEFENSE (Continued)

Field Command
Defense Nuclear Agency
ATTN: FCPRK, LTC Wells
ATTN: LCIT, G. Ganong
ATTN: FCIT, W. Summa
ATTN: FCPR
ATTN: FCIXL

Interservice Nuclear Wpns School
ATTN: T1V
ATTN: Doc Con

Joint Chiefs of Staff
ATTN: SAGA/SFD
ATTN: J-3
ATTN: J-5 Nuc/Chem Pol Br, J. Steckler
ATTN: SAGA/SSO
ATTN: GD10, J-5 Nuc & Chem Div
ATTN: J-5 Nuc Div/Strat Div
3 cy ATTN: J-5 Nuc Div/Strat Div/EP&P Div

Joint Strat Tgt Planning Staff
ATTN: JLTN
ATTN: JLTW
ATTN: J1, Nat Strat Tgt List Dir
2 cy ATTN: JLTW-2

National Defense Univ
ATTN: ECAI Tech Library

DEPARTMENT OF THE ARMY

Harry Diamond Labs
ATTN: DEUHD-HW-P
ATTN: DEUHD-DE
ATTN: DEUHD-TA-1
ATTN: 00100 Cdr/Tech Dir/Div Dir
ATTN: DEUHD-ID, Tech Dir

US Army Ballistic Research Labs
ATTN: DRDAR-VI
ATTN: DRDAR-BI
ATTN: DRDAR-15B-5
ATTN: DRDAR-BIV, Dr Rami
ATTN: DRDAR-BII, Effects Anal Br
ATTN: DRDAR-15B-5
2 cy ATTN: DRDAR-BIB, J. Maloney

US Army Chemical School
ATTN: AT7H-CM-C5
ATTN: AT7H-CM-A5
ATTN: AT7H-CM-CC

US Army Concepts Analysis Agency
ATTN: CUSA ADI

US Army Foreign Science & Tech Ctr
ATTN: DRXST SP 1

US Army Nuclear & Chemical Agency
ATTN: Library
3 cy ATTN: MOHA-OPs, J. Ratway

US Army War College
ATTN: Library

DEPARTMENT OF THE NAVY

Naval Postgraduate School
ATTN: Code 1434, Library

Naval Research Lab
ATTN: Code 2627

Naval Surface Wpn's Ctr
ATTN: Code 041
ATTN: Code R 4
ATTN: Code F 1
ATTN: Code F 30

Naval War College
ATTN: Code 1-11, Tech Svc

Naval Wpn's Eval Facility
ATTN: G. Rimes

Office of the Deputy Chief of Naval Ops
Atty ATTN: NOP 654, Strat & Eval Anal Br

Office of Naval Research
ATTN: Tech Info Svcs

DEPARTMENT OF THE AIR FORCE

Air Force Weapons Lab
ATTN: M-36
ATTN: SHU

Air University Library
ATTN: AUL-USL

Air War College
ATTN: LORA

Air Weather Svc
ATTN: AW&AI

Assistant Chief of Staff
Studies & Analysis
Atty ATTN: AI/SA
Atty ATTN: AI/SAI, Tech Info Div

Strategic Air Command
ATTN: HRI-51110 Library
ATTN: XPI, Col Condyne
ATTN: SAC/TH
ATTN: XP

USAF Academy Library
ATTN: Library

USAF Scientific Advisory Bd
ATTN: AI/NS

USAF School of Aerospace Medicine
ATTN: Radiation Sciences Div

OTHER GOVERNMENT AGENCIES

Central Intelligence Agency
ATTN: O&WR/HIO
ATTN: O&R/41
ATTN: HIO, Strat Sys

Federal Emergency Management Agency
ATTN: Of. of Rec/HQ, D. Benken
ATTN: Asst Assoc. Dir HP-RI
ATTN: Asst. Associated Dir

OTHER GOVERNMENT AGENCIES (Continued)

Department of State
Office of International Security Policy
ATTN: PM/ISP

US Arms Control & Disarmament Agency
ATTN: C. Thorn
ATTN: Ops & Anal Div, R. Deemer
ATTN: A. Lieberman

US Department of State
Office of Security
ATTN: PM

NAFO

NAFO School (SHAPE)
ATTN: Ops Doc Ofc for LIC Williamson

DEPARTMENT OF ENERGY CONTRACTORS

University of California
Lawrence Livermore National Lab
ATTN: 1-262, J. Knox
ATTN: Tech Info Dept Library
ATTN: 1-21, M. Gustavson
ATTN: 1-9, R. Barker

Los Alamos National Lab
ATTN: Reports Library
ATTN: M/5634, T. Dowler
ATTN: R. Sandoval

Sandia National Lab
ATTN: Tech Library, 3141
ATTN: 5612, J. Keizer

Sandia National Labs, Livermore
ATTN: 3334, J. Steuve

DEPARTMENT OF DEFENSE CONTRACTORS

Academy for Interference Methodology
ATTN: M. Painter

Advanced Research & Applications Corp
ATTN: Doc Con

Atmospheric Science Assoc
Atty ATTN: H. Norment

Decision Science Appl, Inc
ATTN: Dr. Pugh

Horizon Technology, Inc
ATTN: R. Kruger
ATTN: J. Palmer

Institute for Defense Analysis
ATTN: J. Grote
ATTN: D. Moody
ATTN: Tech Library

Kanan Tempo
ATTN: DA/CIAC

28D Associates
ATTN: R. Cooper
ATTN: A. Bell

DEPARTMENT OF DEFENSE CONTRACTORS (Continued)

McDonnell Douglas Corp
ATTN: Tech Library Svcs

McLean Research Center, Inc
ATTN: W. Schilling

Mission Research Corp
ATTN: Tech Library

National Institute for Public Policy
ATTN: C. Gray

Orion Research Inc
ATTN: L. Scholz

Pacific-Sierra Research Corp
ATTN: G. Lang
ATTN: H. Brode, Chairman SAGE

Pacific-Sierra Research Corp
ATTN: D. Gornley
ATTN: G. Moe

R&D Associates
ATTN: J. Marcum
ATTN: J. Lewis
ATTN: P. Haas
ATTN: R. Port
Policy ATTN: Doc Con

DEPARTMENT OF DEFENSE CONTRACTORS (Continued)

Rand Corp
ATTN: Library
ATTN: R. Rapp

S-CUBED
ATTN: K. Pyatt

Santa Fe Corp
ATTN: D. Paulucci

Science Applications, Inc
ATTN: J. Beyster
ATTN: E. Swick
ATTN: M. Drake
ATTN: Doc Con

Science Applications, Inc
ATTN: W. Layson
ATTN: L. Goure
ATTN: Doc Con
ATTN: R. Craver
ATTN: J. McGahan

Science Applications, Inc
ATTN: D. Kaul

SRI International
ATTN: J. Naar
ATTN: P. Dolan

Titan Systems, Inc
ATTN: R. Lee

